Do Physical Analogies of Stock Market Crashes Make Sense?

Beau Coker

Tufts University
Department of Physics and Astronomy

Advisor: Professor Timothy Atherton

May 10, 2013

Abstract

The purpose of this thesis is to critique the analogy between physical systems and stock market crashes. We do this by calculating the intraday correlations between a collection of stocks over the past 20 years and the intrahour correlations over a few particular years. Comparing these results to Monte Carlo simulations of a generic condensed matter system, the Ising model, we find that stocks do not exhibit the same correlation features imposed by the dimension of the lattice of the Ising model, suggesting that a measure of distance between stocks does not exist. Rather, the results resemble a Zero-dimensional Ising model. An investigation of the properties of such a model – one that has not been systematically analyzed in condensed matter physics as there is no physical interpretation – will provide several interesting policy implications, including that stock market crashes may depend on market size. We will also expand the analysis of Kiyono et al. [24] by analyzing the critical behavior of the S&P 500 over the past 30 years.

Contents

Acknowledgments

This thesis has been a yearlong process and I am deeply indebted to the many people that helped me along the way, particularly professor Atherton for his tireless dedication and guidance. I could not have finished this project without such assistance. I would also like to thank professor Atherton's condensed matter research group, consisting of Badel Mbanga, Christopher Burke, Kate Voorhes, Lesya Horyn, Dan Fortunato, and others, for their insightful suggestions and critiques. I will add that this thesis would quite literally not exist if it were not for Badel, who helped me print it. Finally, I would like to thank professor Pierre-Hugues Beauchemin for his accommodation and agreement to serve on the thesis committee.

Chapter 1

Introduction

There is an extensive literature of analogies between physical and economic systems. Among these is the analogy between physical systems exhibiting critical phenomena and the stock market. This analogy has also been discussed by popular academics: Niall Ferguson, the controversial economic historian, used the analogy to further an argument against financial regulation [14]. Malcolm Gladwell's bestselling book *The Tipping Point* [17] could easily be retitled *The Critical Point*. Beyond stock markets, the theory has been extended to many other fields, including virus dynamics, ecological shifts, and traffic jams [45]. With this burgeoning amount of literature, one must be careful that the aesthetic appeal of the analogy does not substitute for a theoretically solid and empirically verified analysis of its validity. Indeed, we need to see if market crashes can be thought of within any kind of universal framework, since, if not, any empirical description seems hopeless. The purpose of this thesis is, then, to critique the analogy between critical systems and stock markets. It is the contention of this thesis that the aforementioned analogy has some validity, but important physics has thus far been neglected. Our means of performing the analysis will be to examine the correlation properties of minute-by-minute stock market data. These results will be compared to a generic condensed matter system, the Ising model, which is a simple and well-studied model of ferromagnetism that exhibits a phase transition in certain dimensions. Our primary result is that stock market crashes provide a unique opportunity to study the "spatial structure" of the stock market, which we find to lack an obvious measure of distance. This leads us to propose a condensed matter system that has similar properties, a zero dimensional Ising model, which similarly has no spatial structure. We will then show that the zero dimensional Ising model does not, strictly speaking, exhibit a phase transition, although it does exhibit something similar to it.

There are eight chapters in this thesis, including the current introduction. The structure of each of these chapters is as follows.

In chapter 2 we introduce the discipline of econophysics, paying attention to the connection between physical and economic systems. This will include discussions of diffusive processes and price variation, hydrodynamic turbulence and price variation, and the statistical properties of price variation.

In chapter 3 we continue the theoretical background discussion, but this time from a purely physics-based perspective. We will begin this chapter with an introduction to the study of statistical mechanics, which is the area of physics most connected to economics and finance. Monte Carlo methods in statistical mechanics will also be discussed. We will then examine a few common examples of critical phenomena while introducing concepts like universality, correlation length, order parameters, and so on. Following this, we will introduce the Ising model and pose the "black box" Ising problem - where we attempt to determine the connectivity of an arbitrary Ising system by observing only its state. A collection of Monte Carlo simulations will then be shown in one and two dimensions.

In chapter 4 we review some of the literature concerning models of market crashes as critical phenomena and then proceed to outline a particular agent-based model of market behavior with spin-like interaction. Following

this we will state our critique of such models.

In chapter 5 we discuss the methods used in this thesis, including the data, software, and computing tools.

This results of these methods are shown in chapter 6. This chapter will be divided into three sections. In section one we will show the results of the autocorrelation of the returns and volatility for both intraday detrended and non intraday detrended data. In the next section we reapply the analysis of Kiyono et al. [24] to the S&P 500 from 1983 to 2012. This is a substantial expansion of the scope of this analysis. Finally, in the last section we analyze the correlation properties of stock returns. It is from this section that we conclude that the stock correlations do not exhibit the same structural properties as exhibited by the spin correlations.

Next, in chapter 7, we introduce a zero dimensional Ising model. This will include a definition of the model, an investigation of the partition function, and the results of several Monte Carlo simulations, including one with a random coupling matrix.

In the final chapter we summarize the conclusions of this thesis and propose several suggestions for further work.

Chapter 2

Econophysics

The connection between physics and economics is not new. For example, the mathematician Daniel Bernoulli developed utility based preferences in the 18th century [4]. Although not a physicist, Vilfredo Pareto's empirical observation of a power law wealth distribution in early 20th century Italy follows physics-like analysis [31]. Also in the 20th century, we have seen the emergence of a number of prominent economists with backgrounds in physics, such as Irving Fisher [15] and Nobel Price winner Jan Tinbergen [46], as well as prominent physicists/mathematicians with a strong interest in economics, such as Benoit Mandelbrot [31]. Since the mid-1990s, during which time H.E. Stanley coined the term *econophysics* to describe the study of economics using physics-like analysis, there has been a particular interest in physics from academics studying statistical mechanics [41], which is the branch of physics concerned with applying the laws of statistics to predict the average, macroscopic behavior of a system with a large number of components, given an understanding of the microscopic mechanics governing interactions between the individual system components. Already, one can see an obvious connection to microeconomics, which looks at the behavior of individual households and firms, and macroeconomics, which looks at the behavior of the economy as a whole. Yet, it still seems odd that there is a connection to physics as a natural science. As economics is often quantifiable, one can certainly see the potential advantages of adopting the rigorous, mathematical language used in physics. Then, one might ask, why not simply bypass physics and connect directly to mathematics? For the most part, this is the direction economics has headed, as economics has become substantially more mathematical since the early 20th Century [11]. Nowadays, one can open a textbook on modern economics and see little immediate distinction between it and a textbook in mathematical analysis. Nonetheless, a connection to physics remains, particularly because the idea of falsifying economic models is grounded in science and not mathematics. On one level, we can see this connection in terms of the people that study physics and economics. Both disciplines deal with complex, unsolved problems concerning the nature of the world around us and attempt to develop widely applicable models to explain and predict phenomena. Certainly, one could imagine how this would attract like-minded, analytical academics. The interest of physicists in economics was undoubtable intensified with the explosion of available, high frequency stock market data starting in the 1980s [41].

It is also important to remember that the mathematical development in modern economics is much more recent than it is in physics, as finance did not become at all quantitative until the introduction of mean-variance analysis by Markowitz in the 1950s [33]. From a practical perspective, it seems logical to attempt to apply to economics some of the already developed tools from physics. Yet, it is an interesting exercise to consider whether or not there is a more fundamental connection between physics and economics. Is it possible that we can use the knowledge of a physical system to inform our understanding an economic analog, rather than considering it merely as a secondary application of the same tools? For example, can we think of the variation in a stock price in the same way we think of the motion of a grain of pollen in water? Or, can we think of people in the same way we think of particles?

Of course, the obvious objection to this last application is the that unlike particles, we generally consider people to have some form of free will. At this point, this discussion is already exceeding the philosophical scope of this thesis. However, we will offer the following answer to this question: while it is possible that individual people are far too unpredictable to be understood with the same intellectual framework, it is still a worthwhile study, since without some universal properties governing human behavior, the discipline of economics seems hopeless. Moreover, in aggregate, there are certainly commonalities and trends in human behavior. This search for universal properties is really at the heart of physics as well, and it perhaps in is in this respect that the connection between physics and economics is most clear. It is necessary, where an analogy between physical and economic systems is proposed, to scrutinize it as carefully as possible from both sides. The purpose of the present thesis is to examine, from the physics perspective, the stock market—phase transition analogue.

In this chapter we outline a few of the results and tools from econophysics. Although the results of this thesis center on stock market crashes as critical phenomena, we will briefly discuss a few other results in econophysics in an effort to stress the underlying physical analogy, if one exists. We will also try to point out when these analogies fail. Of course, there are plenty of results we will not have time to introduce. For a more thorough review of econophysics and the statistical properties of financial time series, see [44, 32, 8, 27].

2.1 Distribution of Price Variation

An important question in finance is the distribution of the log returns $G(t)$, defined as

$$G(t) = \ln Z(t + \Delta t) - \ln Z(t), \tag{2.1}$$

where $Z(t)$ is a stock price at time t [1]. Although answering this question is not a goal of this thesis, the connection to diffusive processes, as we will see, is illustrative of the connection between physics and economics. This discussion will also illustrate how the connection can fail.

The classical assumption in financial theory is that $G(t)$ follows follows a *Wiener process* W_t, which is a continuous time stochastic process satisfying the following three properties:

1. $W_0 = 0$.
2. The function $t \mapsto W_t$ is almost surely everywhere continuous.
3. For all times t and s, where $0 \leq s < t$, $W_t - W_s$ is normally distributed with zero mean and variance $t - s$.

A Wiener process is a mathematical description of *Brownian motion*, which models the effectively random motion of particles suspended in fluid as they are repeatedly bombarded by smaller atoms of molecules of the fluid. The term derives from the botanist Robert Brown who, in 1827, observed such random behavior in the motion of grains of pollen in water [40]. In 1905, Albert Einstein showed precisely that the grains of pollen were being moved by water molecules, thus confirming the existence of atoms and molecules [10].

Remarkably, the proposition that stock market returns follow a Wiener process (although this term did not yet exist) was made by Louis Bachelor in 1900 [2], five years prior to Einstein's paper, although the theory did not become popular until the 1950s [31]. This is a rare case in which the application to economics predated the application to physics.

On the surface, the analogy between stock prices and grains of pollen in water seems to make sense. A stock price is continually bombarded with news and other unpredictable information in such a way that its returns are, on average, nearly zero. Unfortunately, with stocks we cannot use the physical space and known mechanics to derive a

[1] Note that we may consider $G(t)$ as a finite, discrete time series $\{G_t\}_{t=1}^{N}$. In the above notation, $G : \mathbb{N} \to \mathbb{R}$ is a function.

precise description of their motion, as Einstein did with grains of pollen. Thus, we should be exceedingly cautious in using this description of stock price variation. But not only does a description according to Brownian motion lack a sound theoretical background, it seems to be contrary to empirical evidence, as Mandelbrot first pointed out in 1963 [30], suggesting that we should reject this description. This, however, has not been the case in standard financial theory. The popular Black-Scholes model and, in particular, the Nobel prize-winning Black-Scholes equation, which gives a pricing formula for options, assumes stock prices follow Brownian motion[2] [5].

2.2 Correlation

In section 3.2 on critical phenomena we will see how, in a system exhibiting a phase transition, correlations increase as the system approaches the transition. In this section we will discuss the known statistical properties of stock market correlation.

2.2.1 Intraday Patterns

It is well documented that intraday patterns exist in the volatility of the returns [47, 3]. In order to adjust for intraday patterns we will follow the procedure of [27]. We start by letting t_{day} index the 390 daily trading minutes of a trading day. We then write $G^k(t_{day})$ as the log return on day k at local time t_{day} (so that $G(t) = G(390(k-1) + t_{day})$). Next, we define $A(t_{day})$ as the average log return at time t_{day} over each of the N days in the sample:

$$A(t_{day}) \equiv \frac{\sum_{k=1}^{N} \left|G^k(t_{day})\right|}{N}. \tag{2.2}$$

We then adjust $G(t)$ for intraday patterns by dividing it by $A(t_{day})$:

$$g(t) \equiv \frac{G^k(t_{day})}{A(t_{day})}, \tag{2.3}$$

where we are mapping $t \to (k, t_{day})$ so that $G(t) = G^k(t_{day})$. In words, $g(t)$ is the log return at time t divided by the average absolute value of the log return at that time during the day over each day in the sample.

2.2.2 Autocorrelation

The autocorrelation function $C(\tau)$ of the sequence $y(t)$, where $t = 1, ..., N$, can be written as

$$C(\tau) = \frac{\langle y(t)\, y(t+\tau)\rangle - \langle y(t)\rangle^2}{\langle y^2(t)\rangle - \langle y(t)\rangle^2}. \tag{2.4}$$

It is well established that the autocorrelation of the log returns decays rapidly to zero within a few trading minutes and for $\tau \geq 15$ minutes it may be assumed to be zero for all practical purposes [9]. Eugene Fama has cited this as support for the Efficient Market Hypothesis [12].

However, the same is not true of the autocorrelation of the absolute value of the log returns, which are a measure of volatility. Figure 2.1 shows both the autocorrelation of $g(t)$ and the autocorrelation of $|g(t)|$ (at a resolution of $\Delta t = 1$ minute) for the S&P 500 during the years 1984-1996 [27]. Recall from section 2.2.1 above that $g(t)$ is the log return after intraday adjustment. On the left we see that the autocorrelation of the log returns decays exponentially to near zero in about 20 trading minutes. Specifically, during this decay, $C(\tau) \sim e^{-\tau/T}$ with $T \approx 4.0$ minutes. However, on the right we see power law behavior in the autocorrelation function of $|g(t)|$: $C(\tau) \sim \tau^{-\gamma}$

[2] Actually, the model assumes stock prices follow *geometric* Brownian motion with constant drift and volatility, which is slightly more general.

with $\gamma = 3.0 \pm 0.08$.[3] This power law behavior exists for more than three decades. Note that the horizontal line indicates the white noise level.

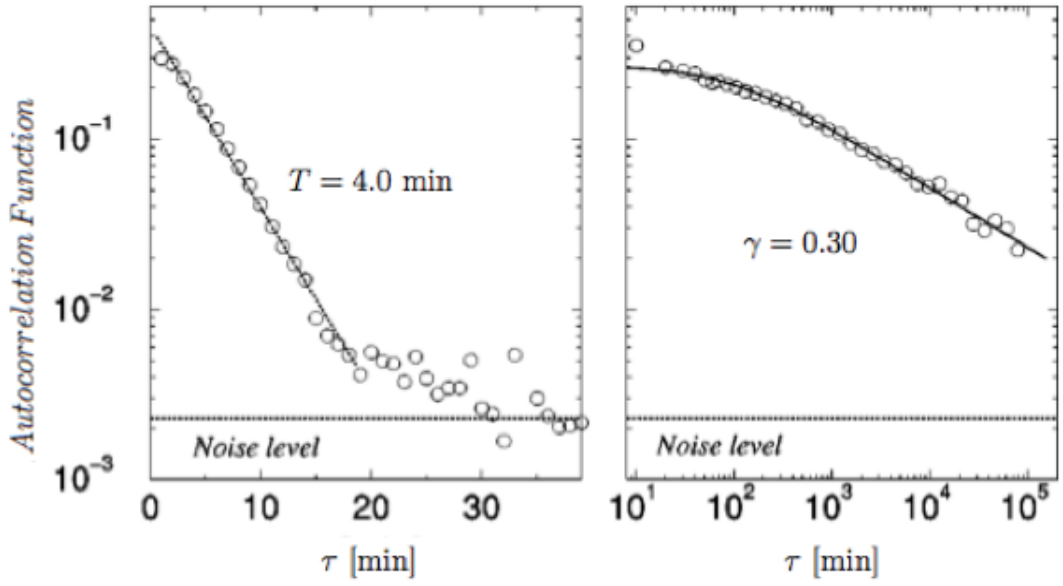

Figure 2.1: Left: Autocorrelation of $g(t)$. Right: Autocorrelation of $|g(t)|$ (reproduced from [27]).

2.2.3 Long Range Autocorrelation

To investigate the long range autocorrelation we will briefly discuss rescaled range (R/S) analysis, which is a method of estimating the Hurst exponent, a number that characterizes the long-term correlations of a time series. A similar method that is slightly more appropriate for financial time series - as it may be applied to non-stationary processes - is detrended fluctuation analysis (DFA) (for a nice discussion see [25]). We will stick with RS analysis as it is has a nice physical motivation (although DFA was originally developed to investigate the long-range power-law correlations of DNA sequences [38]).

2.2.3.1 Rescaled Range Analysis (R/S)

The following method was developed by Harold E. Hurst during his lifetime study of water storage problems related to the Nile river. By observing annual water influx from a lake, his goal was to determine the ideal volume of a reservoir such that a regulated amount of water - equal to the average influx - could be extracted each year without depleting the reservoir [13]. Rather than taking our signal as the water influx, we will use the adjusted log returns, $g(t)$. The analogue of the extracted volume of water will then be the mean of $g(t)$ over the first τ observations. Define $\langle g \rangle_\tau \equiv \frac{1}{\tau} \sum_{t=1}^{\tau} g(t)$ as this mean. We then define $X(t, \tau)$ as the accumulated departure of the signal at time t from $\langle g \rangle_\tau$:

$$X(t, \tau) = \sum_{k=1}^{t} \left(g(k) - \langle g \rangle_\tau \right). \tag{2.5}$$

In Hurst's original formulation, $X(t, \tau)$ represents the amount of water left in the reservoir at time t. As an ideal reservoir is one that never overflows or empties, the quantity of interest to Hurst was the range $R(\tau)$ of $X(t, \tau)$. That is, the difference between the largest accumulated departure and the smallest accumulated departure over the the first τ observations:

[3] Note that we are abusing notation slightly by letting $C(t)$ denote the autocorrelation of both $g(t)$ and $|g(t)|$.

$$R(\tau) = \max_{1 \le t \le \tau} X(t,\tau) - \min_{1 \le t \le \tau} X(t,\tau). \tag{2.6}$$

Notice this quantity depends on the dimensions of the signal. In order to apply this methodology to various phenomena, the range is standardized by dividing it by the (biased) sample standard deviation of the signal over the first τ observations, $S(\tau) = \sqrt{\frac{1}{\tau}\sum_{k=1}^{\tau}\left[g(k) - \langle g \rangle_\tau\right]^2}$. Since $R(\tau)$ and $S(\tau)$ are calculated over τ observations only, we partition the sample into periods of length τ and define the rescaled range as the average ratio of $R(\tau)$ to $S(\tau)$ over each of those periods. We denote this quantity by $(R/S)_\tau$.

We then ask, what is the asymptotic behavior of $(R/S)_\tau$ with respect to τ? The quantity of interest is the Hurst exponent, which comes from the scaling relation $(R/S)_\tau \sim C\tau^H$, where C is a constant. For a statistically independent process with finite variance, H should equal $1/2$. The converse of this statement is not quite true. If $H > 1/2$, the process is positively correlated at all lags, while if $H < 1/2$ the process is negatively correlated at all lags [25].

2.3 Hydrodynamic Turbulence Models

Another physical analogy of economic phenomena is that of price changes as hydrodynamic cascade processes (see [34, 16], for example). More precisely, the analogy is between, on one hand, the probability density function of price changes and the time scale Δt over which these price changes occur, and, on the other hand, the probability density function of the velocity of a fluid at points in space and the physical separation between these points. Analogous to the energy cascade in hydrodynamic turbulence is the information cascade from long-term to short-term investors.

A interesting paper by Kiyono et al. [24] casts doubt on this analogy by showing the existence of scale invariant behavior in the S&P 500 index during the 1987 market crash. This behavior cannot be accounted for by a hydrodynamic cascade process. It does, however, provide evidence that the 1987 crash may be thought of as a phase transition. In the paper, they assume that the inflation detrended returns $\Delta_s Z(t)$ at scale parameter s follow a random multiplicative form given by

$$\Delta_s Z(t) = \xi_s(t)\, e^{\omega_s(t)}, \tag{2.7}$$

where ξ_s and ω_s are Gaussian distributed random variables with mean zero and variance σ_s^2 and λ_s^2, respectively. For a more precise description of the how these returns are detrended for inflation, see section 5.2.2.6. It can be shown that the probability density function of these returns is given by *Castaing's equation*

$$P_s(\Delta_s Z) = \int F_s\left(\frac{\Delta_s Z}{\sigma}\right)\frac{1}{\sigma} G_s(\ln\sigma)\, d(\ln\sigma), \tag{2.8}$$

where $F_s(\xi_s)$ and $G_s(\omega_s)$ and both Gaussian distributions with mean zero and variance σ_s^2 and λ_s^2, respectively. λ_s^2 is a measure of the non-Gaussian nature of the returns and will cause Castaing's equation to converge to a Gaussian as $\lambda \to 0$. Castaing's equation may be used to describe hydrodynamic turbulence [7] as well as heartbeat interval fluctuations [23].

Figure 2.2 shows both the temporal and scale dependence of λ_s^2. For a given s, the detrended log returns $\Delta_s Z$ are partitioned into overlapping intervals of about two month's worth of data and each interval is offset by about 5 days. The horizontal axis T gives the midpoint of the interval. The value $T = 0$ corresponds to the 1987 crash and the region C corresponds to the set of intervals that include data from the 1987 crash. In the results section of this thesis we will calculate this same figure for other crashes.

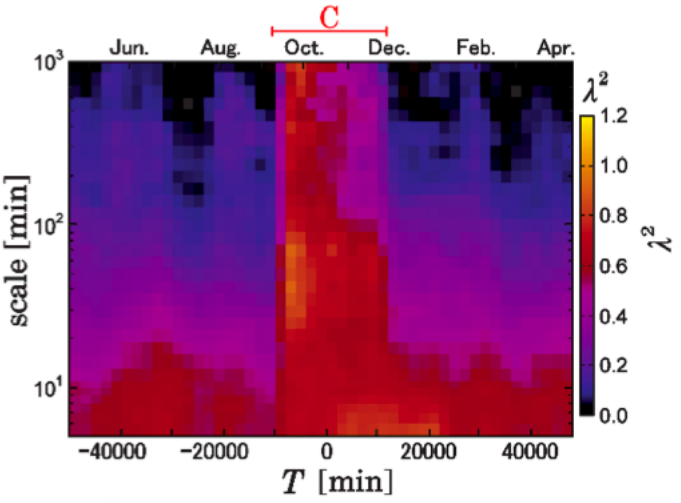

Figure 2.2: Plot of λ_s^2 near the 1987 crash (reproduced from [24]).

Chapter 3

Statistical Mechanics

The area of physics most connected to economics is statistical mechanics. In this chapter we will discuss the perspective of statistical mechanics, the theory of Monte Carlo simulations in statistical mechanics, the theory of critical phenomena, and the Ising model, including Monte Carlo simulations of the Ising model.

3.1 Basic Concepts

3.1.1 Microstates and Macrostates.

Consider a one liter box containing oxygen gas at standard temperature and pressure. This box will contain about 3×10^{23} oxygen molecules. Although the mechanics of this system are simple and well understood, the sheer number of particles makes resolving the motion of each particle prohibitively difficult. Yet, despite this computational barrier, many questions about this system are quite simple to answer. At high temperature and low pressure, the ideal gas law effectively relates pressure, volume, temperature, and the number of particles in the system. This law was originally stated nearly 200 years ago as a combination of Boyle's law and Charles' law, both of which were derived from empirical observations. How is it possible that such an important result could be derived with such simple methods when the number of interacting system components is so large? Bridging the gap between a system consisting of a large number of components and the behavior of the system from a broader, macroscopic perspective, is the task of statistical mechanics. Indeed, a description of the subject can be derived from the two words in its title: mechanics and statistics. We begin with a knowledge of the mechanics of the interactions between the system components and we use the laws of statistics to estimate how the system will behave on a larger scale.

We will call the exact configuration of the system components (particles, for example) and this large-scale condition of the system the *microscopic* and *macroscopic* states, respectively. Notice the microstate contains all of the information about the state of the system. If we were to change anything about the system (for example, the position of a single particle) then we would change the microstate. A macrostate is a complete collection of macroscopic variables, each of which is an average over microstates. Specifically, let Q be a quantity that takes the value Q_μ in microstate $\mu \in M$, where M is the collection of all possible microstates. We define the macroscopic variable $\langle Q \rangle$ at time t as the expectation of Q over each of the microstates. That is,

$$\langle Q \rangle = \sum_{\mu \in M} Q_\mu w_\mu (t) \tag{3.1}$$

where $w_\mu (t)$ is the probability of being in state μ at time t. Later we will show how we can also think of this as a time average, but for now we will stick with this definition. As is common in textbooks, we will often abuse notation and write Q in reference to the macroscopic variable $\langle Q \rangle$. Note that although much of the macroscopic

behavior of a system may be understood by classical equilibrium thermodynamics, which does not consider the microscopic interactions, there are many quantities which thermodynamics cannot describe (for example, fluctuations in macroscopic variables). The results of thermodynamics may be derived from statistical mechanics.

Notice how we allowed the probability of being in a state to depend on time. We define a system to be in equilibrium when this is no longer the case. That is, when $w_\mu(t) = p_\mu$ for all microstates μ, where p_μ is a constant. In order to calculate a macroscopic variable in equilibrium, we will need to say something about these equilibrium probabilities, p_μ. To answer this question we must first introduce the concept of a statistical ensemble.

3.1.2 Statistical Ensembles

Central to this thesis will be the introduction of the Ising model, and the Monte Carlo simulations of its evolution. In order to develop an algorithm to govern these simulations (the Metropolis algorithm, as we will see in section 3.1.4) we will need to understand the equilibrium probability distribution of states, p_μ. To do this we will introduce the concept of a *statistical ensemble*, which is a collection of mental copies of a system, each in a different microscopic configuration, but satisfying the same prescribed set of macroscopic constraints. For a more complete description we refer the reader to [20, 42].

We can think of an ensemble as a region in the *phase space*, which is the space of all possible states of the system. Classically, each microscopic configuration corresponds to a point in the $6N$ dimension phase space of position and momentum (three dimensions for each position vector and three dimensions for each momentum vector). In this case, the distribution of these points, which we characterize by a density function, represents the ensemble.

In general, we derive statistical properties of the system by prescribing a probability measure to the phase space. Such a prescription of the probability measure relies on the postulate that in thermal equilibrium, an isolated system does not have a preference for any of its available microstates. That is, they are all equally probable. We call this the fundamental postulate of statistical mechanics (or, the equal *a priori* probability postulate). In a classical system, the probability measure follows from Liouville's theorem, which implies that that the distribution of points in the phase space evolves like an incompressible fluid. In other words, the density representing the ensemble is constant in time.

We will now consider the micro canonical, canonical, and grand canonical ensembles, as these are the most important ensembles in statistical mechanics. The *microcanonical ensemble* applies to any system with a fixed number of components N (usually particles), a fixed volume V, and a fixed energy E. By fixed energy we mean that $E \in [E - \Delta, E + \Delta]$, where Δ is a number and $E \ll \Delta$. These are the macroscopic constraints. Each member of the ensemble is then a copy of the system, with the same N, V, and E, but with a different microscopic configuration.

Notice that fixed N, V, and E imply an isolated system. This means that the probability measure follows directly from the fundamental postulate. Thus, for all microstates μ, we write the probability of observing the system in this microstate as $p_\mu = 1/\Omega$, where $\Omega = \Omega(N, V, E)$ functions as a normalization constant. Formally, Ω equals the volume occupied by the ensemble in the phase space. If the phase space is discrete and the number of microscopic configurations corresponding to the prescribed N, V, and E is finite, then Ω equals this number of configurations (since we would take the volume integral with respect to the counting measure).

In the *canonical ensemble* we replace the assumption of fixed energy with the assumption of fixed temperature. Specifically, each member of the ensemble is the system taken together with a reservoir. The system and the reservoir are assumed to be in thermal contact and together they are assumed to be isolated from the surroundings. We still require that the number of particles and the volume of the system are fixed; however, we allow the system to exchange energy with the reservoir in such a way that the temperature remains fixed. This can be achieved by assuming the heat capacity of the reservoir to be so large that any heat flow to or from the system has a negligible effect on the temperature of the reservoir. In summary, the macroscopic constraints are fixed N, V, and T. Since

the energy of the system is no longer fixed, the system is no longer isolated from the surroundings and so the probabilities will no longer be constant. However, the composite of the system and the reservoir *is* isolated from the surroundings. Thus, we may apply the fundamental postulate to this composite system. It is a fundamentally important result in statistical mechanics that for a system in the canonical ensemble, the probability of being in a state μ is proportional to the Boltzmann factor, $e^{-\beta E_\mu}$, where $\beta = 1/kT$. To normalize the probabilities, we divide each by the constant Z, called the partition function, where

$$Z = \sum_\mu e^{-\beta E_\mu}. \tag{3.2}$$

The probabilities are then

$$p_\mu = \frac{1}{Z} e^{-\beta E_\mu}. \tag{3.3}$$

One can derive this result with the method of most probable distribution, or the method of steepest descents, for example. A simple derivation writes the a ratio of probabilities as a ratio of the number of configurations of the reservoir, $\Omega(N, V, E)$, and connects these configurations to energies of the states using the thermodynamic identity. The exponential term comes from the definition of entropy as $S = k \log \Omega$. As a full derivation can be readily found in any statistical mechanics textbook, we will not say any more about the derivation here. Finally, notice that in the canonical ensemble, equation 3.1 becomes

$$\langle Q \rangle = \frac{1}{Z} \sum_\mu Q_\mu e^{-\beta E_\mu}. \tag{3.4}$$

The Ising model (which we will introduce in section 3.3) falls under the umbrella of the canonical ensemble and for this reason we will limit the remaining discussion of statistical ensembles. However, we will quickly note that when we replace the assumption of fixed N with the assumption of fixed chemical potential, we are led to the *grand canonical ensemble*. The construction is the same as the canonical ensemble, except that we allow each system to exchange particles with the reservoir. Certainly, in an experimental setting this is an attractive idea, since it seems unreasonable to expect knowledge of the exact number of particles in the system (of course, the same argument can be made with respect to energy in favor of the canonical ensemble over the microcanonical ensemble). Analogous to the volume of the phase space Ω in the microcanonical ensemble, and the partition function Z in the canonical ensemble, is the grand partition function $\mathcal{Z}$ in the grand canonical ensemble. This grand partition function can be written as a weighted sum of the canonical partition functions, each corresponding to a different number of particles. We may think of the grand canonical ensemble as a distribution over canonical ensembles.

3.1.3 Partition Function

Recall the result from the previous section, that for a system described by the canonical ensemble, the probability of observing the system in a particular microstate is proportional to the Boltzmann factor (equation 3.3). We called the constant of proportionality Z the partition function. It is important to briefly discuss this function as we will need it to derive the formula for the internal energy and magnetization of the Ising model.

The partition function encodes much of the information about how probabilities are partitioned amongst the microstates. It is really at the heart of statistical mechanics because although its calculation depends entirely on the microscopic configuration of the system, many macroscopic variables may be extracted from it through simple algebraic manipulations. For example, using equation 3.1 and our definition of the equilibrium probabilities p_μ we have

$$U \equiv \langle E \rangle = \sum_{\mu} E_\mu p_\mu = \frac{1}{Z} \sum_{\mu} E_\mu e^{-\beta E_\mu} = -\frac{1}{Z} \sum_{\mu} \frac{\partial}{\partial \beta} e^{-\beta E_\mu} = -\frac{1}{Z} \frac{\partial}{\partial \beta} \sum_{\mu} e^{-\beta E_\mu} = -\frac{1}{Z} \frac{\partial Z}{\partial \beta}. \tag{3.5}$$

Therefore,

$$\langle E \rangle = -\frac{\partial \log Z}{\partial \beta}. \tag{3.6}$$

In a similar manner, one may show that the Helmholtz free energy F, given by $F \equiv U - TS$, where S is the entropy, may be written as

$$F = -\frac{1}{\beta} \log Z. \tag{3.7}$$

One can likely see from the previous two equations how macroscopic variables may be expressed as derivatives of the free energy (which we write without the $\langle \cdot \rangle$ notation as this is the way it is usually written). Unfortunately, the large number of microstates makes the computation of the partition function quite difficult, except in special cases.

3.1.4 Introduction to Monte Carlo Methods and the Metropolis Algorithm

Recall our definition of a macroscopic variable as a weighted average of a particular quantity over the available microstates of the system (equation 3.1), where the weights were shown to be determined by a normalized Boltzmann factor. Unfortunately, we have seen that the sheer number of available microstates makes this average exceedingly difficult to compute. Luckily, as we will now show, we can also think of a macroscopic variable as an average over *time*. This is the key insight that allows the use Monte Carlo methods, which will later be used to simulate the Ising model in a several dimensions. As we will use the correlation data from these simulations to provide insight into the spatial structure of the stock market, the discussion of Monte Carlo methods is important to this thesis. This discussion of Monte Carlo methods will follow [35] and this text is highly recommend to anyone interested in a more detailed treatment.

Consider first the following question: is it possible to choose a finite sequence of states $\mu_1, ..., \mu_n$ such that the arithmetic mean of the macroscopic variable Q over these states gives a good estimate of the actual expectation value, defined by equation 3.1? Loosely speaking, to do this we would need some assurance that this finite sequence of states is in some way representative of the full set of available states. On the surface, this might seem like a difficult problem. For example, a good computer will be able to sample about 10^8 states in a few hours [35], while the Ising model - one of the simplest models in statistical mechanics - on, say, a $10 \times 10 \times 10$ lattice will have $2^{10 \times 10 \times 10} \sim 10^{301}$ possible states. However, we should be encouraged by the following fact: a system with a large number of components spends the vast majority of its time in a very small number of states.

Consider for a moment a real system consisting of a box of particles that is in thermal contact with a reservoir. Suppose that the system and the reservoir are allowed to exchange energy but not particles. In other words, this system falls into the canonical ensemble. In equilibrium, the system and the reservoir will have the same temperature. However, the energy will fluctuate in time. To estimate a macroscopic quantity (like the energy) we may average the value of this quantity over time.

In a Monte Carlo simulation *we do essentially this*, except we map our system onto a computer. In both cases we choose some initial state and watch the system evolve. The longer we wait, the more accurate our estimates become. Of course, on a computer, we measure time in terms of iterations of our Monte Carlo algorithm (this idea will be refined later). The main difference is that on a computer we must completely specify the system by a model, which inevitably introduces some degree of simplification. Our task is then to specify the time evolution of this

model in such a way that once the model system reaches equilibrium, states will appear with probability according to the Boltzmann distribution.

To do this, most Monte Carlo simulations define a stochastic time evolution according to a *Markov process*, which is a type of stochastic process in which the probability of transition between a state μ and a state ν depends only on the states μ and ν, and not on any of the previous states. We will denote this transition probability by $P(\mu \to \nu)$. For a Markov process to generate a sequence of states according the the Boltzmann distribution, two conditions must be satisfied.

The first condition is that of detailed balance. Using our notation from earlier sections, we will let $w_\mu(t)$ denote the probability of being in state μ at time t. Therefore, $w_\mu(t) P(\mu \to \nu)$ is the rate at which the system transitions out of the state μ and into the state ν, while $w_\nu(t) P(\nu \to \mu)$ is the at which the system transitions into the state μ from the state ν. The state probabilities $w_\mu(t)$ then evolve according to the master equation

$$w_\mu(t+1) - w_\mu(t) = \sum_\nu \left[w_\nu(t) P(\nu \to \mu) - w_\mu(t) P(\mu \to \nu) \right] \tag{3.8}$$

Recall that we defined a system to be in equilibrium when $w_\mu(t)$ no longer depends on time, for all states μ. We wrote these equilibrium state probabilities as p_μ. Thus, in equilibrium, the master equation becomes

$$\sum_\nu p_\mu P(\mu \to \nu) = \sum_\nu p_\nu P(\nu \to \mu). \tag{3.9}$$

In order to rule out the possibility of limit cycles in our Markov process, we must further assume that these sums agree term-wise. That is, for all μ,

$$p_\mu P(\mu \to \nu) = p_\nu P(\nu \to \mu). \tag{3.10}$$

This is the condition of *detailed balance*. Since we want $p_\mu = \frac{1}{Z} e^{-E_\mu / kT}$, we can rewrite the condition of detailed balance as

$$\frac{P(\mu \to \nu)}{P(\nu \to \mu)} = \frac{p_\nu}{p_\mu} = e^{-\beta(E_\nu - E_\mu)}. \tag{3.11}$$

The second condition is that each state must be accessible from each other state. This is the condition of *ergodicity*. Note that it is not necessary for the each state to be accessible in a single transition. Indeed, most Monte Carlo methods set the majority of transition probabilities to zero [35]. Rather, it must only be that there is at least one path of non-zero probability between any pair of states. Assuming a valid probability distribution (that is, one that sums to one) if the condition of ergodicity as well as equation 3.11 are satisfied, then the equilibrium distribution will be Boltzmann distribution [35].

At this point we have still not specified a way to construct a Markov process satisfying the conditions above. To change this, we first break the transition probability into a product of two other probabilities:

$$P(\mu \to \nu) = g(\mu \to \nu) A(\mu \to \nu). \tag{3.12}$$

The first term, $g(\mu \to \nu)$, is called the *selection probability* and it gives the probability of selecting a target state ν while the system is in state μ. Once the target state has been selected, the system will actually transition to it with probability $A(\mu \to \nu)$, called the *acceptance probability*. If the system rejects the target state ν it will remain in the current state μ. An ideal algorithm is one in which the selection probabilities are equivalent to the transition probabilities, making the acceptance ratio unity and a good algorithm is one that approximates this as best as possible.

The most widely used algorithm to this problem is Metropolis algorithm. Recall that setting some of the

transition probabilities to zero will not violate the condition of ergodicity, as long as there is at least one path of non-zero probability between each pair of states. In the so-called single-spin-flip dynamics, we set the transition probability to zero for all states except those differing by a single spin. The Metropolis algorithm then sets the probability of selecting one of these states, $g(\mu \to \nu)$, to be the same number for each pair μ and ν, where μ and ν differ by a single spin. For a system of N spins, this assumption along with the normalization of the probability distribution gives

$$g(\mu \to \nu) = \frac{1}{N}. \tag{3.13}$$

Using equations 3.11 and 3.12 we have

$$\frac{A(\mu \to \nu)}{A(\nu \to \mu)} = e^{-\beta(E_\nu - E_\mu)}. \tag{3.14}$$

Recall that a more efficient algorithm, the acceptance ratios are near unity. One way to exploit this fact is to set the larger acceptance ratio to unity and adjust the other accordingly. We can do this since it is only the ratio of acceptance probabilities that matters. The Metropolis algorithm does exactly this, giving

$$A(\mu \to \nu) = \begin{cases} e^{\beta(E_\nu - E_\mu)} & \text{if } E_\nu - E_\mu > 0 \\ 1 & \text{otherwise} \end{cases}. \tag{3.15}$$

This is equation is the distinguishing feature of the Metropolis algorithm. We will discuss our implementation of the Metropolis algorithm in section 5.3.

3.2 Critical Phenomena

A system may exist in different states - called phases - that are distinguished by their qualitative features, e.g. density, average molecular orientation, magnetization, etc. It is difficult to give a clear definition of a phase as there is no canonical system to consider. The prototypical view of phases in physics is they are distinguished by the symmetries of the system, including translational, rotational and inversion symmetries. A phase transition, generically, is when such a symmetry is broken as some thermodynamic variable is adjusted through a critical value. A central idea in condensed matter physics, known as *universality,* is that the critical properties of a system depend only on the symmetries broken and not on the detailed nature of the interactions. This means that many of the tools from critical phenomena may be adapted to non-physics systems. Indeed, systems with widely different objects of interest and interactions, in disciplines ranging from biology to, as has already been stressed, sociology and economics, have been analyzed under this approach.

In other sections we discuss in detail the validity of the extension of the theory of critical phenomena to non-physics systems. This discussion is, of course, centrally important to this thesis. To this end, it is important to discuss critical phenomena in a purely physics-based context, as this is the field in which the theory of critical phenomena is most properly developed. This section is an attempt at such a discussion. We have chosen to develop these concepts in context, beginning with a simple pressure-temperature phase diagram and ending with an introduction to ferromagnetic systems. We will then settle on a more careful definition of a phase transition in the next section. The discussions on phase diagrams and ferromagnetic systems will follow [43].

3.2.1 Phase Diagrams

Figure 3.1 shows a phase diagram, in pressure-temperature space, of a typical substance. Each point in the diagram corresponds to a particular phase of the substance. The solid curves, called *phase boundaries* (or *coexistence curves*),

represent the boundaries between the different states. If a system crosses a phase boundary, a phase transition will occur. For concreteness, consider a system at (P_1, T_1). If the system were heated at constant pressure until it reached (P_1, T_2), following path 1, the system would transition from a liquid to a gaseous phase. The important fact is that this transition will occur abruptly. More precisely, a parameter that allows us to distinguish between the phases, called an *order parameter*, will change discontinuously (in higher order transitions the order parameter is changes continuously). In our example, the parameter of interest is the difference in the densities between any two states. Now, recall that macroscopic variables may be expressed as derivatives of the free energy. We define the *order* of a phase transition as the lowest order derivative of the free energy that behaves discontinuously at the transition. This is called the *Ehrenfest classification*. Note that higher order phase transitions are often called *continuous phase transitions*. The density may be expressed as a first order derivative of the free energy and for this reason we classify the transition as a first order phase transition.

Now, in principle, a system may trace out any path in the diagram. Since the liquid-gas phase boundary terminates at the so-called critical point, if the system follows path 2, the same initial and final states can be achieved without crossing the liquid-gas phase boundary. This implies a continuous phase transition. The termination of the liquid-gaseous phase boundary – indicated by a red dot in the phase diagram – is an example of a *critical point*. In general, a critical point is the point in the phase space at which a continuous phase transition occurs. As a system approaches a critical point from the high temperature side, the system begins to adjust itself on a microscopic level. Correlations over long distances will begin to occur, signaling the emergence of the order parameter which becomes nonzero upon reaching the critical point. These long-range correlations become the only relevant length scale of the system and dominate over the microscopic physics of the system. Mathematically we say the *correlation length* ξ diverges, where $\xi = \xi_0 \tau^{-\nu}$ and $\tau = (T - T_c)/T$ is the reduced temperature. Rendering the microscopic physics unimportant explains why the divergence in the correlation length is crucial to the understanding of *universality*, which is the term used to describe the remarkable degree of similarity observed near critical points in systems with different physics. Universality includes similarity in the so called *critical exponents*, one of which is given by the parameter ν in the expression for the correlation length. Other critical exponents are β, γ, δ, and α, which correspond to the order parameter, the susceptibility, the critical isotherm, and the specific heat, respectively.

Near a phase transition we also tend to observe a change in the symmetry of the system, a phenomena known as *symmetry breaking*. For example, in the liquid-solid and gas-solid transitions, the translational symmetry of the high temperature phase is broken as the system transitions to the low temperature, solid phase. This is true since in the liquid and gas phases, the average particle density is independent of position and therefore is invariant under translation, while in solid the solid phase the average particle density is periodic and hence not invariant under translation. Mathematically we can think of the transformations describing symmetries as forming a group. We could then say that the liquid and gaseous phases are invariant under the translation group, while the solid is phase is only invariant under a subgroup of the translation group. Notice there is no such symmetry breaking upon crossing the liquid-gas phase boundary. Therefore, a first order phase transition may or may not exhibit a phase transition. Continuous phase transitions, on the other hand, will always exhibit symmetry breaking.

Finally, we also tend to observe *ergodicity breaking*, where the assumption that the system will explore its entire phase space given sufficient time (called the *ergodic hypothesis*) ceases to hold.

The mathematical origin of phase transitions are the branch cuts in the logarithm of the partition function. To see this, recall that macroscopic variables may be expressed as derivatives of the free energy F, which is may be expressed as $F = -(1/\beta) \ln Z$. Branch cuts in $\ln Z$ cause nonanalyticities in F, which cause singular behavior in the derivatives of F. Notice that for a finite system, the partition function is a sum of a finite number of exponential terms and it is thus analytic. Therefore, phase transitions can only occur in systems of infinite system size. The finite size of the system will smooth out any discontinuous changes in macroscopic variables. Finally, we note that a critical point should be an *intensive* property of the system. That is, it should not not depend on the size of the

system.

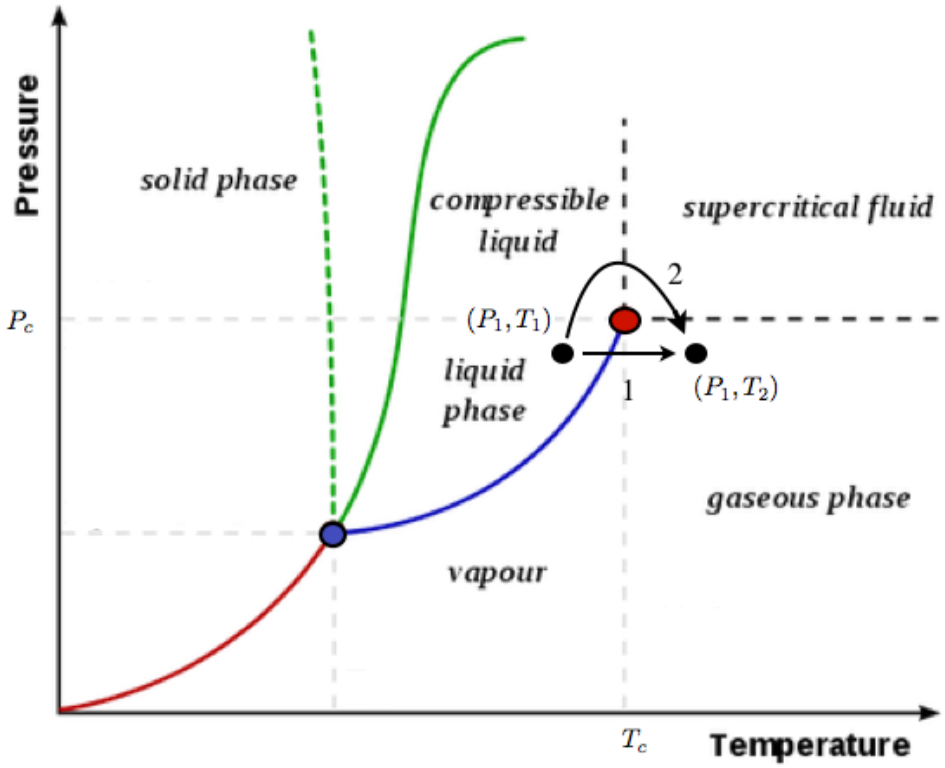

Figure 3.1: Phase diagram in pressure-temperature space of a typical substance.

3.2.2 Ferromagnetic Systems

Ferromagnetism is the phenomena wherein a system forms a permanent magnetic field. We commonly refer to ferromagnetic materials as permanent magnets. Examples include iron, nickel, and cobalt. The exact origins of ferromagnetism are not particularly important to our discussion so we will only give a brief discussion in the next few sentences. Due to the effect of quantum mechanical spin, electrons behave as tiny magnetic dipole moments. Although the dipoles will tend to align in opposite directions, an effect known as the exchange interaction will tend the dipoles towards alignment in the same direction. Magnetism will be observed at a macroscopic level if the system is such that a large number of dipoles align. If the dipoles are not, in general, aligned, and will only align at this temperature in the prosiness of an external magnetic field, the system is in *paramagnetic* state.

Figure 3.2 shows an illustrative phase diagram of a ferromagnetic system. To understand this diagram, first suppose that the system is in zero external magnetic field with a temperature $T > T_c$, so that the system is in a paramagnetic state. As the system is cooled to $T < T_c$ a second order phase transition occurs. During the transition the magnetization jumps spontaneously – but continuously – to some non-zero number (either positive or negative), causing the system to form a ferromagnet, and the magnetic susceptibility, which is a second order derivative of the free energy, to diverge (this is path number 2 in the diagram). The magnetization functions as the order parameter. At the transition we observe a break in the rotational symmetry of the system, as the spontaneous magnetization defines a direction in space, and a break in the ergodic hypothesis, as the system will choose a state of nonzero magnetization, but will not reach a state corresponding to a magnetization of opposite sign in any amount of time. In the ferromagnetic state, a change in the sign of the external magnetic field will cause the magnetization to flip

signs discontinuously, resulting in a first order phase tradition (path 1 in the diagram). Notice that the phase boundary is symmetric about the T axis in the $M - T$ plane. This is because the system is symmetric with respect to a flipping of all spins.

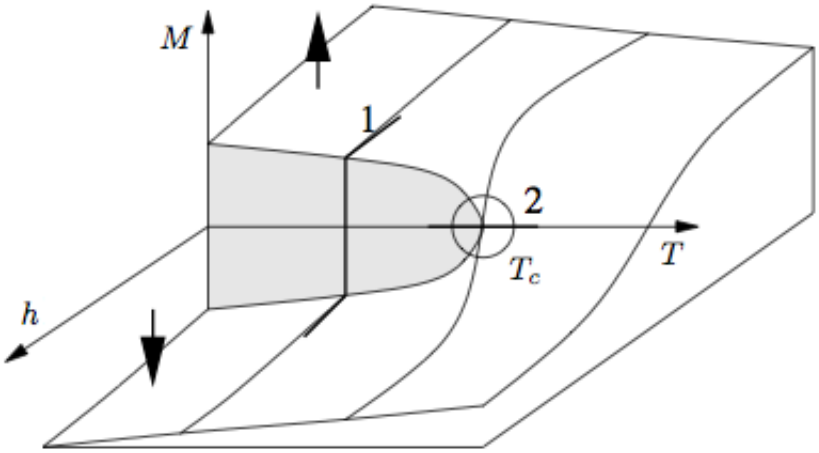

Figure 3.2: Phase diagram in (M, h, T) space of a typical ferromagnetic system.

3.3 Ising Model

A simplified model of ferromagnetic systems is given by the Ising model, which is likely the most widely studied model in all of condensed matter physics. In it, we make three primary assumptions: that the dipoles are arranged on a graph (usually a lattice), that each magnetic dipole can point either parallel or antiparallel along a single axis of magnetization, and that interactions exist only between adjacent dipoles (that is, dipoles connected by a single edge in the graph). We call the two spin orientations "spin up", often denoted by $\uparrow$, and "spin down", often denoted by $\downarrow$. Glauber succinctly describes the motivation for simplified models like the Ising model:

> *"The property most desired in these models is mathematical transparency. The deeper insights offered by the possibility of exact treatment are intended to compensate for any unrealistic simplifications in the formulation* [18]*."*

We would now like to formulate a more precise description of the model. Consider an arbitrary graph Λ. To each vertex i of Λ we associate a number $\sigma_i \in \{-1, +1\}$ called the spin, where $\sigma_i = -1$ indicates the spin down orientation and $\sigma_i = 1$ indicates the spin up orientation of the dipole. We also define the scalar J_{ij} as the interaction strength between spins σ_i and σ_j and we let h_i denote the strength of the external magnetic field acting on spin σ_i. The Hamiltonian of the system is then given by the following equation:

$$H = -\sum_{(i,j)} J_{ij}\sigma_i\sigma_j - \sum_i h_i\sigma_i, \tag{3.16}$$

where the notation (i, j) indicates that the sum is taken over all pairs of spins. However, since the matrix J is symmetric, we will only count each pair once (i.e. will will count (i, j) but not (j, i)). Recall that only adjacent spins are allowed to interact. Therefore, for any non-adjacent spins σ_i and σ_j, we require $J_{ij} = 0$. This means that the first sum is effectively taken over all pairs of adjacent spins. This notation is more generally than simply stating that the sum is taken over all pairs of adjacent spins. However, it does allows us to encode topological information

about the space of spin interaction in the matrix J and for this reason we choose this notation. From now on we will assume that the graph Λ is a hypercubic lattice of arbitrary integer dimension.

As each σ_i represents a magnetic dipole moment, the mean magnetization M is the average spin value:

$$M = \frac{1}{N}\sum_{i=1}^{N}\sigma_i. \tag{3.17}$$

The minus sign on the right-hand side of the Hamiltonian is conventional. It implies that if $J_{ij} > 0\ \forall i, j$, the energy of the system will decrease if any pair of adjacent spins σ_i and σ_j have the same sign (that is, if they are aligned). We call this type of interaction ferromagnetic. On the other hand, if $J_{ij} < 0\ \forall i, j$ the spins will tend to antialign and we call this type of interaction antiferromagnetic. Furthermore, notice that the presence of a positive or negative external magnetic field tends to decrease or increase the energy of the system, respectively.

We can also derive the expression for the mean magnetization in a constant external magnetic field h in terms of the partition function, as we did with the internal energy in section 3.1.3. To do this first notice that we can use equation 3.17 to write the Hamiltonian as

$$H(\sigma) = -\sum J_{ij}\sigma_i\sigma_j - hNM, \tag{3.18}$$

which gives $M = -\frac{1}{N}\frac{\partial H}{\partial h}$. Them, since the Hamiltonian gives the energy of the system, we can use equation3.4 (where the state is now denoted by σ) to write

$$\langle M\rangle = \frac{1}{Z}\sum_{\sigma} M_\sigma e^{-\beta H(\sigma)} = \frac{1}{Z}\sum_{\sigma}\frac{1}{N}\left(\frac{\partial H(\sigma)}{\partial h}\right)e^{-\beta H(\sigma)} = \frac{1}{NZ}\sum_{\sigma}\frac{1}{\beta}\frac{\partial}{\partial h}e^{-\beta H(\sigma)} = \frac{1}{N\beta}\left(\frac{1}{Z}\frac{\partial}{\partial h}\sum_{\sigma}e^{-\beta H(\sigma)}\right). \tag{3.19}$$

Therefore, using the definition of the partition function we have

$$\langle M\rangle = -\frac{1}{N\beta}\frac{\partial \log Z}{\partial h}. \tag{3.20}$$

This is the mean magnetization. We will use this result in chapter 7 when we introduce a 0D Ising model.

3.3.1 Ising Model by Dimension

We will now demonstrate how the behavior of the Ising model depends very much on the dimension of the lattice. This is a remarkable result, as it demonstrates how systems with equivalent physics but different physical spaces can have dramatically different behavior. *It is this fact that has been previously neglected in the proposed analogy between stock market crashes and phase transitions, and the elucidation of this point is the central result of this thesis.* Specifically, it has been shown analytically that a 2D Ising model will exhibit a phase transition at a finite, positive temperature, while a 1D model will not. Due to the prominence of this result to the present thesis, we discuss separately the behavior of the Ising model in low dimensions. Attention will be paid to the adjacency matrix of the lattice in anticipation of the correlation matrix of spins during a Monte Carlo simulation, shown in section 3.3.3.

3.3.1.1 1D

In the 1D Ising model, the N spins are arranged in a line. Each spin interacts with the spin to its left and the spin to its right. Usually, periodic boundary conditions are imposed by allowing the $1st$ andNth spins to interact. This model was first solved analytically by Ising himself in his 1924 thesis [21] when he found the following expression for the free energy per spin (this form of the equation is reproduced from [19]):

$$\frac{F}{N} = -J - \frac{1}{\beta} \ln \left(\cosh(\beta h) + \sqrt{\sinh^2(\beta h) + e^{-4\beta J}} \right). \tag{3.21}$$

Figure 3.3 shows a plot of this equation in as a function of T and h, where we let $k = J = 1$. Notice that for any fixed h, the free energy is a smooth function of T, suggesting that there is no singular behavior in the derivatives of the free energy and hence no phase transition.

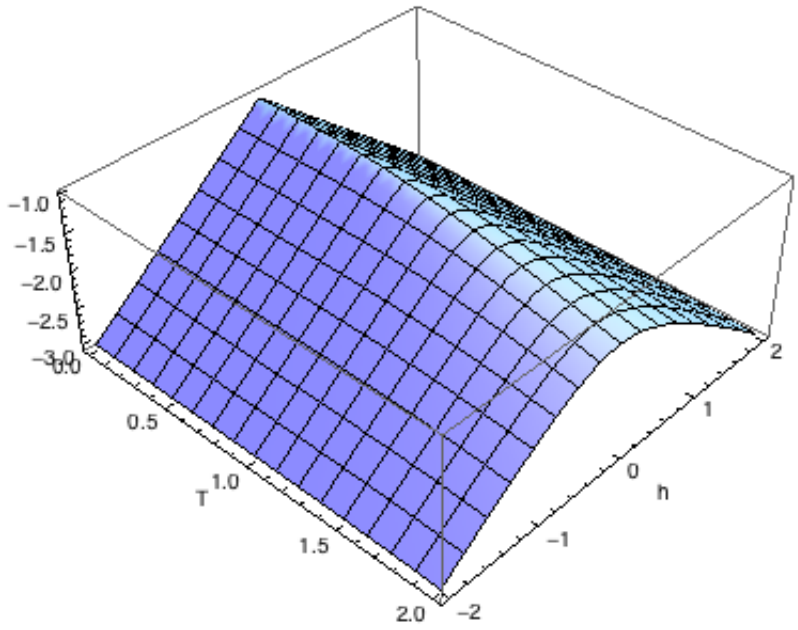

Figure 3.3: Plot of the free energy as a function of the temperature T and external magnetic field h assuming $k = J = 1$ according to Ising's exact solution of the 1D Ising model.

From this expression for the free energy the magnetization follows immediately (see [19] for details):

$$M = -\frac{1}{V}\frac{\partial F}{\partial h} = \frac{\frac{N}{V}\sinh(\beta h)}{\sqrt{\sinh^2(\beta h) + e^{-4\beta J}}} \tag{3.22}$$

Notice that in zero external magnetic field, the magnetization is zero for all T. This shows that there is no phase transition in a 1D Ising model.

To illustrate the topology of spin interaction, we will introduce the adjacency matrix of a lattice. If we assume that the interaction strength between interacting spins is always 1, then the adjacency matrix of the lattice is equivalent to the interaction strength matrix J introduced in the definition of the Ising model. Therefore, J_{ij} will take the value 1 if spins σ_i and σ_j can interact and 0 if they cannot. Figure 3.4 shows the adjacency matrix of a 1D lattice of size $N = 25$. Notice that the matrix is symmetric, as each of the interactions is mutual. The two nonzero entries off the the diagonal indicate that any spin σ_i not on the boundary is related to spins σ_{i-1} and σ_{i+1}. The fact that $J_{1,25} = J_{25,1} = 1$ indicates the imposed periodic boundary condition. The diagonal itself is zero as the spins do not interact with themselves. Finally, notice that we can easily compute the number of nearest neighbors of spin σ_i by summing along either row or column i (the result will be the same as the matrix is symmetric).

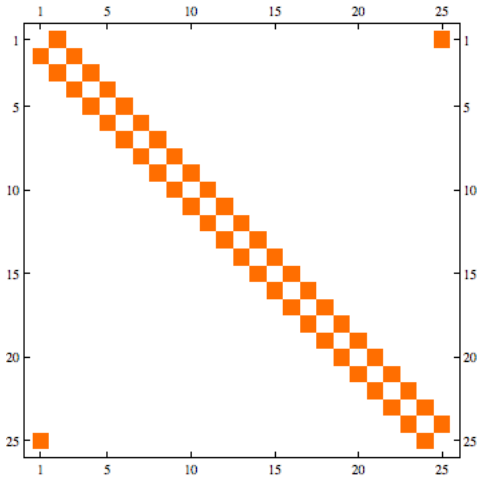

Figure 3.4: Adjacency Matrix of a 1D Lattice.

3.3.1.2 2D

The 2D Ising model in zero magnetic field was first solved by Onsager in 1944 [37]. In particular, he found the following analytical expression for the spontaneous magnetization for $T < T_c$ (this form of the equation is reproduced from [19]):

$$M = \frac{1}{2}\left[1 - \sinh^{-4}\left(2\beta J\right)\right]^{1/8}, \tag{3.23}$$

where

$$T_c = \frac{2J}{k\log\left(1+\sqrt{2}\right)} \tag{3.24}$$

is the critical temperature at which the system exhibits a phase transition. For $T > T_c$ the magnetization is zero. Note that in the limit $T \to T_c$, one can show that

$$M = 1.224\left(\frac{T_c - T}{T_c}\right)^{1/8} \tag{3.25}$$

Therefore, the critical exponent is $1/8$.

To illustrate the topology of the 2D Ising model we once again analyze the adjacency matrix of the lattice. To do this we must map each index pair (i, j) to a single index. We do this by counting down columns. That is, for a 2D square lattice of N spins, $(i, j) \mapsto i + N^{1/2}\left(j - 1\right)$. Since this is a square lattice, $N^{1/2}$ is the number of spins along each row or column of the lattice.

We will also impose toroidal boundary conditions, as illustrated in Figure 3.5. The dashed lines show how spins on the top and bottom rows interact, while the dotted lines show how spins on the left-most and right-most columns interact. Note that to avoid too much clutter in the figure, the interactions between the spins at the corners of the lattice are omitted. For example, the spins at the top-left and top-right corners should interact.

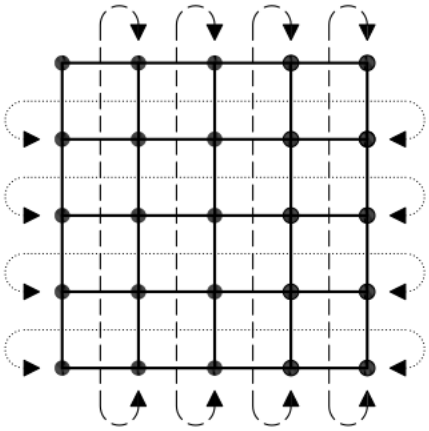

Figure 3.5: Illustration of toroidal boundary conditions on a 2D lattice.

To see why we describe these boundary conditions as toroidal we note that the adjacency graph of a 2D lattice with these boundary conditions (figure 3.6) has a toroidal structure.

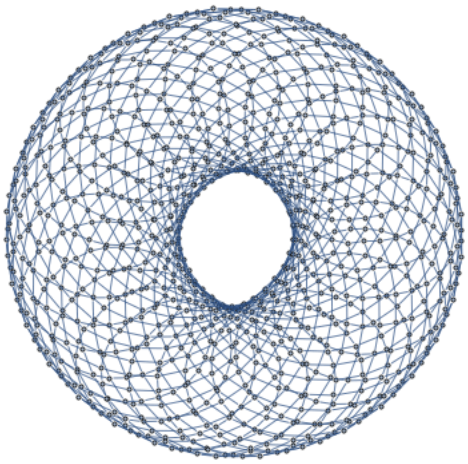

Figure 3.6: Adjacency graph of a 2D lattice with toroidal boundary conditions for a system of $N = 1000$ spins.

Now that we have an understanding of the boundary conditions we can show that associated adjacency matrix. Figure 3.7 depicts such a matrix for system of $N = 25$ spins. The four diagonal bands represent the four nearest neighbors. Since we map the index pair (i, j) in the lattice to a single index in the correlation matrix by counting down rows, the two interior bands represent the nearest neighbors that are above and below a given spin. The two exterior bands represent the nearest neighbors separated to the left and right of a given spin, since they will be mapped to single indices that are 5 less and 5 more than a given spin, respectively. In general, the exterior bands will be separated from the diagonal by $N^{1/2}$ matrix elements, where, once again, $N^{1/2}$ is the number of spins along each row or column of the square lattice.

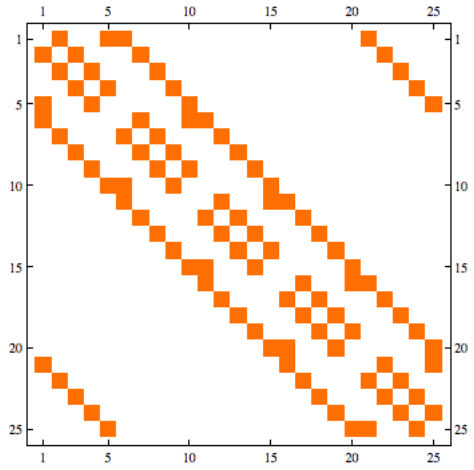

Figure 3.7: Adjacency matrix of a 2D lattice.

3.3.1.3 Higher Dimensions

The Ising model in all dimensions higher than 2 exhibits a phase transition, although the critical exponents differ. There is no existing analytical solution to the 3D Ising model, which remains, famously, one of the great unsolved theoretical problems in condensed matter physics. In dimensions greater than four, the Ising model can be effectively described by a mean field theory, where the local field is defined as the average spin value over the local region. Since these results are not of central importance to the present work, details are left to the established literature.

3.3.2 "Black Box" Ising Problem

Typically, in physics, the dimension of the system of interest is fully known beforehand. Where the methods of physics are applied to other systems, as in econophysics, it need not be given and hence must be determined empirically. It is of central importance to this thesis, as we will later ask this same question of a stock market, which does not operate in an obvious physical space.

In order to illustrate an important difficulty that this presents, we propose the following *gedanken* experiment, which will be henceforth referred to as the "black box" Ising problem: Consider a physical system described by an Ising model of unknown dimension enclosed in a closed box and which cannot be accessed. The box is equipped with a paper tape that periodically reports the state of the system. Hence, although we are able to observe the state of the system at different times, we have no *a priori* knowledge of its connectivity. We therefore pose the following *inverse problem*: is it possible to infer the connectivity of the Ising model, including its dimensionality, simply from the contents of the tape?

Generally speaking, fluctuations in the system will prevent us from concluding much about the connectivity by observing the tape at any given point in time. The best that can be done is to compare the contents of the tape at different times, that is to say to examine the correlations present between states. The question may therefore be reposed: can the connectivity of the system be deduced from the correlation matrices and autocorrelation functions of the system? In order to answer this problem, we use Monte Carlo simulations to generate quantitative data as we describe in more detail in the next section.

3.3.3 Monte Carlo Simulations of the Ising model

With an eye on the black box problem posed in the previous section, we will now show the results of various Ising model Monte Carlo simulations in 1D, 2D, and 3D. Although these simulations were performed specifically for this

thesis, the Ising model is such a well-studied system in these dimensions that we have kept this discussion separate from the results chapter (chapter 6).

Among the reported results is the time-averaged correlation matrix C of the spins, where C_{ij} is the time-averaged correlation between spins σ_i and σ_j. We compute this matrix as follows. After allowing the system to reach equilibrium, for each spin we record the sequence of spin values over M Monte Carlo sweeps, $\{\sigma_i^t\}_{t=1}^{M}$, where $i \in \{1, .., N\}$ indexes the spin. We then partition each of the N sequences into overlapping subsequences $\left\{\sigma_i^{t_k}\right\}_{k=1}^{S}$ of length L (corresponding to L Monte Carlo sweeps), where the starting point of each interval is offset by K sweeps. This gives $S \equiv (M - L)/K + 1$ subsequences. The time-averaged correlation between spins σ_i and σ_j is then the average of the correlations over each subsequence. That is,

$$C_{ij} = \frac{\sum_{t=1}^{S} corr\left(\sigma_i^{t_k}, \sigma_j^{t_k}\right)}{M/S}, \; k = 1, ..., S. \tag{3.26}$$

We have found that taking this time average gives a better result than computing a single correlation over the M Monte Carlo sweeps.

3.3.3.1 1D Simulations

Figure 3.8 shows the time-averaged correlation matrix for a Monte Carlo simulation of the 1D Ising model with $N = 100$ spins at $T = 1$ and $T = 1000$. Notice the diagonal of each matrix is identically 1, as each spin is perfectly correlated with itself. Off the diagonal, the correlations are so close to zero that they are barely visible in the plot, reflecting that the system is in paramagnetic state. This is true for both $T = 1$ and $T = 1000$. Of course, this does not prove the nonexistence of a phase transition, but as the analytical solution of the 1D Ising model shows that indeed there is no phase transition, we need not run any further simulations. The correlation of a 1D Ising model simulation will always look like figure 3.8.

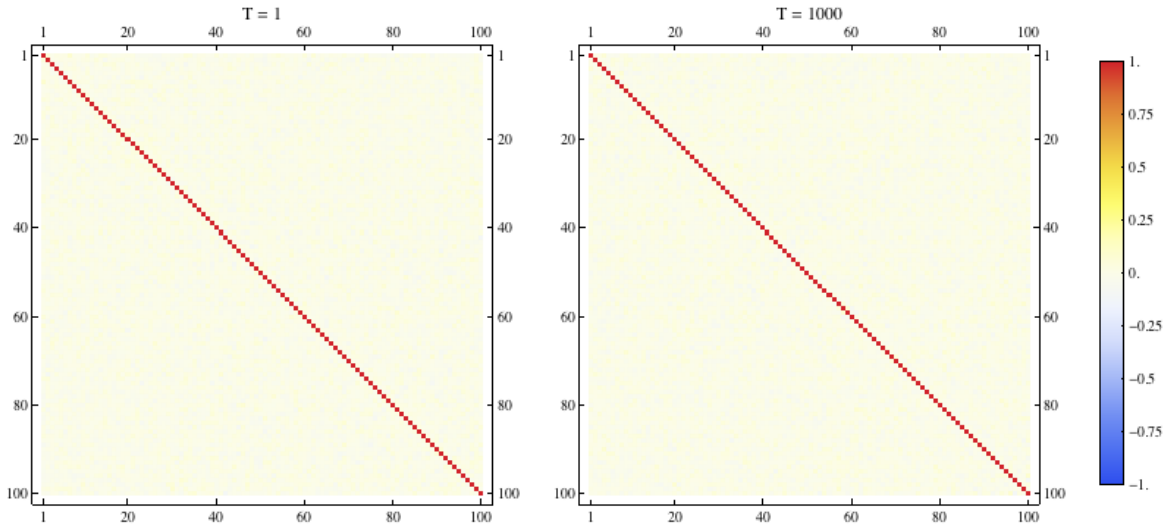

Figure 3.8: 1D correlation matrices at $T = 1$ and $T = 1000$.

3.3.3.2 2D Simulations

We will begin by showing the results of simulations for a 10×10 lattice at a selection of temperatures. For each simulation we will run for 1000 sweeps to reach equilibrium and and then run for an additional 10,000 sweeps to calculate the mean magnetization M, the internal energy U, and the time-averaged correlation matrix C. The

time-averaged correlation matrix will be calculated with a subsequence length of $L = 1000$ sweeps and an offset of $K = 1$ sweeps, according to the notation defined above. As always, we assume $J = k = 1$.

Figure 3.9 shows M as a function of T. Recall that in an Ising system, M is the order parameter. The sudden jump in M as the system cools is a 2nd order phase transition, as explained in the discussion on ferromagnetic systems. Onsager's solution of the 2D Ising model predicts that the critical temperature T_c at which this transition phase transition occurs is $T_c = 2/\log\left(1+\sqrt{2}\right) \approx 2.269$ (assuming $J = k = 1$). Thus, our results are approximately in accordance with theoretical prediction. Next, 3.10 shows U as a function of T. Notice that the transition is much softer than the transition in the magnetization.

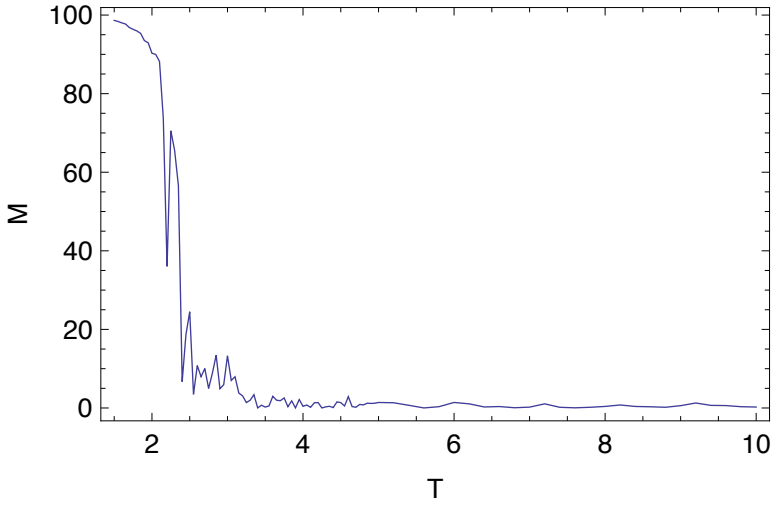

Figure 3.9: Net magnetization as a function of temperature.

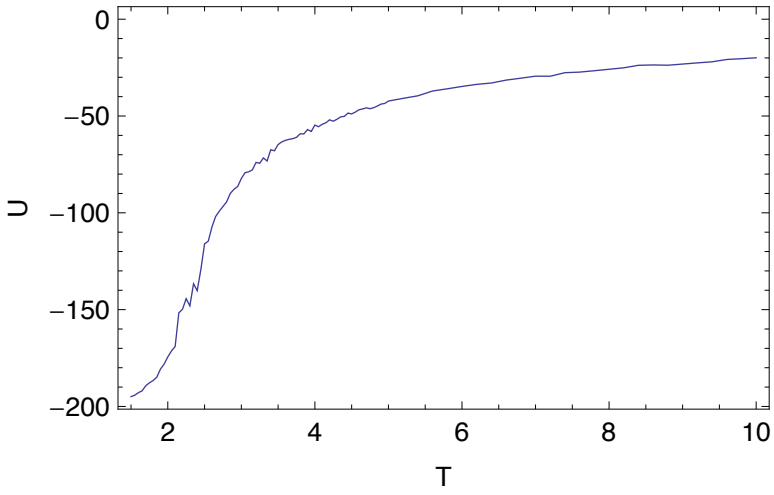

Figure 3.10: Internal Energy as a function of temperature.

Figures 3.11 and 7.3 show the time averaged correlation matrices for a selection of temperatures (note that the temperature spacing between each of the matrices is not uniform). We can see the clear onset of structure as the system approaches the critical temperature, although this onset is more gradual above the critical temperature. A review of the adjacency matrix of a 2D lattice makes the interpretation of the structure of the correlation matrix clear: the diagonal bands of higher correlation correspond to each spin being more highly correlated with its nearest neighbors. The vertical (or horizontal) distance between these bands should be 10 matrix elements, since, for any

given spin in the interior of the 10×10 lattice, the spins to the left and right on the lattice are mapped to single indices that are 10 less and 10 more than the single index of the given spin (this idea is explained in the discussion of the adjacency matrix of a 2D lattice in section 3.3.1.2). Figure 3.13 shows the 2-Norm of the correlation matrix as a function of T. We can see that it clearly spikes near the transition.

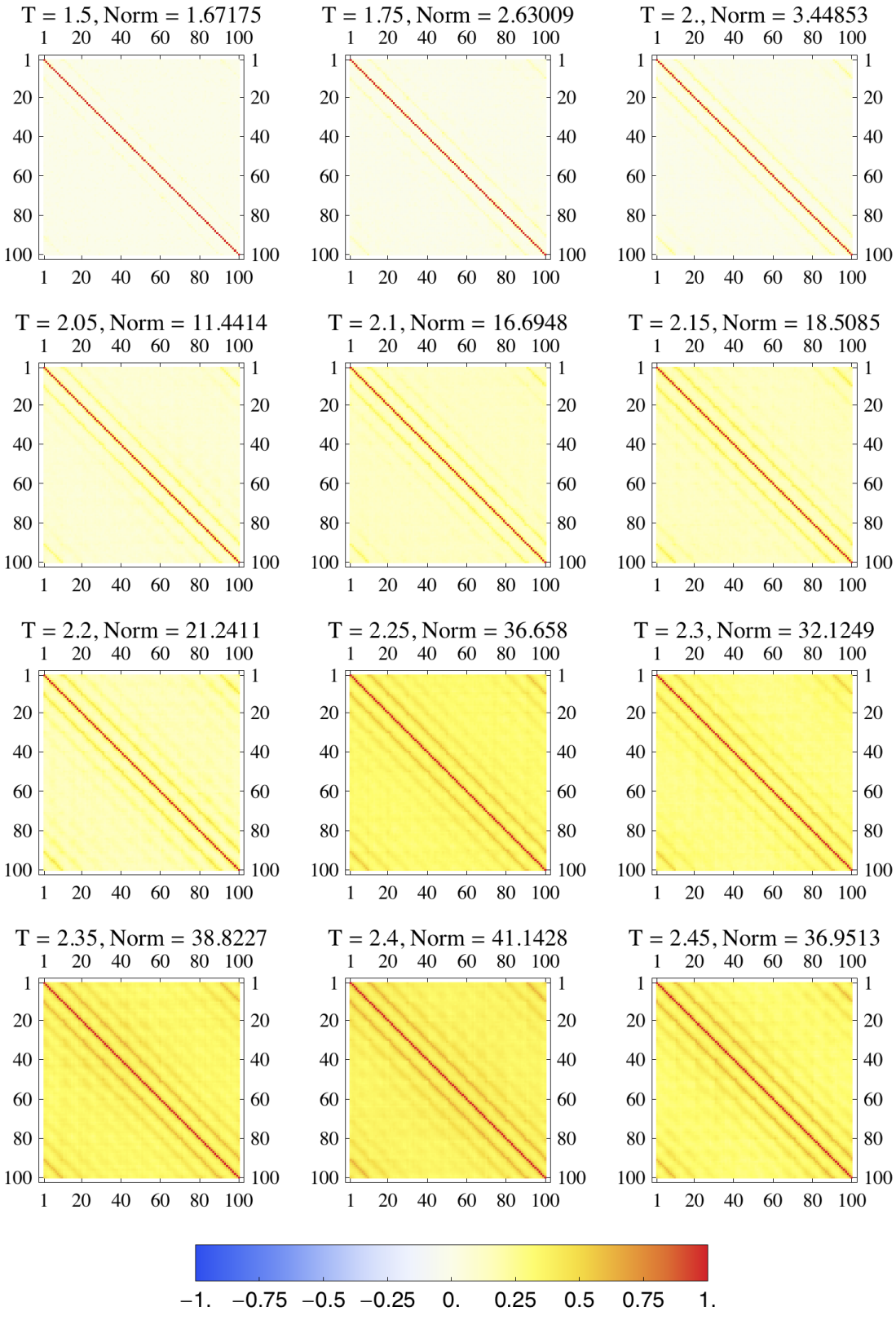

Figure 3.11: Time averaged correlation matrices from 2D Ising model simulations (part 1).

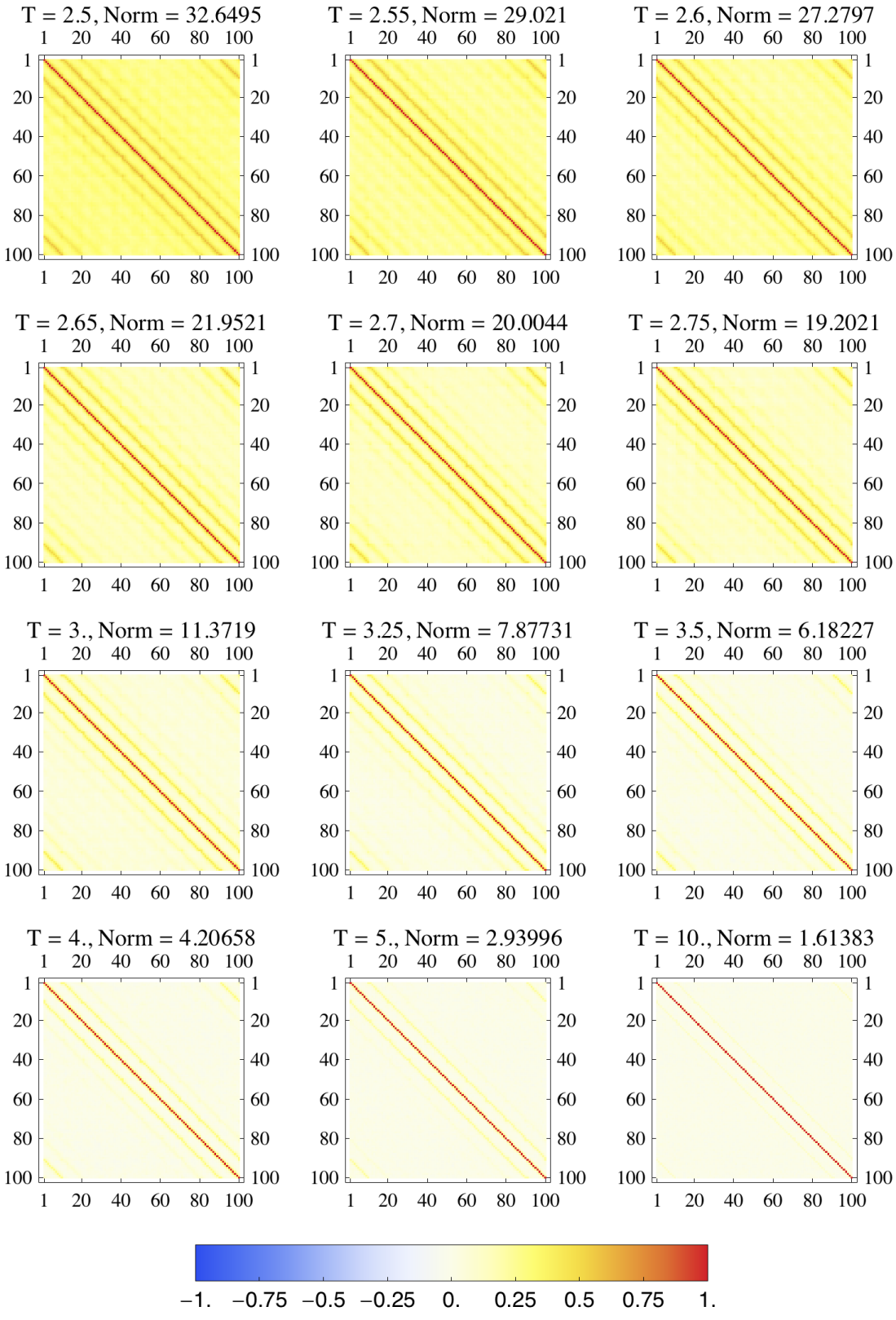

Figure 3.12: Time averaged correlation matrices from 2D Ising model simulations (part 2).

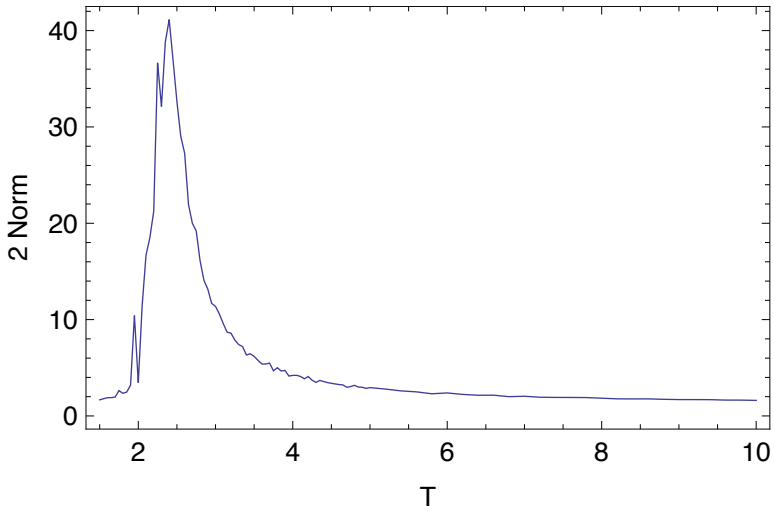

Figure 3.13: 2-norm of the correlation matrix as a function of temperature.

3.3.3.3 Resolution of the Black Box Problem

Recall that our goal is to use the information from these matrices to solve the black box Ising problem outlined above. It is immediately apparent from the above simulations that the inverse problem cannot in general be solved because sufficient information about the connectivity is not always available; correlation matrices for both the 1D and 2D systems are indistinguishable at high temperature. However, it seems that near the critical point we have an excellent means of accomplishing this, since near this point the correlation matrix for the 2D model acquires a rich diagonal structure. Since the 1D model does not possess a transition, it lacks this structure at any temperature. We do not show explicitly that this is the case, but calculations for 3D show a qualitatively similar effect. A problem that remains is that the elegant structure visible in figures 3.11 and 7.3 depends on the ordering of the spins. Once can see this effect in figure 3.14, which shows the matrix corresponding the highest matrix norm from the simulations but with randomly reordered elements. The diagonal structure is lost. It therefore necessary to develop tools for analyzing the correlation matrices that are invariant with respect to a reordering of the matrix. The tools we introduce are the histogram of the correlations and the staircase function of the correlation matrix. We begin with the histogram (which we will also refer to as the distribution of correlations).

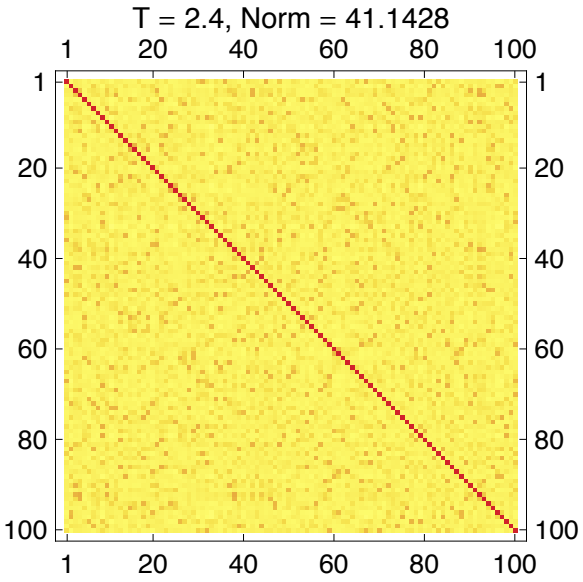

Figure 3.14: Randomly reordered correlation matrix at $T = 2.4$.

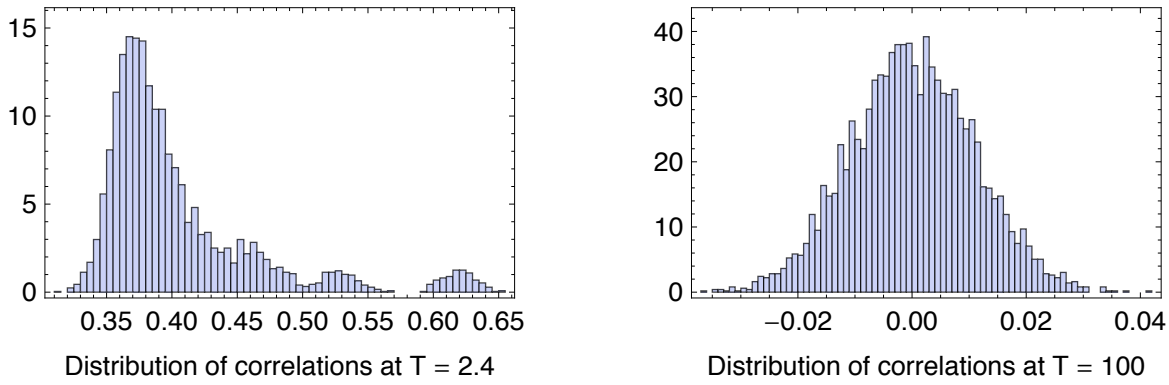

Figure 3.15: Histograms of the off-diagonal correlations at $T = 2.4$ and $T = 100$.

Figure 3.15 shows the histograms of the matrix elements for a temperature near the transition, $T = 2.4$, and a temperature away from the transition, T=100. Since a correlation matrix will always have a diagonal that is identically 1, we actually show the histogram of the off-diagonal elements in each plot. Now, around the transition, the histograms of matrix elements (represented by figure 3.15, left) show multiple peaks and high correlations. The peak centered on 0.7 reflects the strong correlations between adjacent and nearby spins. This structure vanishes above the transition as shown by the typical histogram displayed in figure 3.15 (right), which instead is centrosymmetric and has only one peak. Figure 3.16 shows the histograms for a collection of temperatures (although for a maximum of $T = 10$). Again, near the transition, we see the multiple peaks of the histograms. These peaks fade as the temperature increases, although the outermost peak is still visible at $T = 10$. We also see that the mean of the histogram shifts outward near the transition, reflecting that correlation's are higher everywhere in the system. For a more detailed discussion of how the histograms were calculated, see section 5.2.2.5.

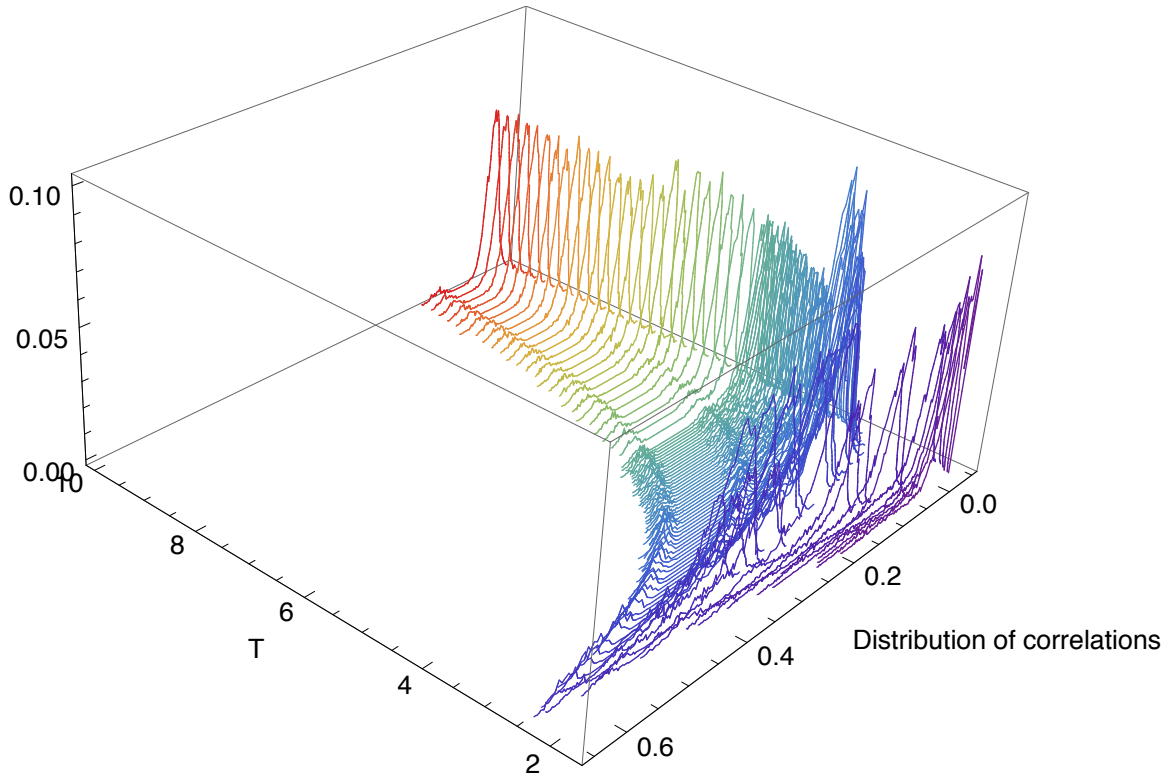

Figure 3.16: Histograms of the off-diagonal correlations for a variety of temperatures.

For an $n \times n$ matrix C we will define the staircase function $S(x)$ as the average of the average number of elements per row that exceed the value x. That is,

$$S(x) = \frac{1}{n^2} \sum_{j=1}^{n} \sum_{i=1}^{n} \chi_{(x,\infty)}(C_{ij}) \tag{3.27}$$

where χ is the characteristic function of the interval (x, ∞). The division by n^2 gives us that $S(x) \in [1, 1]$, since at least zero and at most n^2 elements can exceed a given value x. One could, of course, generalize this to a $m \times n$ matrix, but since we are only interested in the square correlation matrix we will write the staircase function in this form. Figure 3.17 shows the staircase plots of the same two correlation matrices discussed above. The interpretation of the plot is that for small x values (about 0.4 for $T = 2.4$ and about 0 for $T = 100$), nearly all of the correlations exceed this value, whereas for larger x, nearly all of the correlations do not exceed this value. Since the entries of a correlation matrix are bounded by $[-1, 1]$, $S(x) = 0 \ \forall x > 1$ and $S(x) = 1 \ \forall x < -1$.

We can see that the staircase plot of the high temperature correlation matrix has a much steeper transition than the lower temperature matrix. This tells us that the variance of the correlations is smaller in the high temperature case. Also, the point of the transition is lower in the high temperature case implying that the correlations are in general lower. Finally, notice the slight bump in the lower temperature case just above the transition. Again, this is a result of correlations between nearest neighbors. This behavior is more clear in figure 3.18, which shows the staircase plots for a selection of temperatures in the range $[1.5, 10]$. One can see that the staircase function spikes in the neighborhood of the critical temperature.

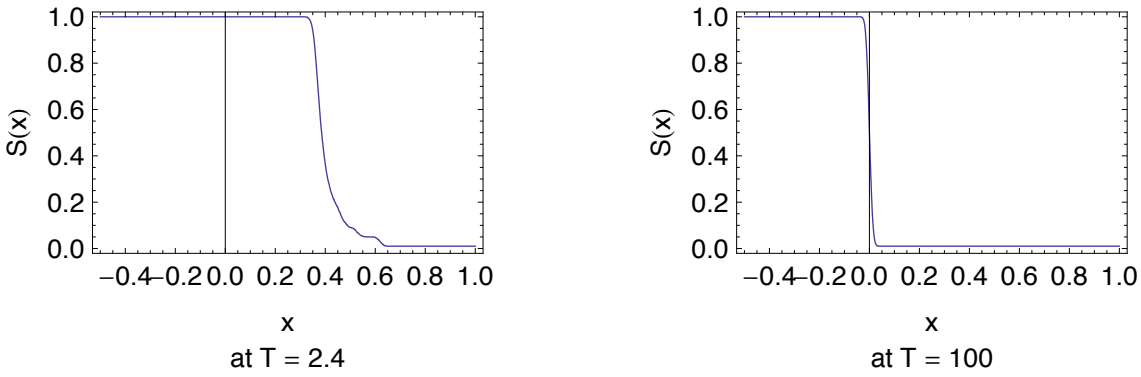

Figure 3.17: Staircase plots near the transition ($T = 2.4$) and at high temperature ($T = 100$).

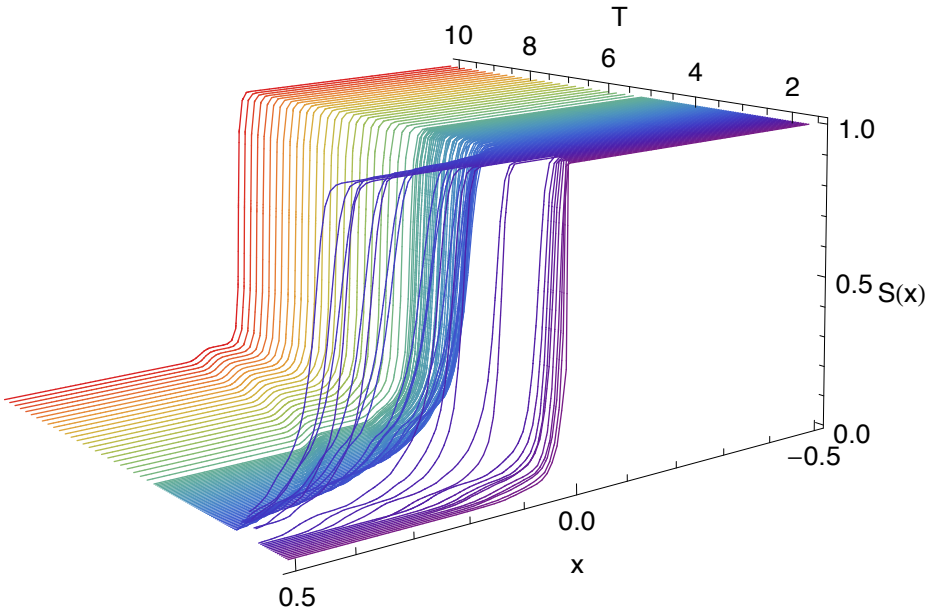

Figure 3.18: Staircase plots for a selection of temperatures.

3.3.3.4 2D with Random Coupling Matrix

It is hardly to be expected that any kind of stock market would be described by a Hamiltonian with constant coefficients. Additional simulations were therefore performed for the 2D Ising model where nonzero elements of J_{ij} were replaced with random numbers on the interval $[0, 1]$. The following figures illustrate results corresponding to those in the previous section; showing that the diagonal structure is still visible, but modulated by the presence of disorder. The primary effect seems to be softened correlations and a lower critical temperature. The latter effect is apparent from figures 3.19 or 3.20, which show a transition temperature of just above 1. To see the former effect, notice from figure 3.20 that the maximum matrix norm is just under 30 (it was over 40 in the previous simulation with constant couplings). Figure 3.21 shows that the diagonal structure is preserved near the critical point, although it is weakened. Finally we see similar but softened behavior in the histograms and staircase functions.

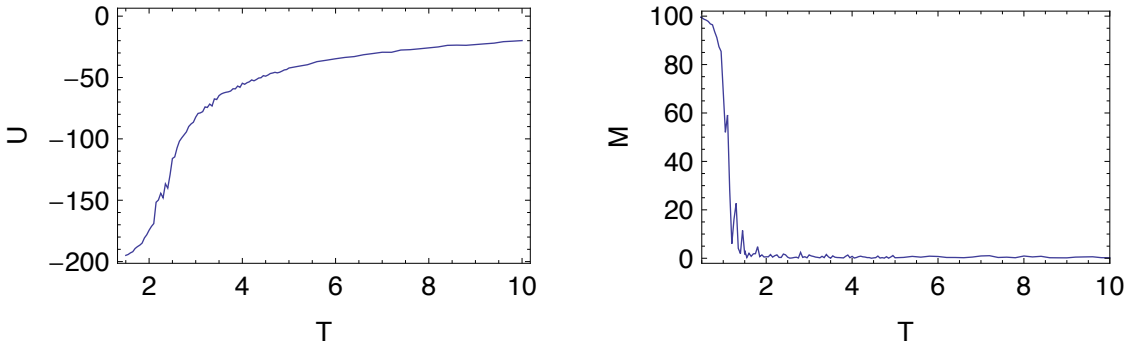

Figure 3.19: Internal energy and magnetization.

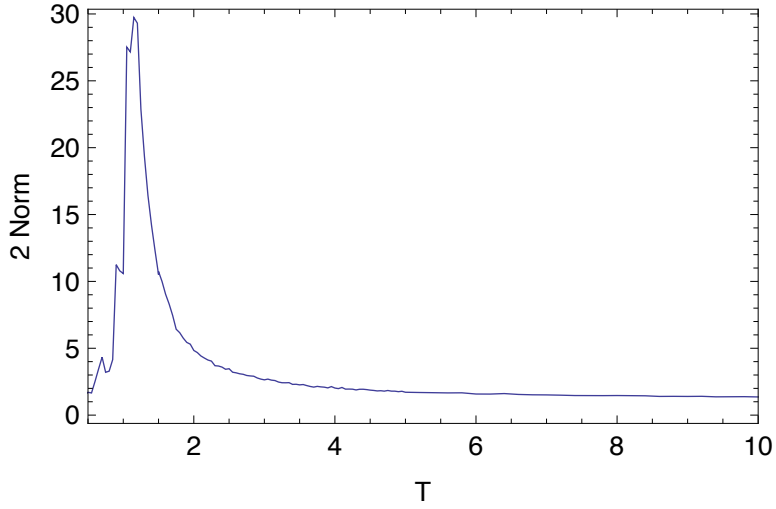

Figure 3.20: 2 norm of the correlation matrix.

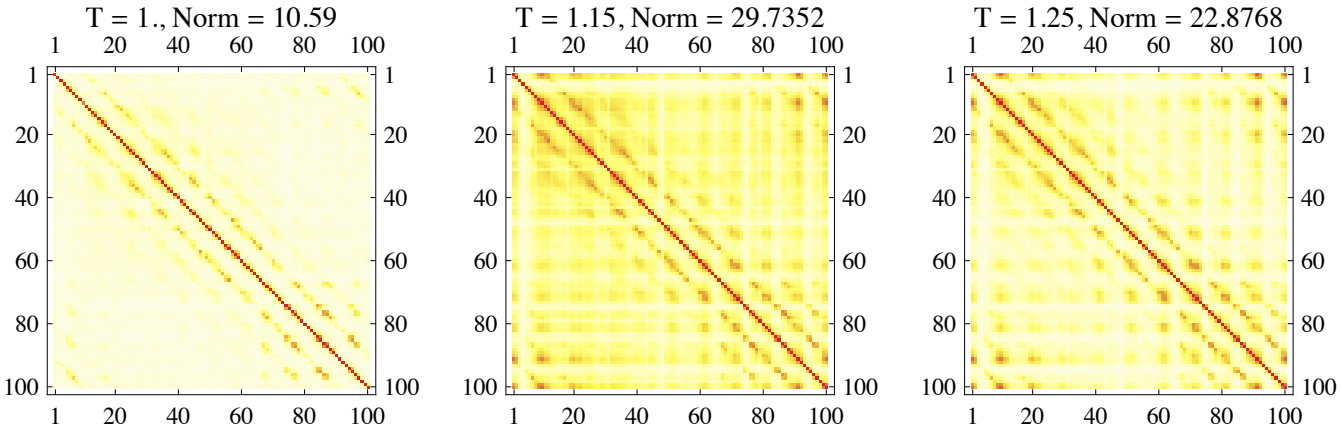

Figure 3.21: A sample of correlation matrices near the transition.

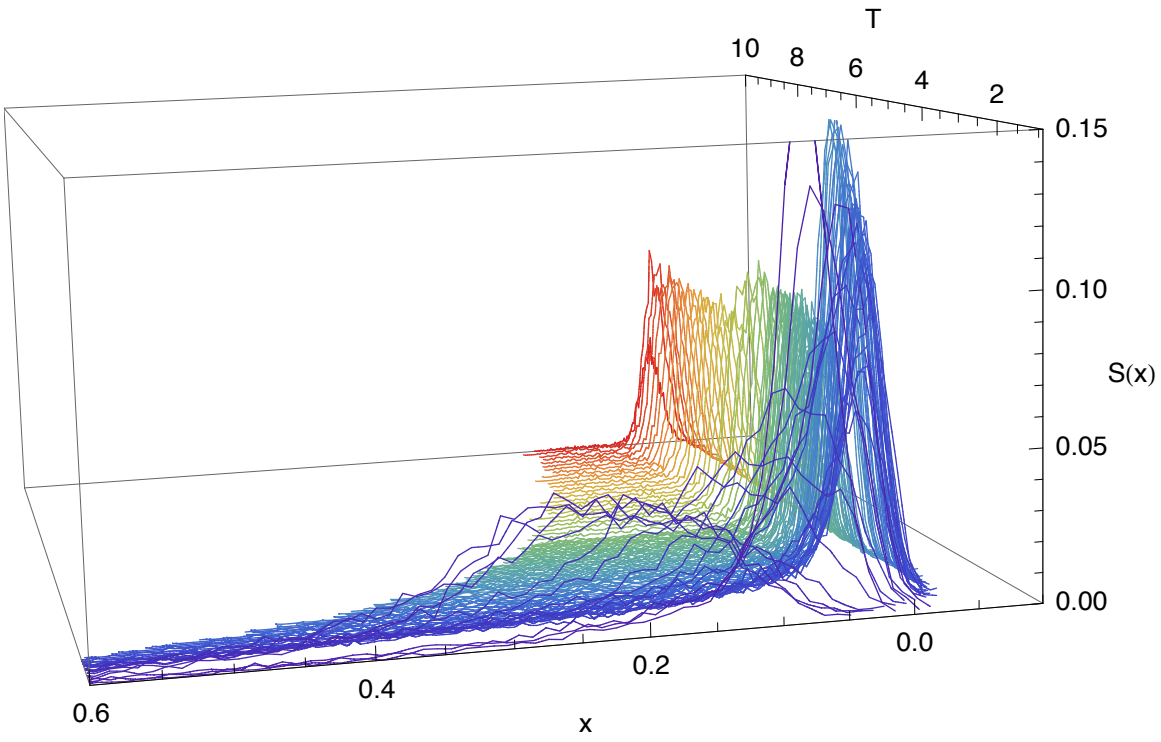

Figure 3.22: Histogram of the off-diagonal correlations for a variety of temperatures.

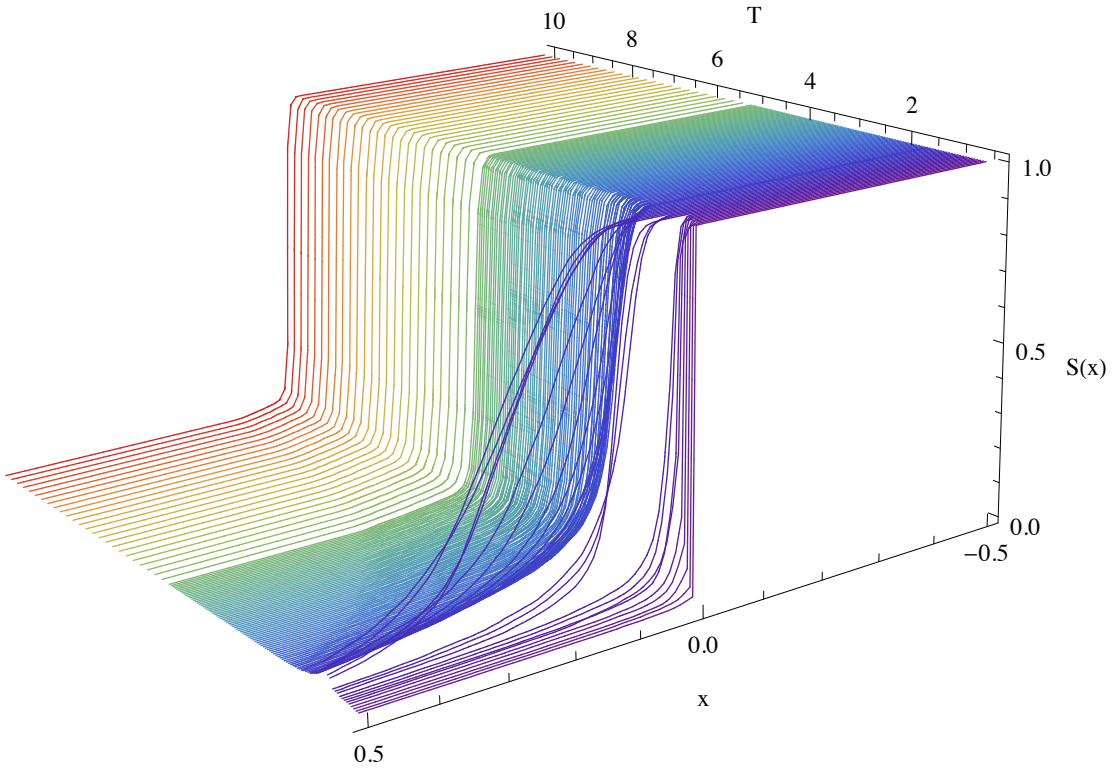

Figure 3.23: Staircase plots for a variety of temperatures.

3.3.4 Summary: Importance of Dimension

We restate the result of this chapter seen that at temperatures far away from the critical temperature, we cannot distinguish between the different dimensional Ising models. The black box Ising problem is therefore not in general solvable. However, near the critical point, the onset of structure to the correlations provides information that can be used to distinguish between dimensions, or at least to identify spins that are "nearby" to one another in some measure of distance. It is clear that a rigorous analysis of this new problem is a worthy topic of further study, and in particular quantitative methods for distinguishing detailed features of the hidden system are not developed here and remain a topic of future work. Rather, the distribution functions and the staircase functions of the correlations matrices, which are independent of the ordering of the matrix, will prove adequate tools for the present analysis of stock market crashes.

Chapter 4

The Analogue between Stock Market Crashes and Phase Transitions

There are an extensive number models of stock market crashes as phase transitions. For example, Levy [26] constructs a simple two asset model where an investor's participation in the market depends his or her degree of conformity, among other factors. The paper argues that in situations of high investor conformity relative to investor heterogeneity, the market is susceptible to a crash. As ought to be obvious from the preceding chapters, a two asset model is incapable of capturing the differences that are caused by the physical space of the system. Yalamova [48] even maps the phase diagram of a substance in pressure-temperature space to the phase diagram of an investor in risk/fundamentals-noise/information space, where the gas, liquid, and solid phases correspond to the buy, sell, and wait decisions of the investor, respectively. A number of these models are based on the Ising model. The central point of this thesis is that these models, and models of market crashes as critical phenomena in general, ignore a detailed discussion of the dimension. As we have seen in the previous discussion of the Ising model, the dimension can dramatically change the behavior of the system.

We will now focus on agent-based models of market behavior with spin-like interaction. Although there are differences among the models, there are a few common concepts. To begin with, we consider a graph (which is usually taken to be lattice, as in the Ising model) of size N. Instead of associating a spin with each vertex of the graph, we associate a buy or sell order σ_i. Generally, $\sigma_i(t) = 1$ implies that agent i places a buy order at time t, while $\sigma_i(t) = -1$ implies a sell order. Notice that this construction limits the model to the consideration of a single asset. The time evolution of this system is specified according to a particular stochastic formulation of the Ising model. Finally, each model relates the magnetization to the asset price. Table 4.1 presents an summary of the analogy.

These models are difficult to verify as we cannot directly observe the buy and sell orders of individual investors. In reference to section 3.3.2 we essentially have a black box Ising problem *without the tape*. However, the collection of all buy and sell orders of a stock determines its price and, according to the famous efficient market hypothesis, the price is all that matters since it contains all of the available information concerning the stock. We therefore consider a second analogy, laid out in table 4.2, in which the spins correspond to individual stocks rather than investors. One can think of this as a "course-grained" version of the first. For this reason, we believe that in order for the first analogy to hold, the second analogy must hold as well. As high frequency stock market data is readily available it is possible to investigate the validity of the second analogy through empirical observation, something we attempt in the results section.

To provide further illustration (of the first analogy, as this appears to be what is discussed in the literature), we will next discuss a particular model, the Bornholdt model [6], in more detail. For examples of other models, see

[22, 49, 44].

	Ising model	Financial model
Variable at each vertex:	Spin	Investor decision
Possible values of the variable:	$\uparrow$ $(+1)$ or $\downarrow$ (-1)	buy $(+1)$ or sell (-1)
Order parameter:	Mean magnetization M	Asset price
Phase transition:	Sudden change in $M(T)$	Stock market crash

Table 4.1: One possible analogy between the Ising model and financial market models based on it.

	Ising model	Financial model
Variable at each vertex:	Spin	An asset
Possible values of the variable:	$\uparrow$ $(+1)$ or $\downarrow$ (-1)	Asset price
Order parameter:	Mean magnetization M	Market Index/Sum of asset prices
Phase transition:	Sudden change in $M(T)$	Stock market crash

Table 4.2: A second possible analogy between the Ising model and financial market models based on it.

4.0.5 Bornholdt Model

Here we will outline the Bornholdt model, a model of agent behavior with spin-like interaction. Note that although $\sigma_i(t)$ refers to demand of an agent, to simplify the discussion we will often refer this number as the spin. The time evolution of the model follows the heat-bath Monte Carlo algorithm, which is an alternative to the Metropolis algorithm. In it, the probability p of spin σ_i taking the value $+1$ at time $t+1$ is given by

$$p = \frac{1}{1 + e^{-2\beta h_i(t)}}, \tag{4.1}$$

where $h_i(t)$ is the local field. This mean,

$$\sigma_i(t+1) = \begin{cases} +1 & p \\ -1 & 1-p \end{cases}. \tag{4.2}$$

The local field is given by

$$h_i(t) = \sum_j J_{ij}\sigma_j - \alpha C_i(t) \frac{1}{N} \sum_{i=1}^{N} \sigma_i(t), \tag{4.3}$$

where, as in our notation on the Ising model, the matrix J encodes the topology of spin interaction, so $J_{ij} = 0$ if spins σ_i and σ_j do not interact. This equation shows the two important interactions in this system. The first term represents the interaction between each agent and his or her neighbors. Since p depends positively on the local field, the term implies that each agent is inclined to follow the investment decisions of his or her neighbors. However, this is potentially frustrated by the second term, which represents the interaction between each agent and the market as a whole. The factor $\frac{1}{N}\sum_{i=1}^{N}\sigma_i(t)$ represents the excess demand of the market, per agent. In the Ising system, it is the net magnetization. As the parameter α is assumed to be positive, the value of $C_i(t)$ determines the direction of the interaction. As the strength of the interaction may be adjusted by choice of α, there are only two cases to consider. If $C_i(t) = 1$, agent i is inclined to follow the minority (in the language of an Ising system, there is an anti-ferromagnetic coupling between spin σ_i and the net magnetization). On the other hand, if $C_i(t) = -1$, agent i is inclined to follow the majority.

This is the basic construction of the model. The model is then simulated on a 32×32 lattice and the results reproduce some of the observations from real economic data, including power-law distributed returns and clustered

volatility.

4.1 Critique of Phase Transition Models

Our critique of the above models centers around the previous neglect of the physical space component in constructing the analogy, which is important because in physical systems this space actually determines the qualitative behavior. It is not *a priori* obvious what the physical space that either assets (or investors, depending on how the analogy is constructed) occupy in a financial market. We stress that what is really meant by "physical space" in this context actually encodes a measure of distance. While it is certain that both stocks and investors exist in the 4(+) dimensional space we all occupy, it is really the idea of locality between objects that is not well defined. For example, two investors in different states can just as easily buy and sell shares on the time scale of seconds, so it is clear that the geographic measure of distance need not be the relevant one. As we have seen, the behavior of the Ising model—including the very existence of a phase transition—depends on the dimension of the lattice. Stock market data provides a way to investigate the validity of the above models. If the stock market can indeed by thought of as an Ising-like system, with a market crash corresponding to a phase transitions, we should observe some of the same properties of the correlations as observed in Monte Carlo simulations of the Ising model. This is the application of the black box Ising problem introduced in section 3.3.2.

Chapter 5

Methods

5.1 Software and computing

Almost all of the programs used in this thesis were written in Mathematica 8. For a list of important programs, see table 5.1. Although some of the small calculations were performed on a personal computer, most calculations were performed on the Tufts Research Computing Cluster, provided by Tufts Technology Services.[1]

5.2 Financial Data Methods

5.2.1 Data

Our data is the HIstorical Market Data package, purchased from the Pi Trading Corporation[2]. It contains minute-by-minute observations of over 300 time series, including 18 indices, all 30 components of the Dow Jones Industrial Average, and 201 other actively traded stocks. Each observation includes the open, close, high, and low price as well as the trading volume during that minute. By an observation we mean a single line of the data file in its raw format. The start date of each series varies, although no individual stock data is available before 1991. The S&P500 index is available starting in 1983. Each series continues until 06/15/2012. Below we show the first few lines and the last few lines of a typical data file, this one corresponding to IBM.

```
"Date","Time","Open","High","Low","Close","Volume"
01/02/1991,0931,28.22,28.22,28.22,28.22,122000
01/02/1991,0933,28.25,28.25,28.25,28.25,94000
01/02/1991,0934,28.25,28.25,28.25,28.25,26000
01/02/1991,0936,28.22,28.22,28.22,28.22,8400
01/02/1991,0937,28.19,28.19,28.19,28.19,93200
.
.
.
06/15/2012,1558,199.13,199.19,199.10,199.18,43625
06/15/2012,1559,199.19,199.25,199.16,199.18,59425
06/15/2012,1600,199.19,199.27,199.06,199.11,155332
```

[1] For more information on the cluster, see http://wikis.uit.tufts.edu/confluence/display/TuftsUITResearchComputing/Home.
[2] http://pitrading.com/historical_data.htm

The time variable is given in a standard 12-hour clock notation (so, for example, 0931 corresponds to 9:31 a.m.). Notice that, for this particular stock, the time skips from 0931 to 0933 and again from 0934 to 0936. We will explain this in the next section.

5.2.1.1 Omitted observations

In its raw format, an observation of any particular time series is omitted if it is identical to the observation from the previous minute (that is, if each price variable price and the volume do not change). Obviously, if left in this form, cross sectional comparisons would be difficult. To correct for this, we replace each omitted observation with the most recently available observation prior to the omitted observation. In the example of the IBM file above, the omitted observation at 9:32 would be replaced with the observation at 9:31, while the omitted observation at 9:35 would be replaced with the observation at 9:34. Note that it is often the case that consecutive observations are omitted. In this case we use the same procedure, meaning we replace the entire sequence of omitted observations with the most recently available observation prior to the omitted observation. To reduce run time we performed this procedure with a simple program written in C++. Below we show a sample of the output for the IBM data given above. Since we only use the open price in this thesis, we do not record the other variables.

"Date","Time","Open"
01/02/1991,0931,28.22
01/02/1991,0932,28.22
01/02/1991,0933,28.25
01/02/1991,0934,28.25
01/02/1991,0935,28.25
01/02/1991,0936,28.22
01/02/1991,0937,28.19
.
.
.
06/15/2012,1558,199.13
06/15/2012,1559,199.19
06/15/2012,1600,199.19

5.2.1.2 Unusable data

The following stocks were excluded, as their price often went below zero (making it impossible to calculate at the log returns): McDermott International (MDR), Motorola Solutions Inc. (MSI), Time Warner Inc. (TWX), Verisign Inc. (VRSN), and Wynn Resorts Limited (WYNN).

5.2.1.3 Storage

As indicated above, the raw data and the data after filling-in omitted observations for each stock was stored in a comma separated text file. All other data was stored in Mathematica form using the Put and Get functions.

5.2.2 Analytical Tools

5.2.2.1 Log Returns

After filling-in the omitted observations, we denote the opening price of a particular stock at time t by $Z(t)$. The log returns $G(t)$ are defined by $G(t) = \ln Z(t + \Delta t) - \ln Z(t)$.

5.2.2.2 Intraday Detrending

Unless otherwise noted, we will always examine data that has been detrended for intraday patterns, as explained in section 2.2.1.

5.2.2.3 Correlations

The standard Mathematica function $Correlation\,[x, y]$ computes the standard sample Pearson correlation coefficient between two vectors x and y in the following form:

$$Correlation\,[x, y] = \frac{Covariance\,[x, y]}{StandardDeviation\,[x]\,StandardDeviation\,[y]} \tag{5.1}$$

where $Covariance\,[x, y]$ is the Mathematica function that gives the unbiased estimate of the correlation between x and y and $StandardDeviation\,[x]$, for example, is the Mathematica function that gives the unbiased estimate of the standard deviation of x. To be clear, they are mathematically equivalent to

$$Covariance\,[x, y] = \frac{1}{N-1}\sum_{i=1}^{N}(x_i - \bar{x})(y_i - \bar{y}) \tag{5.2}$$

and

$$StandardDeviation\,[x] = \sqrt{\frac{1}{N-1}\sum_{i=1}^{N}(x_i - \bar{x})^2}. \tag{5.3}$$

The division by $N-1$, rather than N, is a degrees of freedom adjustment required for unbiasedness. The mathematical equivalent of equation 5.1 is therefore

$$Correlation\,[x, y] = \frac{\sum_{i=1}^{N}(x_i - \bar{x})(y_i - \bar{y})}{\sqrt{\sum_{i=1}^{N}(x_i - \bar{x})^2 \sum_{i=1}^{N}(y_i - \bar{y})^2}}. \tag{5.4}$$

Unfortunately, it is sometimes the case that a stock price (and hence the log returns) will not change during a window over which we want to calculate the sample correlations. This can happen either if all of the price and volume data did not change (and so these observations were omitted in the raw format but added as constant values by the Repair Price program) or if only the open price did not change. This will cause the estimated covariance between this stock and any other stock to be zero. The trouble is that estimated standard deviation of this stock will also be zero, which will cause the Mathematica function given by equation 5.1 to return an error flag. As the these Mathematica functions are substantially faster than an equivalent but manually written function we would like to find a way to use these functions. Therefore, we define the function $Correlation^*$ by

$$Correlation^*\,[x, y] = \begin{cases} 0 & StandardDeviation\,[x] = 0 \text{ or } StandardDeviation\,[y] = 0 \\ Correlation\,[x, y] & otherwise \end{cases} \tag{5.5}$$

Since we are generally interested in calculating the correlations between more than two stocks, it is more useful to compute the correlation matrix C, where $C_{ij} = Correlation^*\left[x^i, x^j\right]$.

Now, if given a matrix M, the same mathematica functions evaluated on this matrix, $Covariance\,[M]$ and $Correlation\,[M]$, will return the covariance matrix corresponding to the columns of M. Therefore, in practice, we calculate C by $Correlation^*\,[M] = Correlation\,[M]$ if $StandardDeviation\left[x^i\right] = 0\ \forall i$. If this condition does not hold we construct C manually by $C_{ij} = Correlation^*\left[x^i, x^j\right]$.

5.2.2.4 Matrix Norms

Throughout our analysis of correlation matrices we will often report the 2 norm of the matrix. We briefly note here that the 2 norm is equivalent to the *spectral norm*, which, for a symmetric matrix, gives the largest eigenvalue. Recall that a norm $\|\cdot\|$ on $\mathbb{R}^n$ induces a norm on the space of $n \times n$ matrices in the following manner

$$\|A\| = \sup \{\|Ax\| : \|x\| = 1\}. \tag{5.6}$$

The p *norm* is defined as

$$\|x\|_p \equiv \left(\sum_{i=1}^{n} |x_i|^p \right)^{1/p}. \tag{5.7}$$

One can show that the 2 norm is equivalent to the spectral norm, given by

$$\|A\|_2 = \sqrt{\lambda_{max}(A^* A)} = \sigma_{max}(A), \tag{5.8}$$

where $\sigma_{max}(A)$ is called the singular value of A. If A is a symmetric matrix, a singular value and a non-negative eigenvalue are equivalent. Thus we have

$$\|A\|_2 = \lambda_{max}(A). \tag{5.9}$$

5.2.2.5 Histograms

The histograms of the correlations (alternatively called the distribution of the correlations) were calculated, in part, with the Mathematica function *HistogramList*, which divides the elements of a list into bins. Although we always adjust the height of the bins so that the area under the distribution is 1, in general we adjust the width of the bins to optimize the look of the particular plot. For example, if the bin width is too small there will only be a single but large bin at the mean correlation. For the 3 dimensional histogram plots we used the results from *HistogramList* to construct a piecewise linear plot connecting the midpoints of the tops of the bins. We always show the histogram of correlations off the diagonal of the correlation matrix.

5.2.2.6 Fitting Castaing's equation

Following [24] we would like to fit the detrended the log returns to Castaing's equation (equation 2.8). To do this, we partition the data into intervals of length $2s$. On each of these intervals we fit $\ln Z(t)$ with a linear function and let $x(t)$ denote the deviation of $\ln Z(t)$ from the fitted function. Then, we define the detrended log returns at scale parameter s as

$$\Delta_s Z(t) = x(t+s) - x(t). \tag{5.10}$$

Next we detrend for intraday patterns in the usual fashion (see section 5.2.2.2). We then fit Castaing's equation to the observed PDF of the these doubly detrended returns using the Mathematica function *FindFit* to find optimal values of λ_s^2 and σ_s^2. We find that optimizing with respect to the 1 norm gives qualitatively better results than optimizing with respect to the 2 norm as the latter will give a poor fit if there is a large number of zero returns in the sample (see section 5.2.1.1 for a discussion of why this might happen). All optimizations were run with an accuracy goal of 5 digits.

5.2.3 List of programs

Name	Language	Description
Repair Price	C++	Fills in omitted observations (see section 5.2.1.1)
Log Returns	Mathematica 8	Computes the log returns $G(t) = \ln Z(t + \Delta t) - \ln Z(t)$ (see section 5.2.2.1).
Detrend Intraday	Mathematica 8	Performs intraday detrending procedure on the log returns (see section 5.2.2.2)
Detrend Inflation	Mathematica 8	Detrends for inflation, as described in 5.2.2.6.
*Correlation**	Mathematica 8	Computes sample correlation (or correlation matrix) as outline in section 5.2.2.3.
Calculate Correlations	Mathematica 8	Computes a sequence correlation matrices (using the function *Correlation**) between a collection of stock returns. The length and the overlap of the window over which the correlation matrix is calculated may be specified.

Table 5.1: List of programs.

5.3 Condensed Matter Methods

The Monte Carlo simulations of the 0D, 1D, and 2D Ising models were straightforward applications of the Metropolis algorithm (the results of the 0D simulations will be shown in chapter 7). Each program was written in Mathematica and run on the aforementioned cluster. Since we have already derived the Metropolis algorithm (section 3.1.4) and described our procedure for calculating the time averaged correlation matrix (section 3.3.3) we need not say much more concerning the implementation and so we will only make a few brief remarks.

In the forthcoming discussion of the 0D Ising model we will mention that equation 7.4, which gives a simplified expression for the Hamiltonian in terms of the number of negative spins, can be used to reduce the computation time required in a Monte Carlo simulation. To see this, note that in any dimension the change in energy ΔE_i obtained by flipping single spin σ_i is

$$\Delta E_i = -2 \sum_{j \in \mathcal{N}_i} J_{ij} \sigma_i \sigma_j, \tag{5.11}$$

where the sum is over the set $\mathcal{N}_i$ of all nearest neighbors of spin σ_i. The cardinality of this set is given by the *coordination number* of the lattice. For example, a 2D lattice has coordination number of 4. Since each spin is adjacent to each other spin in a 0D model, the coordination number is $N - 1$. To compute ΔE_i in 0D we will thus need to perform $N - 1$ operations, rather than just 4 in a 2D simulation. To speed up the computation we can use equation 7.4 to give

$$\Delta E_i = \begin{cases} H(n+1) - H(n) & \text{if } \sigma_i = +1 \\ H(n-1) - H(n) & \text{if } \sigma_i = -1 \end{cases}. \tag{5.12}$$

Of course, this formula may only be used when the nonzero elements of J_{ij} are constant for all i and j.

Chapter 6

Results

6.1 Autocorrelation

We are interested in understanding the effect of the intraday detrending procedure on the autocorrelation. To this end, we will analyze the S&P 500 index for entire window we have available, 2/01/1983 to 6/15/2012. For a complete discussion of the intraday detrending procedure and a general discussion of the autocorrelation properties of financial time series, please see section 2.2.1.

We begin by showing a plot of $A(t_{day})$, the average of the volatility at local time t_{day} over each day in the sample. This U-shaped pattern is typical of $A(t_{day})$ as it indicates the know pattern: that trading is more volatile at the beginning and end of the trading day. Figure 6.2 shows the autocorrelation function $C(\tau)$ of the detrended and non-detrended volatility. Once again, the daily pattern in the non-detrended data is quite clear. Furthermore, it seems to be the case that the detrending procedure effectively removes this pattern. Notice that this detrending procedure has almost no effect on the returns (figure 6.3). Note that τ is of course measured in minutes. In this thesis we will only analyze stock market data that has been adjusted for intraday patterns.

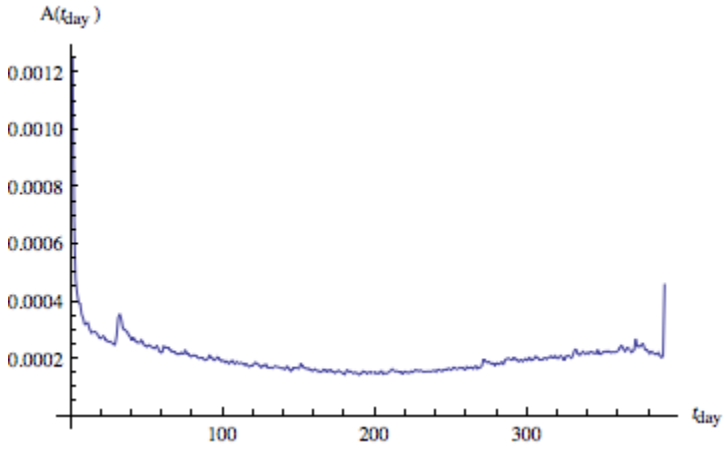

Figure 6.1: $A(t_{day})$.

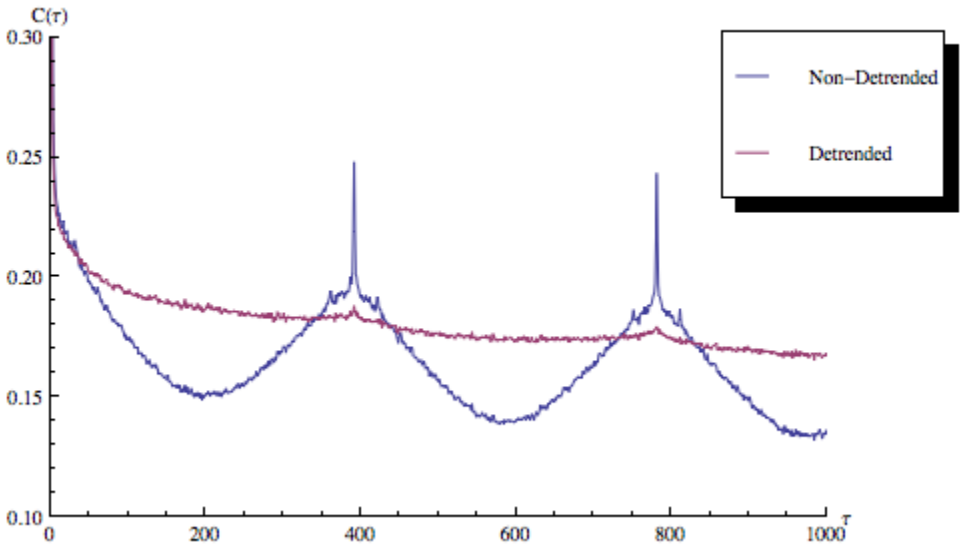

Figure 6.2: Autocorrelation of detrended and non-detrended volatility.

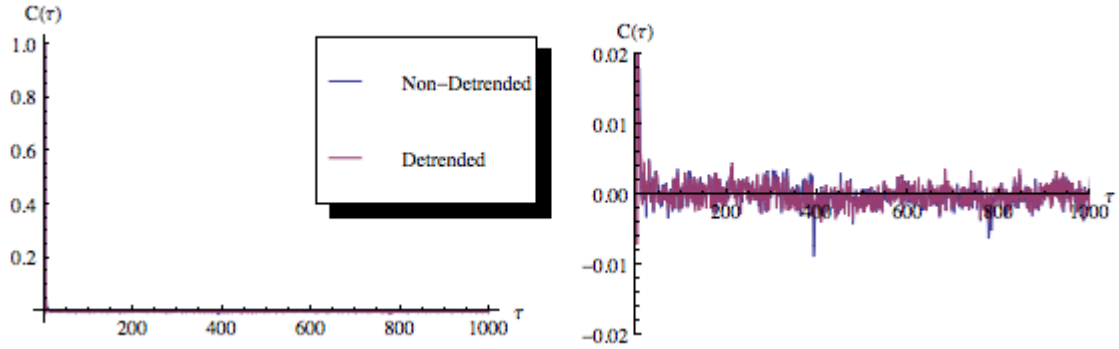

Figure 6.3: Autocorrelation of the detrended and non-detrended returns (with different axes).

6.2 Scale Invariance

We would like to expand the analysis of Kiyono et al [24] from the 1987 crash to the 30 year history of available, intraday S&P 500 returns. To do this we partition the intraday and inflation detrended returns for a collection of scale parameters s (see sections 5.2.2.2 and 5.2.2.6) into overlapping intervals of length 50 days and increment 5 days. We then fit Castaing's equation to the observed PDF of these returns, as described in section 5.2.2.6. Recall that λ_s^2 is a measure of the non-Gaussian behavior in the returns. The vertical "bars" in figure 6.4 of high λ_s^2 – – indicate scale invariance at a particular point in time. Near the 1987 crash, the results are qualitatively similar to Kiyono, as can be seen in figure 2.2. However, our expansion of this analysis shows that this scale invariant in behavior in λ_s^2 did not occur in other market crashes to nearly the same degree, suggesting that this analysis does not provide a universal framework for analyzing market crashes. We also notice large values of λ_s^2 in the years following the 1987 crash. Although the U.S. experienced a mild recession in the early 1990s, by any metric it was nothing in comparison to the recession following the 2008 financial crisis. In the figure, the U.S. invasion of Kuwait in summer of 1990 is noted for context.

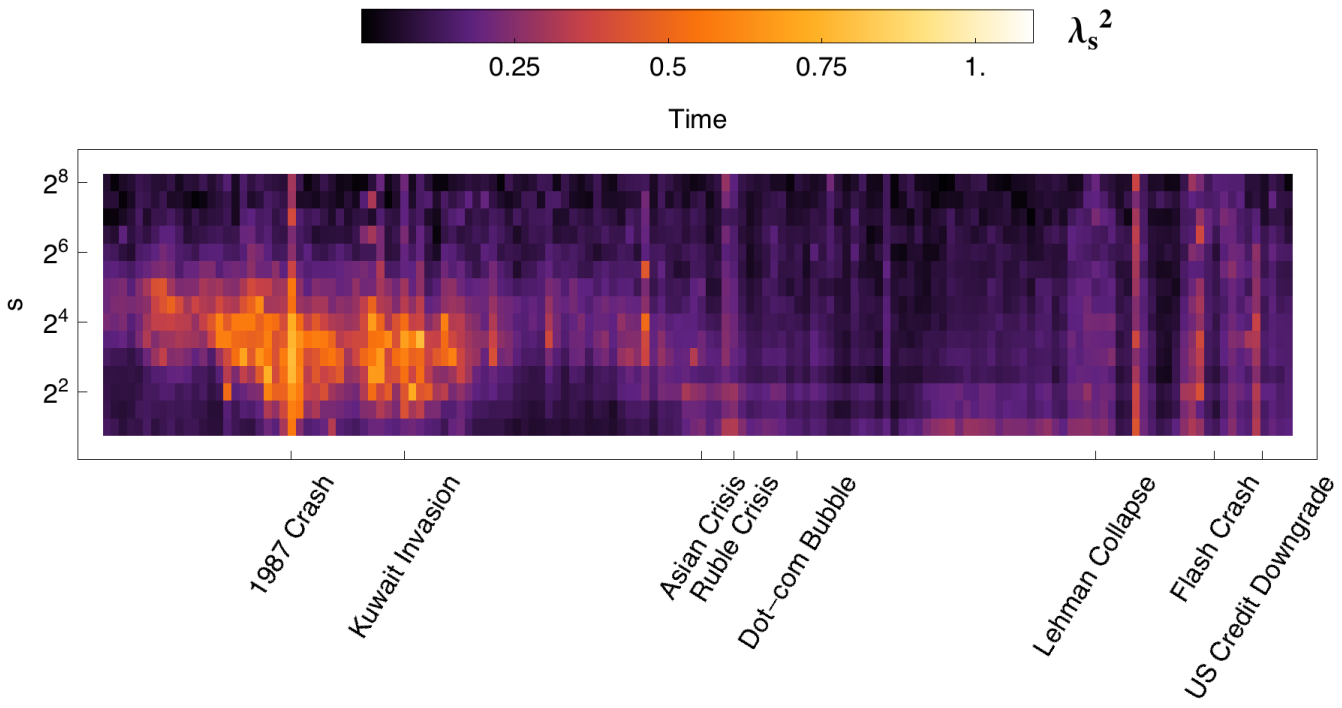

Figure 6.4: Fit of the parameter λ_s^2 in Castaing's equation to the probability density functions of the detrended log returns.

6.3 Stock Correlations

We are now ready look at the correlations between stocks. Unfortunately, the variance in the start dates of the stock price time series prevents us from consider the complete set of stocks, unless we only look at data after the last start date, or we allow the number of stocks in our calculations to change over time. As the last start date is not until 2011, we avoid the first option. We also avoid the second option as it would complicated comparisons between correlation matrices at different time periods. Instead, we we choose the start date 04/1/1993 for the calculation of daily correlations, as this date is early enough to not eliminate too much data, late enough to allow us to include the majority of stocks, and as it coincides with the start date of the Dow Jones Industrial Average (in our dataset, that is). Note that we do not have individual stock data before 1991 and so we are therefore unable to study the 1987 crash. This is especially disappointing as the size and compactness of the 1987 crash makes it ripe for analysis as a phase transition. Many of the other financial crises correspond to a sequence of stock market drops that took place over a matter of weeks or months. Recall that our goal is to look for evidence of spatial structure in the correlations between stocks. Rather than showing a legend next to each plot of a correlation matrix, we will state here that all of the following correlation matrices are plotted on the following color scale:

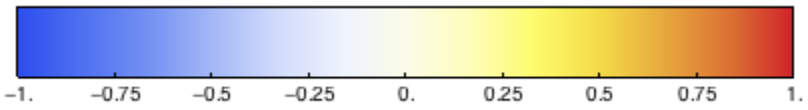

Figure 6.5: Color map used in each of the correlation matrix plots.

6.3.1 Intraday

We begin by providing 6.6, which shows the intraday price changes as for each day in the sample. To compute this, over each day we recorded the maximum and minimum price of the S&P 500 and plotted a vertical line between these two points. Notice how much the index has grown since the early 1990s.

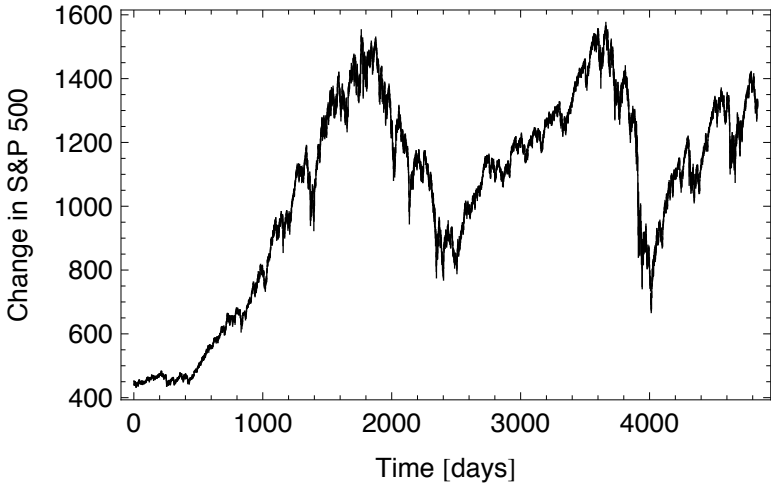

Figure 6.6: Intraday price changes in the S&P 500 over the sample, (1993-2012).

Table 6.1 shows the 2 norm of the correlation matrix, the variance of the eigenvalues of the correlation matrix, the price change of the S&P 500, and the volatility (defined here as the standard deviation of the S&P 500) on the 20 days corresponding to the 20 highest norms of the correlation matrix. We define the price change as the difference between the maximum and minimum price over the course of the day, as in figure 6.6. We also define the volatility as the standard deviation of the returns over the day. Notice the dominance of late 2011 in this table. On August 6th, 2011, Standard and Poor's downgraded the U.S. credit rating for the first time [1]. One must wait until the 17th day of largest norm to find a day in 2008. Finally, notice that although the flash crash and the day after the flash crash appear relatively high in the list.

Rank	Date	2 Norm	Eigenvalue Variance	Price Change	Volatility
1	08/09/2011	73.68	49.93	68.60	64.63
2	08/05/2011	72.71	48.63	49.68	62.69
3	08/10/2011	73.08	49.11	52.95	54.29
4	05/07/2010	71.32	46.78	40.11	50.99
5	05/06/2010	53.04	26.43	101.41	106.88
6	08/08/2011	68.17	42.70	77.41	52.43
7	05/20/2010	65.50	39.38	34.23	24.07
8	10/04/2011	64.11	37.73	50.13	33.22
9	08/26/2011	63.98	37.56	45.00	17.66
10	08/11/2011	63.98	37.56	64.70	28.92
11	09/01/2011	63.58	37.08	25.08	11.93
12	09/12/2011	63.24	36.68	26.00	13.80
13	09/09/2011	63.41	36.88	36.97	15.43
14	09/26/2011	63.47	36.93	33.10	17.87
15	09/22/2011	62.76	36.13	50.33	29.69
16	08/16/2011	63.40	36.86	23.69	16.75
17	10/23/2008	63.33	36.77	63.38	156.37
18	10/16/2008	62.28	35.57	80.61	208.02
19	11/01/2011	61.71	34.93	35.18	18.81
20	08/25/2011	62.17	35.44	34.26	16.22

Table 6.1: Some statistics of the 20 days corresponding to the dates with the 20 highest 2 norms of the daily correlation matrix of returns.

In figure 6.7 we see that the 2 norm of the correlation matrix increased substantially in both mean and variance over the sample.

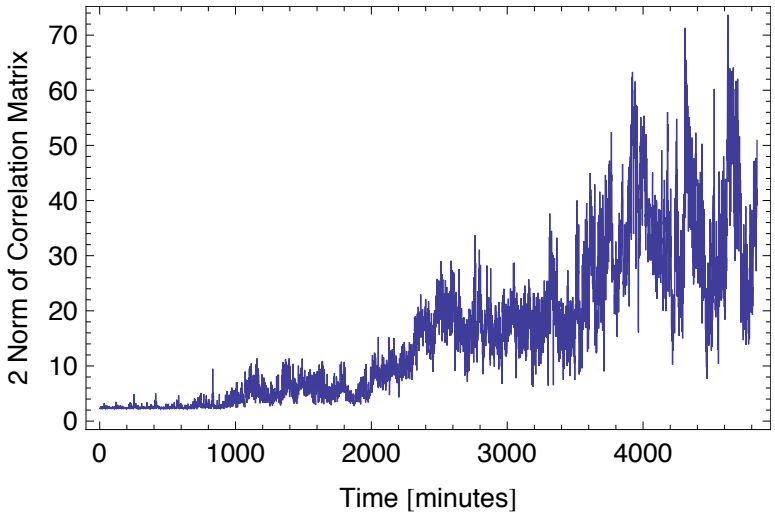

Figure 6.7: Norm of the daily correlation matrix over the sample (1993-2012).

We will now show a few correlation matrices and histograms of these matrices near a few important events, beginning with the most recent.

6.3.1.1 August 2011

Here we can see the very large correlations near the U.S. credit downgrade. As we have already discussed, however, the arbitrary ordering of the stock market correlation matrix makes it impossible to determine spatial structure

from the matrices in this form. We therefore look at the histograms for the same dates. Notice we do not see additional peaks of correlation, which are our telltail sign of spatial structure. However, these peaks are different: whereas in the Ising model simulation we observed smaller peaks of higher correlation above the mean correlation, here we observe the peaks below the mean correlation. We will show in the next discussion that these peaks are a result of a few stocks being nearly uncorrelated with the rest.

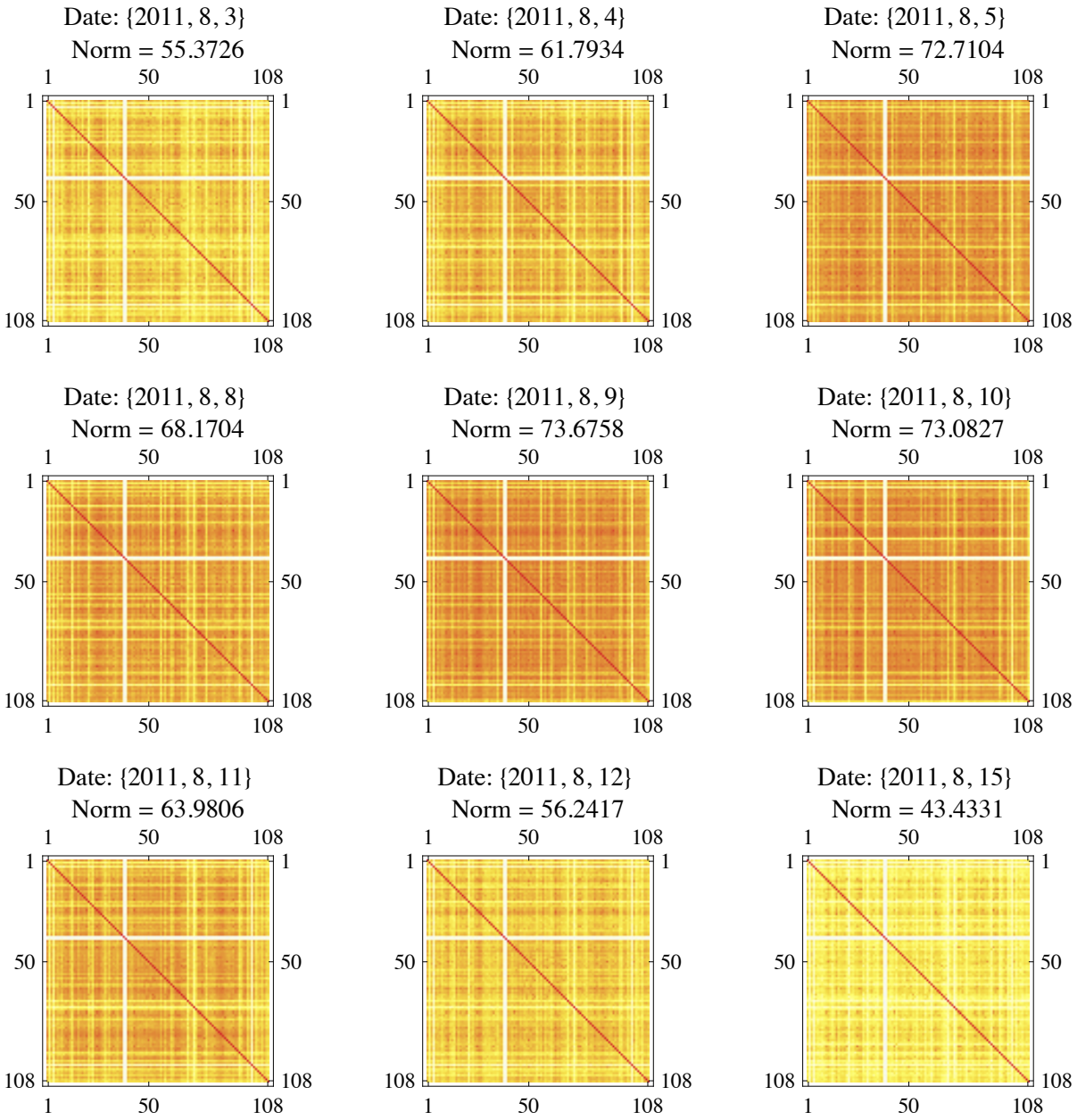

Figure 6.8: Correlation matrices near the U.S. credit downgrade on 08/05/2011.

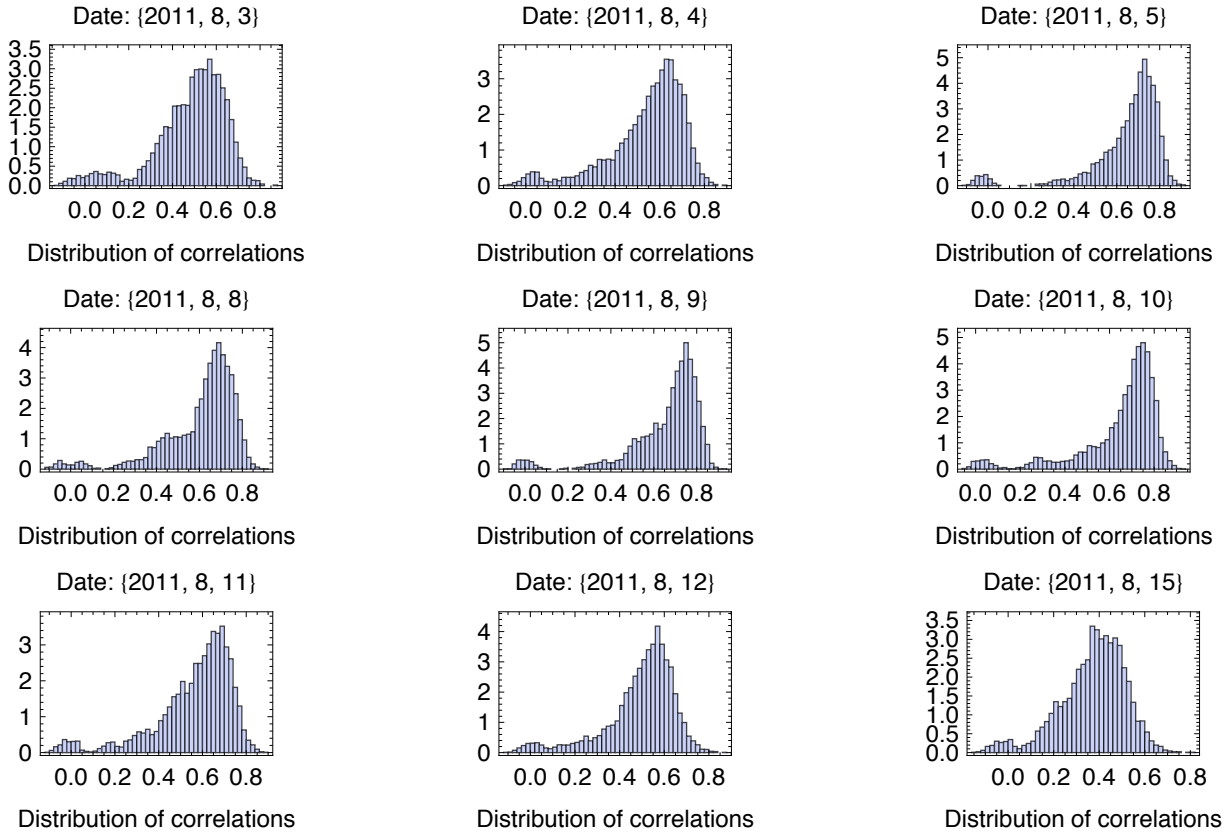

Figure 6.9: Distribution of correlations near the U.S. credit downgrade.

6.3.1.2 Flash Crash

We now show the same figures near the flash crash of 05/06/2010. Notice that rows 38 and 39 (or, alternatively, columns 38 and 39 as the matrix is symmetric) are nearly white, implying approximately zero correlation of stocks 38 and 39 with the rest of the stocks in the sample over this period. These stocks are the cause of the lower peaks of correlation discussed above and observed, once again, in near the distribution of correlations near the flash crash (figure 6.11). To see this, we remove stocks 38 and 39 from the correlation matrix and recalculate the histogram. The results for 05/07/2010 can be seen in 6.12. Notice that the peaks of lower correlation completely disappear. Interestingly, stocks 38 and 39 are correspond to Fannie Mae and Freddie Mac, the government-sponsered enterprises. Following the 2008 financial crisis, during which time both companies were bailed out by the U.S. government, both were delisted from the New York Stock Exchange on July 7th, 2010, months after the flash crash [39].

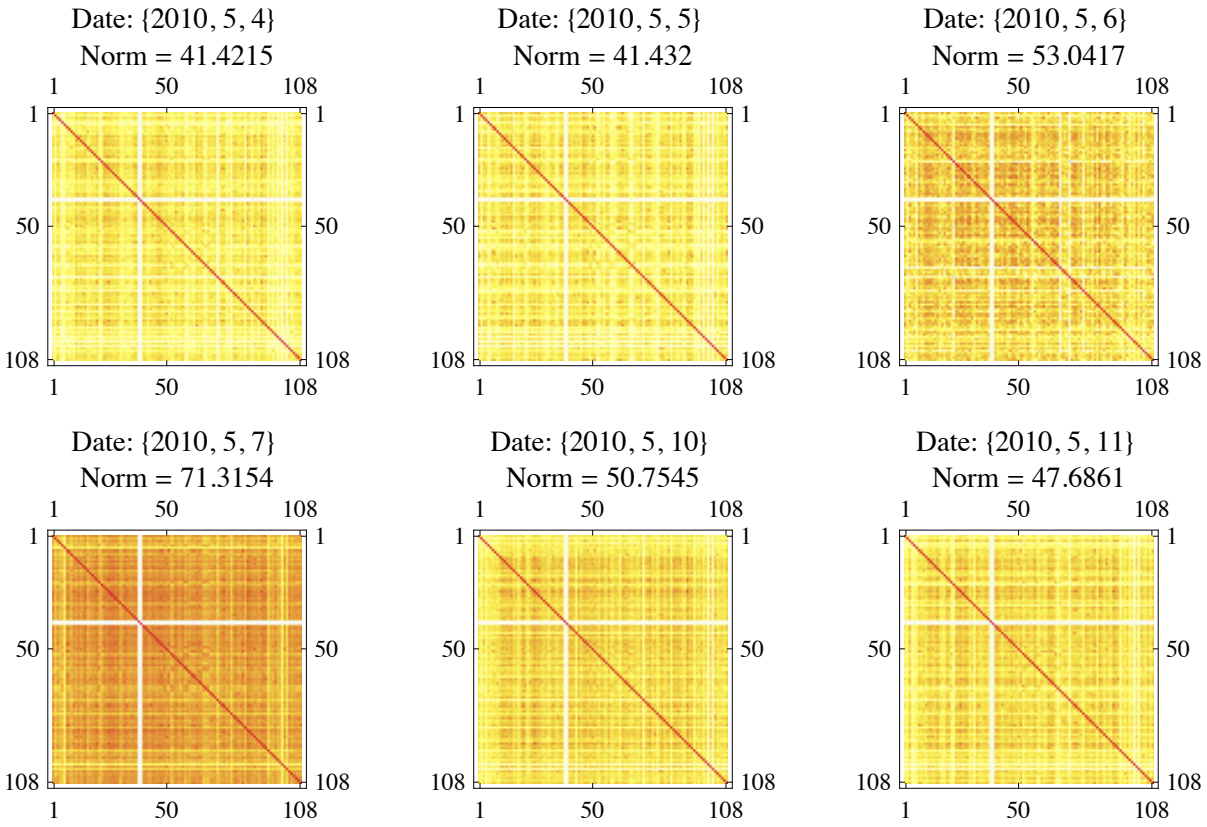

Figure 6.10: Correlation matrices near the flash crash of 05/06/2010.

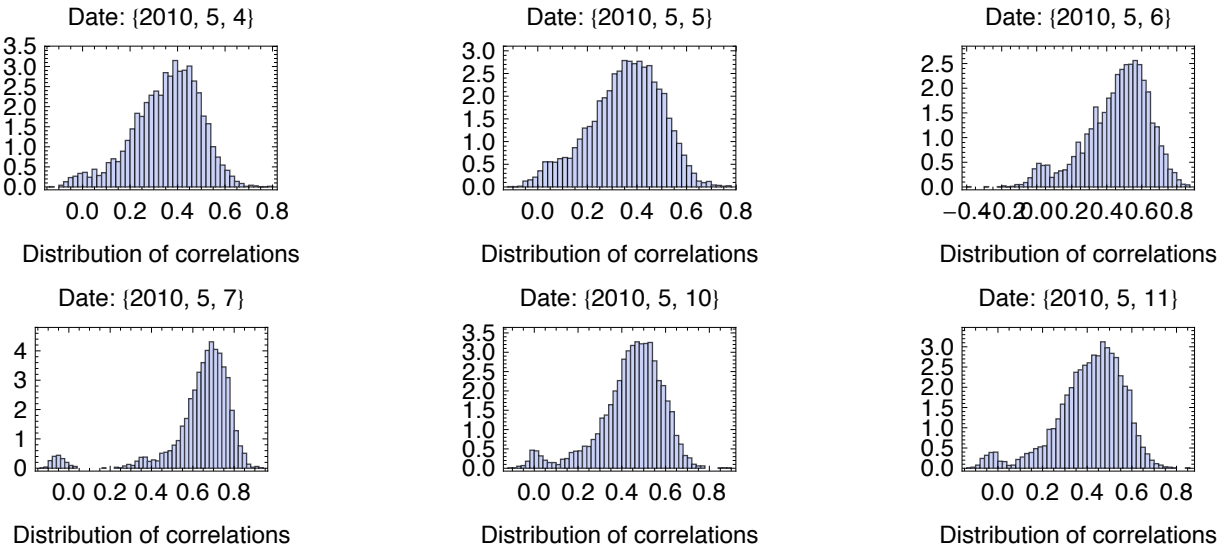

Figure 6.11: Distribution of correlations near the flash crash of 05/06/2010.

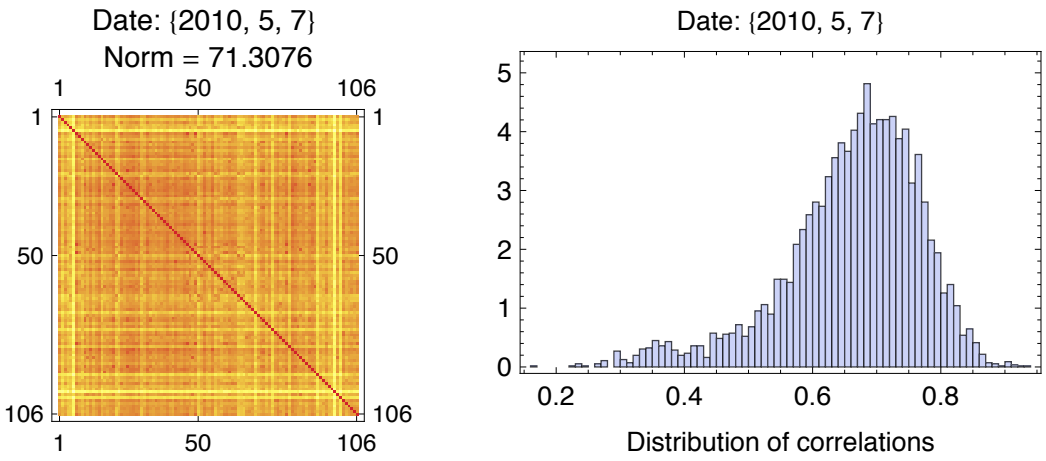

Figure 6.12: Correlation matrix and histogram from 05/07/2010 after removing Fannie Mae and Freddie Mac.

6.3.1.3 2008 Financial Crisis

Here we observe the correlation matrices and the histograms of the correlations near the collapse of Lehman brothers, which occurred on September 15, 2008 [29]. Once again, we do not see peaks of higher correlation.

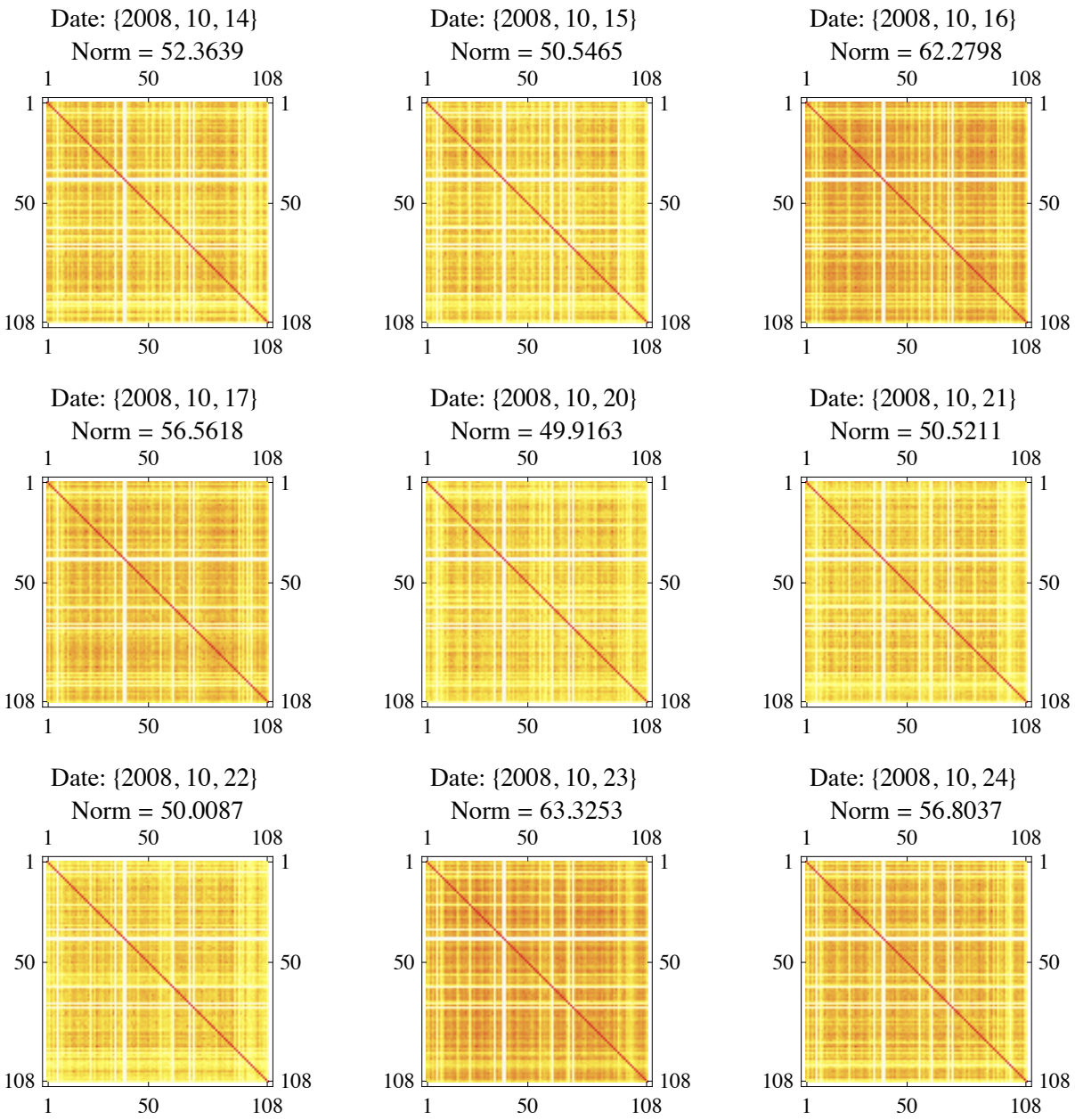

Figure 6.13: Correlation matrices near the collapse of Lehman Brothers.

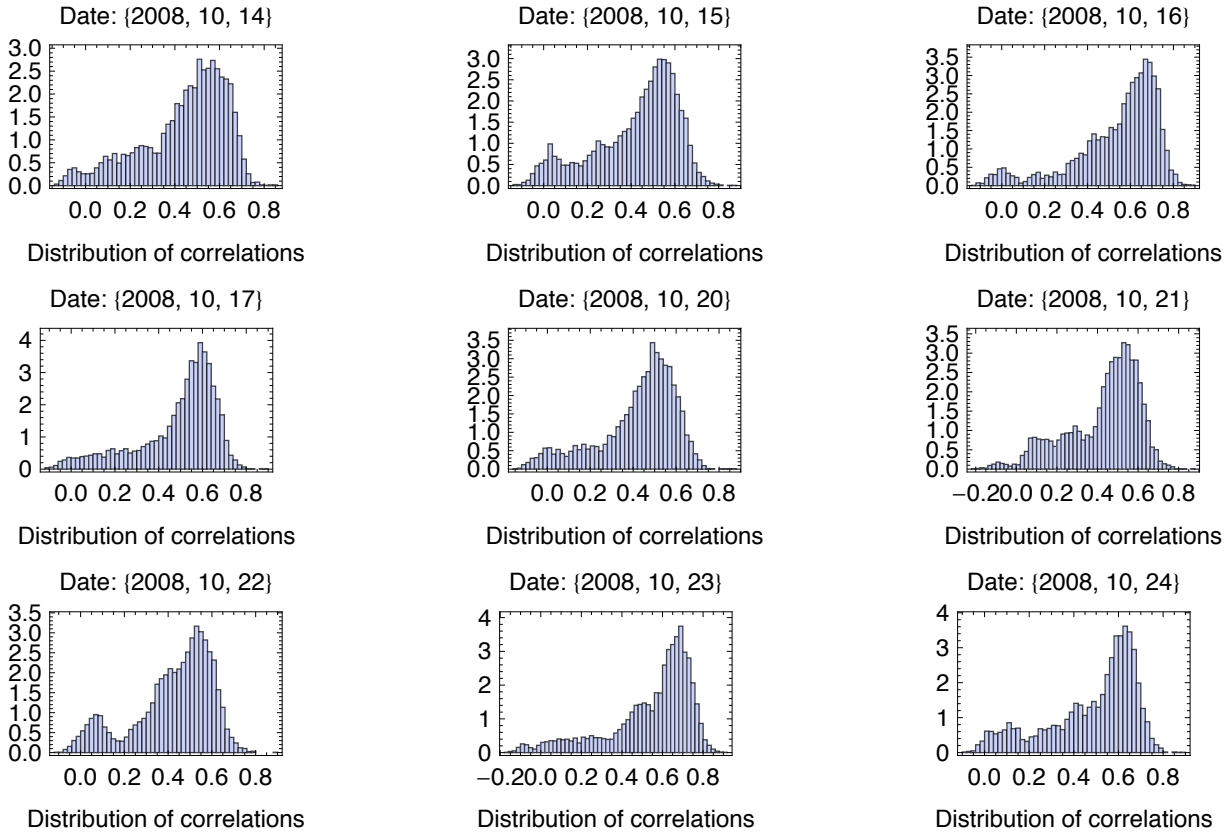

Figure 6.14: Histograms near the collapse of Lehman Brothers.

6.3.1.4 Dot Com Bubble

It is generally considered that the Dot-com bubble burst on March 10th, 2000 [28]. Here we show the correlation matrices histograms in the surrounding days. Notice that the correlations are much smaller than in the more recent crashes. Once again, we do not see evidence of spatial structure to the correlation correlations.

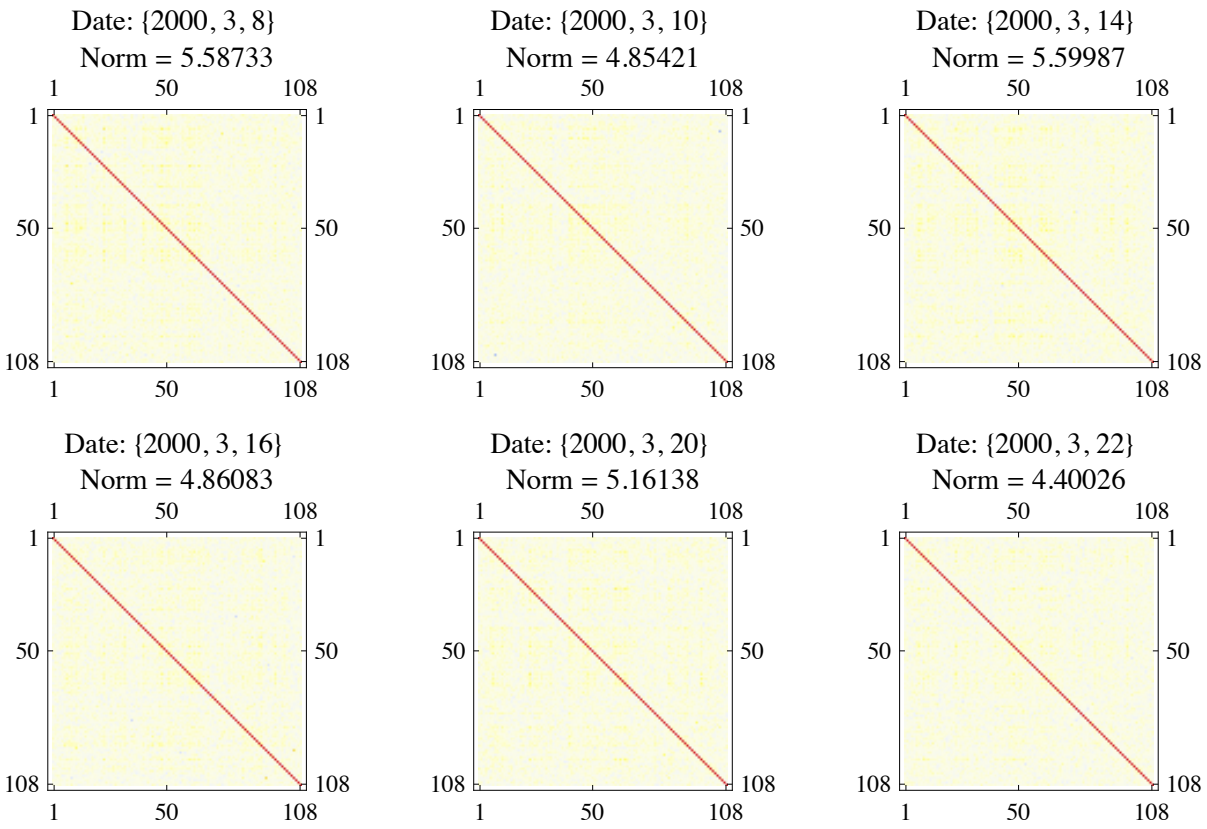

Figure 6.15: Correlation matrices near the bursting of the Dot-com bubble.

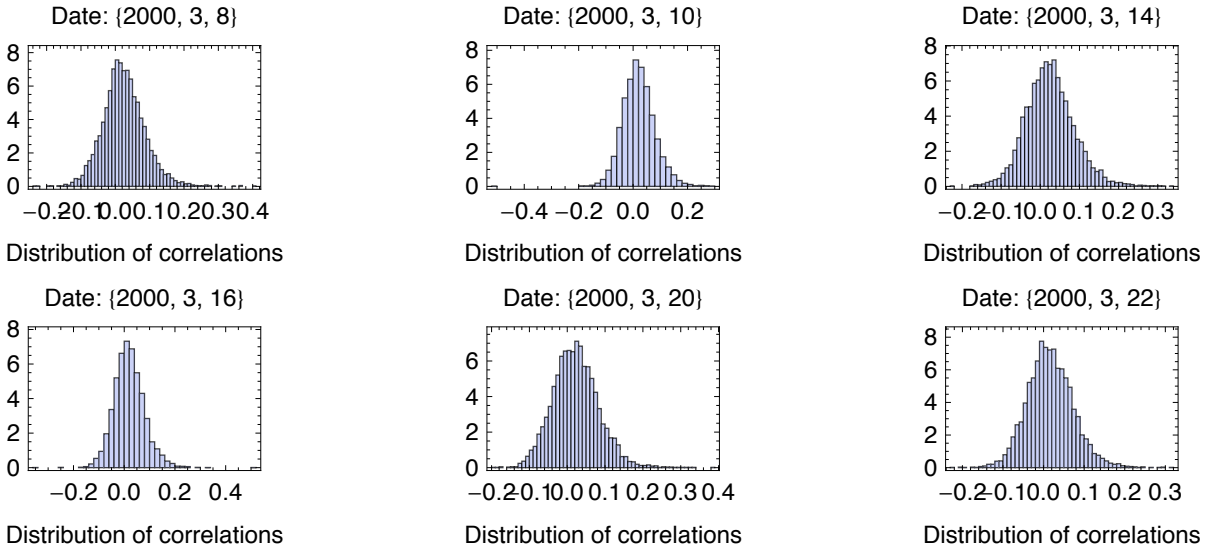

Figure 6.16: Correlation matrices near the bursting of the Dot-com bubble.

6.3.1.5 Asian Financial Crisis

The stock market crash associated with the Asian Financial Crisis is the October 27th, 1997, mini-crash, during which time the Dow Jones industrial average plunged 554.26 points [36]. Although the 2 norm on this date is small relative to the more recent crashes, we note that the mean norm for a 200 day interval centered on this date is 5.46 with a standard deviation of 1.76. The histograms do not exhibit evidence of spatial structure.

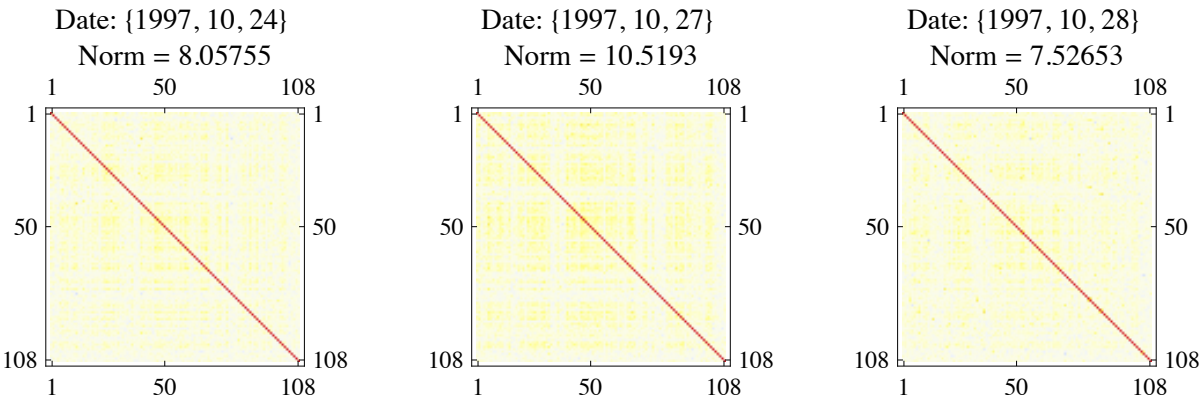

Figure 6.17: Correlation matrices near the mini-crash of 10/27/1997.

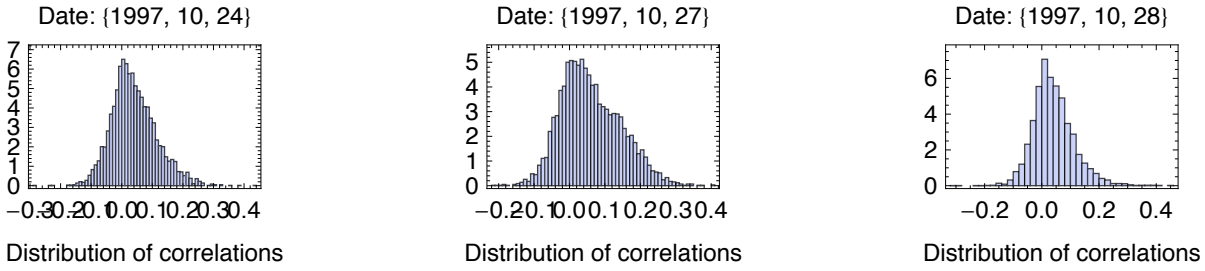

Figure 6.18: Histograms near the mini-crash of 10/27/1997.

6.3.1.6 Distribution of Correlations

We would now like to show the analogue of figure 3.16, which shows the distribution of spin correlations for a 2D Ising model as a function of temperature. Of course, a financial market does not have a temperature, but there are a few analogies of temperature that we may explore. As with distribution of 2D returns we will only consider the off-diagonal elements of the correlation matrix.

Figure 6.19 shows the histogram of stock correlations as a function of the 2 norm of the correlation matrix. We can see that the distributions scale nicely with the norm. Notice that we do not see the additional bumps of higher correlation seen in the distribution of spin correlations for a 2D Ising system. This suggests that stock markets do not have a well-defined same spatial structure. Figure 6.20 shows that the histograms scale nicely with the variance of the eigenvalues as well.

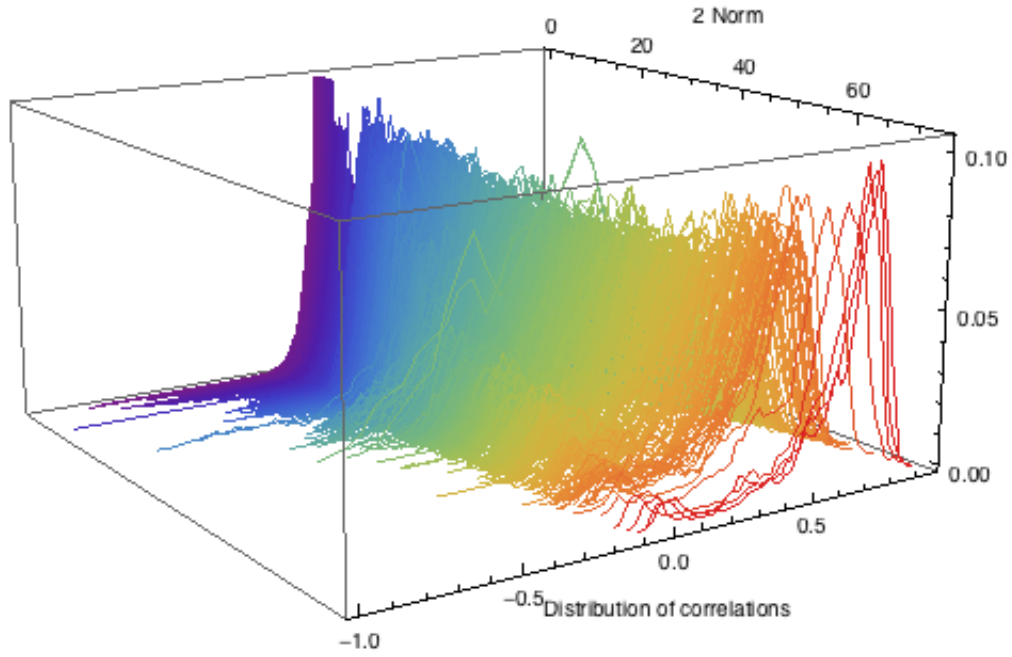

Figure 6.19: Distribution of stock correlations as a function of the 2 norm of the correlation matrix.

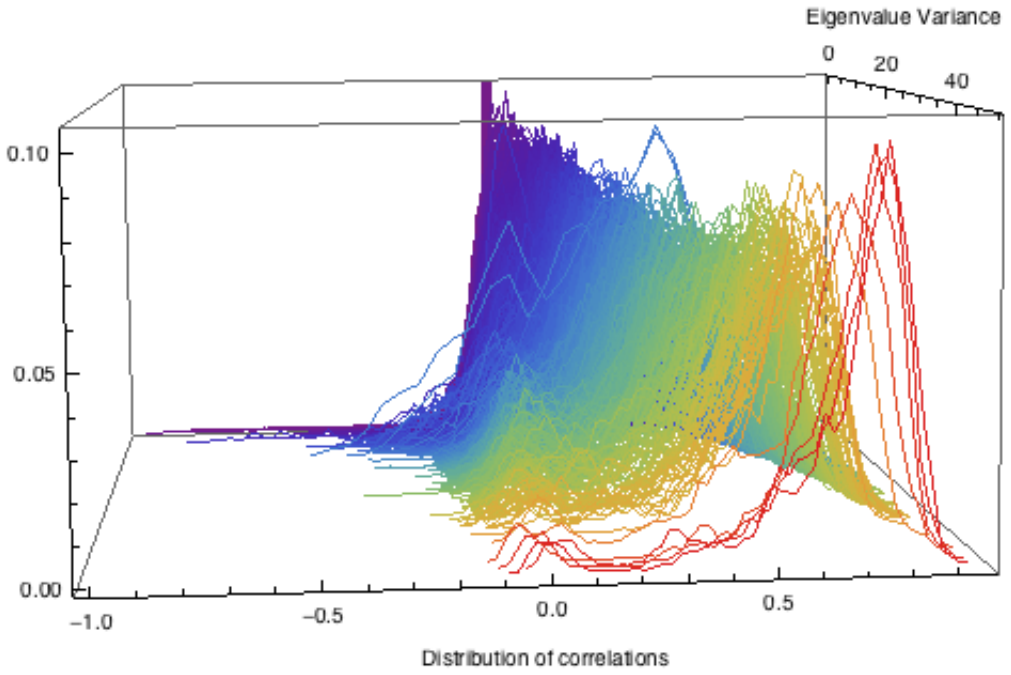

Figure 6.20: Distribution of stock correlations as a function of the variance of the eigenvalues of the correlation matrix.

6.3.1.7 Staircase Function

Finally we will show the staircase plots of each correlation matrix in the sample (figure 6.21). Note that we choose to sort the plots by the 2 Norm of the correlation matrix. Notice that we do not see the additional peak in the staircase plot as observed in the analogous plot of the 2D Ising model. Again, this suggests the nonexistence of

spatial structure to a stock market.

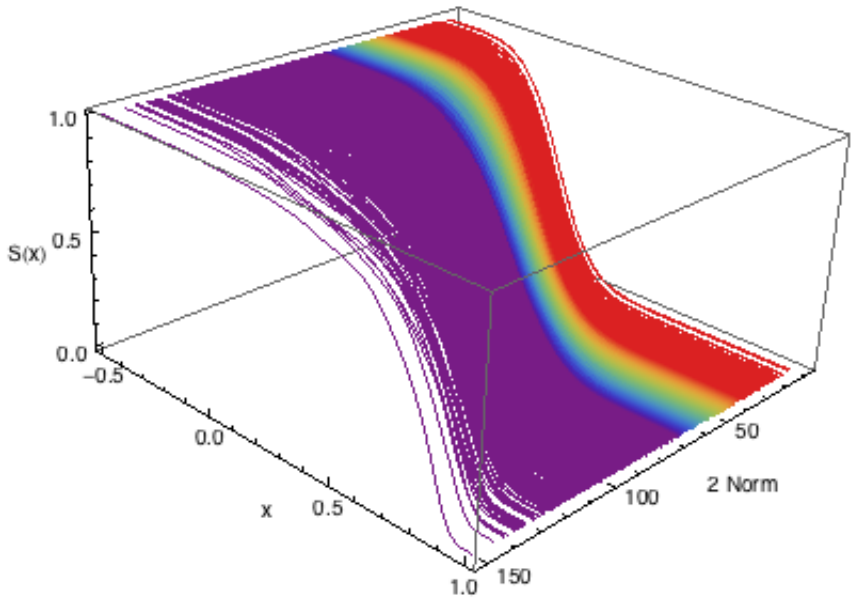

Figure 6.21: Plot of the staircase plots for each correlation matrix in the sample.

6.3.2 Intrahour

We will now examine intrahour correlation matrices, where we define an hour as 60 trading minutes. As showing the actual correlation matrices would quickly fill up a great deal of space, we will focus on the histograms and staircase plots of the correlations, which are the results we are more interested in anyway, since, as already explained, they are independent of the ordering of the matrix. We will also focus on more recent data. This enables us to expand the number of stocks in our sample.

6.3.2.1 2008

Here we observe the data on intrahour correlations in 2008. First we will note a few minor observations, beginning with the peak of correlations near zero. As in the daily case, this is the result of a small number of stocks consistently having nearly zero correlation with other stocks. Although we will spare the details, it appears that the small correlations are due to little variation in the price, not uncorrelated movement in the price. Next, we note the histogram corresponding to June 12, 2008 looks different from the rest (it corresponds to a 2 Norm of about 115 in figure 6.24). As there does not appear to be any significant event that occurred on that day, it is possible the dataset contains an error. The final observation, and, indeed, the most important one, is that the lack of peaks of higher correlation demonstrate a lack of spatial structure, as in the daily case. The other figures are similar to the ones above and require no further explanation.

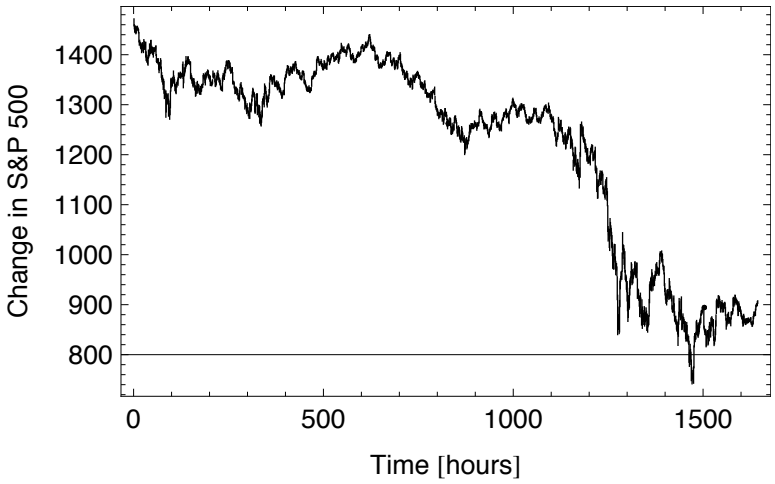

Figure 6.22: Intrahour price changes during the year 2008.

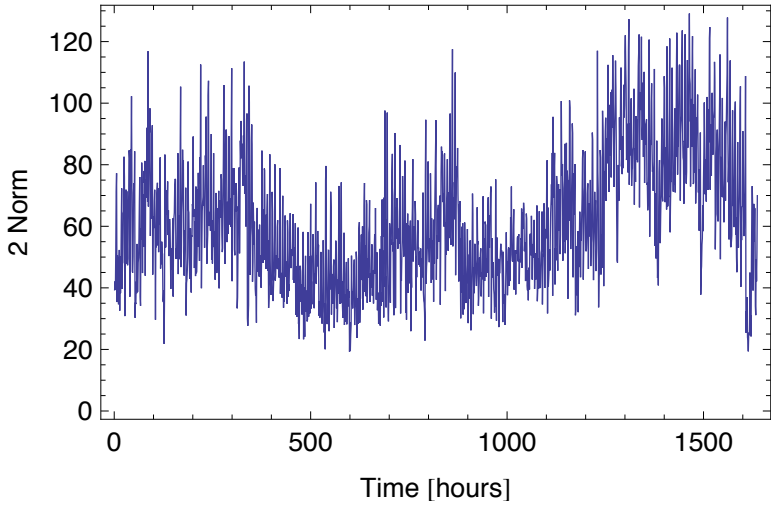

Figure 6.23: Norm of the hourly correlation matrices during 2008.

Rank	Date	Time	2 Norm	Eigenvalue Variance	Price Change	Volatility
1	11/20/2008	10:01-11:00	129.12	81.11	17.44	160.82
2	12/12/2008	9:31-10:30	127.82	79.51	19.82	42.71
3	10/17/2008	12:01-13:00	127.30	78.89	29.50	76.24
4	12/03/2008	10:01-11:00	124.72	75.70	25.17	33.41
5	11/17/2008	11:31-12:30	123.63	74.42	10.88	71.04
6	11/13/2008	10:31-11:30	122.89	73.57	32.56	56.82
7	11/18/2008	12:01-13:00	122.36	72.94	30.22	49.56
8	10/23/2008	12:01-13:00	122.32	72.88	44.51	156.72
9	10/16/2008	9:31-10:30	122.06	72.65	15.79	154.99
10	11/21/2008	11:31-12:30	121.75	72.22	32.47	129.38

Table 6.2: Statistics concerning the hourly correlation matrices in 2008 with the 10 highest 2 norms.

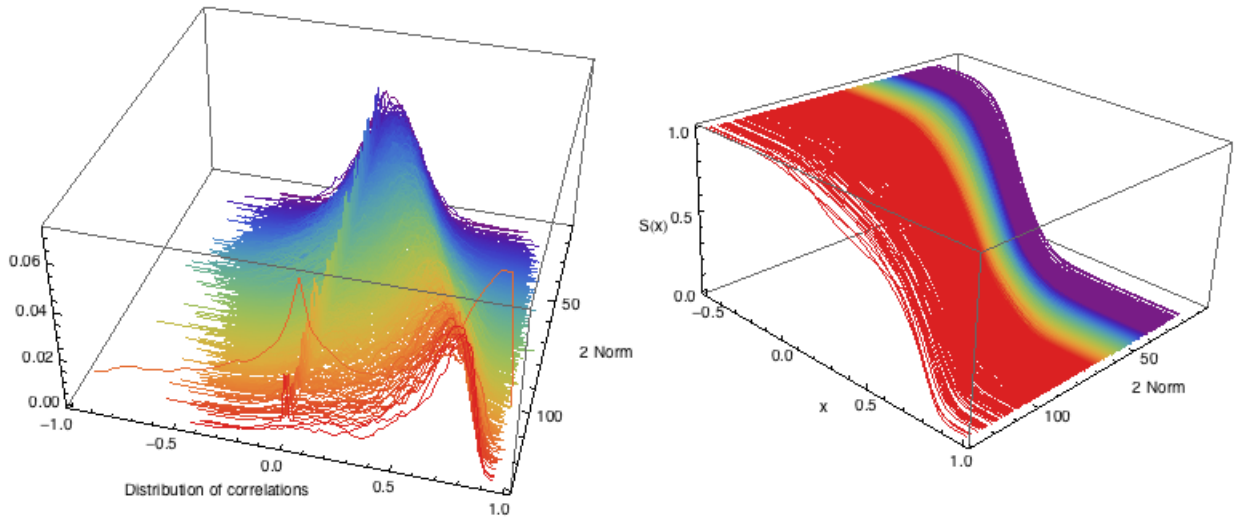

Figure 6.24: Distribution of correlations and staircase plots for 2008 hourly correlations.

6.3.2.2 2010

Here we show the same figures for 2010. Notice the flash crash (which occurred on 05/06/2010) is not on table 6.3, although the day after it is. In figure 6.27 we see the same behavior in the histograms and the staircase plots of the correlations that has been discussed above.

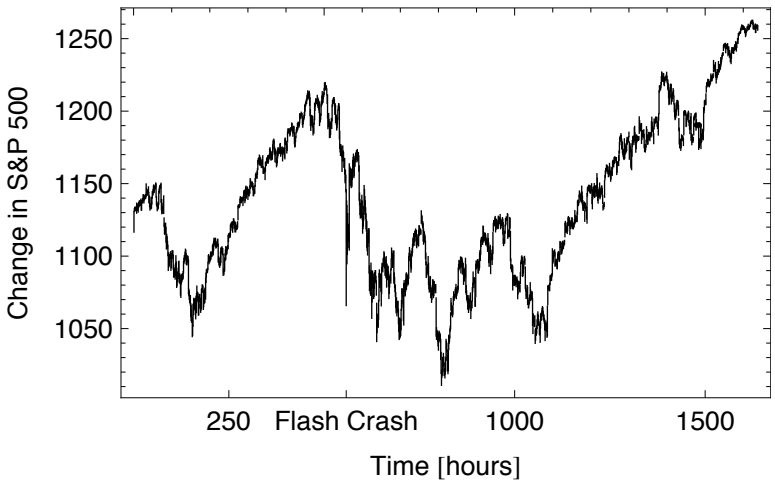

Figure 6.25: Intrahour price changes during the year 2010.

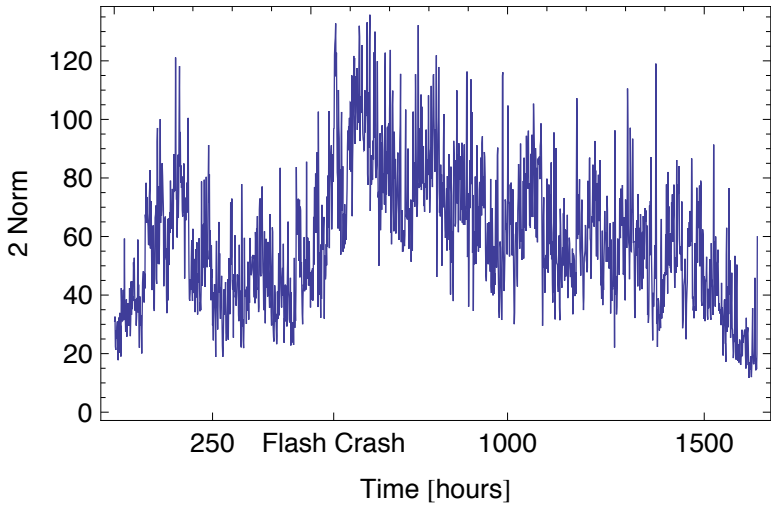

Figure 6.26: Norm of the hourly correlation matrices during 2010.

Rank	Date	Time	2 Norm	Eigenvalue Variance	Price Change	Volatility
1	05/26/2010	15:01-16:00	135.75	89.61	15.28	24.36
2	05/25/2010	14:31-15:30	133.17	86.23	12.95	21.76
3	05/07/2010	12:31-13:30	132.80	85.85	10.46	55.48
4	06/23/2010	14:31-15:30	132.20	85.03	10.98	18.97
5	05/20/2010	14:01-15:00	131.98	84.70	16.68	27.61
6	05/28/2010	15:01-16:00	129.97	82.26	9.58	14.97
7	05/20/2010	15:01-16:00	128.28	80.20	16.47	23.48
8	05/07/2010	11:31-12:30	127.77	79.45	17.98	76.48
9	05/26/2010	14:01-15:00	126.71	78.15	10.46	18.27
10	05/07/2010	10:31-11:30	125.78	77.16	25.78	74.62

Table 6.3: Statistics concerning the hourly correlation matrices in 2010 with the 10 highest 2 norms.

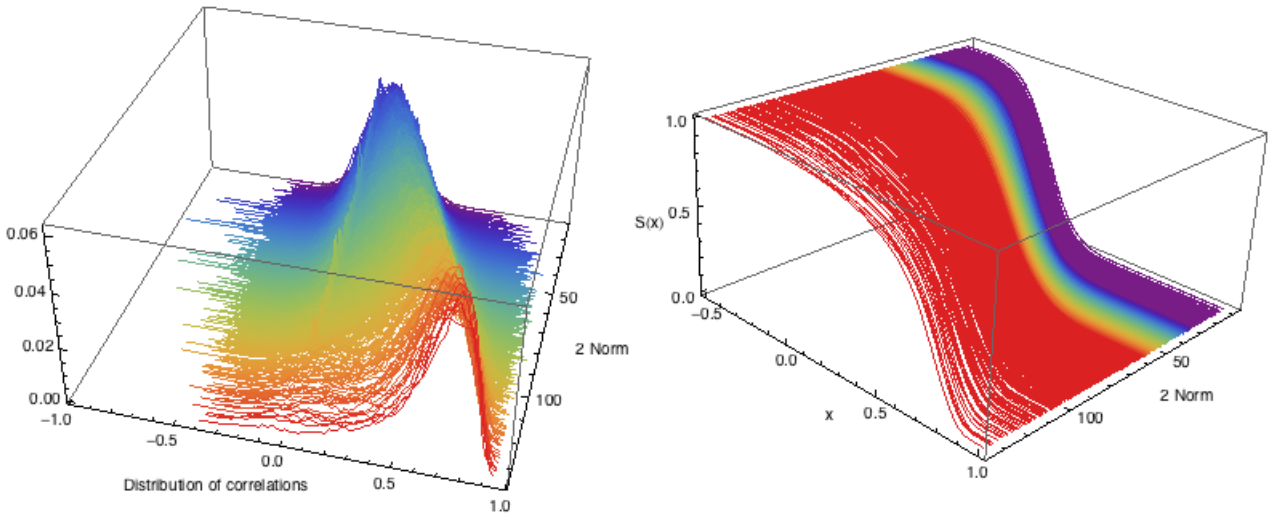

Figure 6.27: Distribution of correlations and staircase plots for 2010 hourly correlations.

6.3.2.3 2011

Finally, we show the results for 2011. Notice from figure 6.30 that the peak of zero correlation is smaller than in 2008 and 2010, suggesting that stocks were more actively traded. Also, notice the prevalence of August 2011 (near the U.S. credit downgrade) in table 6.4. The other figures require no further explanation at this point.

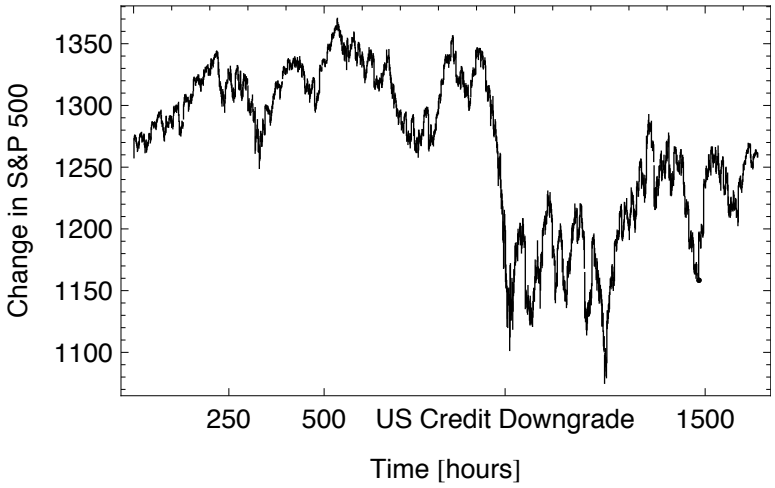

Figure 6.28: Intrahour price changes during the year 2011.

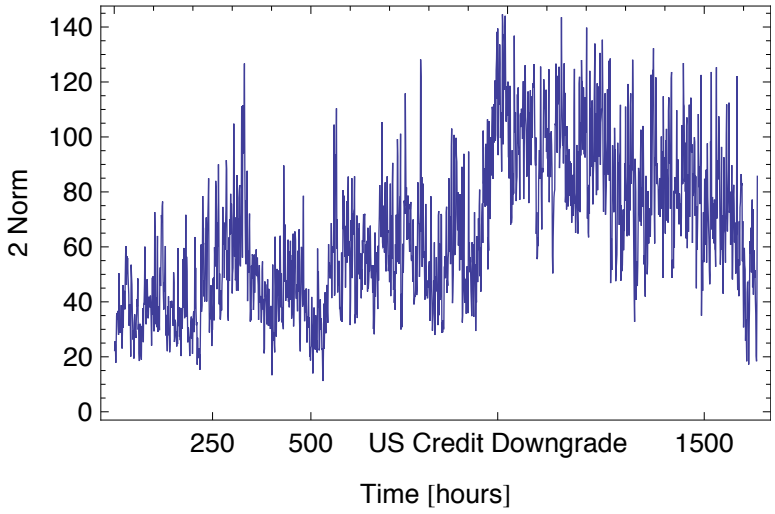

Figure 6.29: Norm of the hourly correlation matrices during 2011.

Rank	Date	Time	2 Norm	Eigenvalue Variance	Price Change	Volatility
1	08/09/2011	14:01-15:00	144.62	101.72	38.34	204.70
2	08/10/2011	14:31-15:30	144.09	100.80	21.35	54.74
3	09/12/2011	14:31-15:30	143.56	100.08	11.17	21.76
4	08/09/2011	15:01-16:00	140.10	95.35	57.57	89.31
5	09/26/2011	13:31-14:30	139.78	94.94	9.14	31.92
6	08/05/2011	15:01-16:00	139.49	94.55	13.44	34.34
7	08/05/2011	13:01-14:00	138.24	92.83	16.43	84.29
8	08/10/2011	12:31-13:30	137.48	91.85	12.05	57.08
9	08/16/2011	11:31-12:30	136.85	91.03	10.63	41.82
10	10/04/2011	14:31-15:30	135.38	89.10	14.10	35.65

Table 6.4: Statistics concerning the hourly correlation matrices in 2011 with the 10 highest 2 norms.

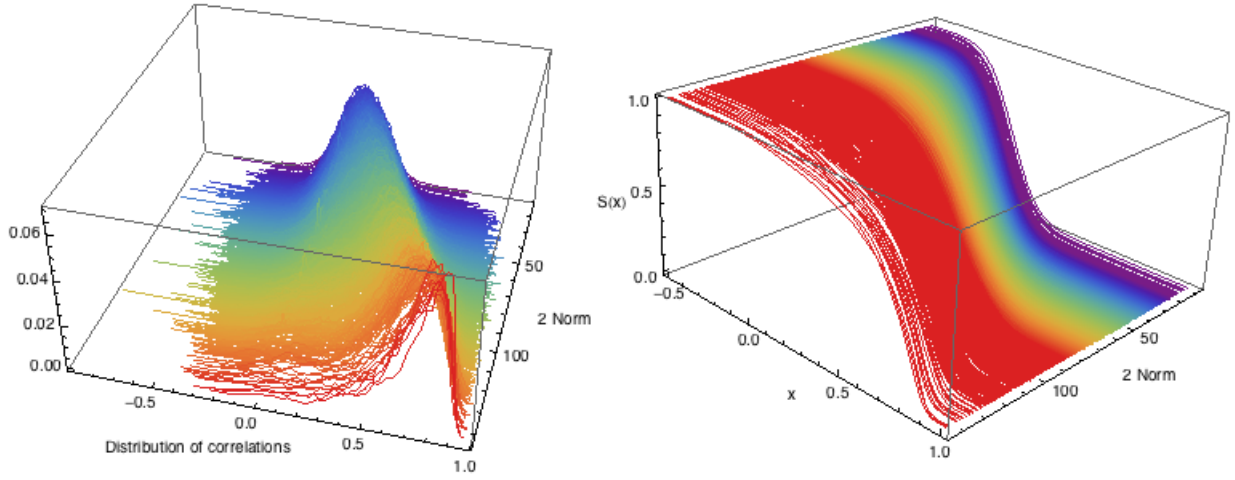

Figure 6.30: Distribution of correlations and staircase plots for 2011 hourly correlations.

Chapter 7

0D Ising Model

We will now propose a 0D Ising model, where each spin interacts with each other spin. This means the adjacency matrix is identically 1 off the diagonal (and zero on the diagonal as spins still do not interact with themselves). Geometrically, one can consider each spin to be concentrated at a single point. Unlike in the other dimensions we have discussed, the Ising model in 0D is not studied in condensed matter physics as there is no physical analogue. In this section we will derive important properties of the 0D model and we will show the results of Monte Carlo simulations. Our primary observation concerning the 0D model is that although it may exist in paramagnetic and ferromagnetic states, strictly speaking it does *not* have a phase transition. To show this we will start by analyzing the partition function.

7.0.3 Partition Function

Recall that the macroscopic behavior of a system may be extracted from the partition function, but that the partition function is often very difficult to compute. Even in the case of an Ising system, the definition of the partition function involves a sum of 2^N exponential terms, as there are 2^N states in an Ising system. We will now show that the partition function of a 0D Ising model may be written as a sum of only N exponential terms. Although this equation is still difficult to handle, for small N we can exploit it to calculate analytical expressions for the internal energy and magnetization. We will then use these expressions to justify the claim that the 0D model does not have a phase transition. Along the way we will obtain a simplified form of the Hamiltonian for a 0D Ising model that will reduce the computation time required for Monte Carlo simulations.

First notice that since the Hamiltonian $H(\sigma)$ gives the energy of the system, where σ represents a particular spin configuration, the expression for the partition function (equation 3.2) becomes:

$$Z = \sum_{\sigma} e^{-\beta H(\sigma)} \tag{7.1}$$

The key to deriving equation a simplified partition function is the following observation: since there is no topological structure to the 0D Ising model, the particular arrangement of spins does not matter (i.e. does not affect the Hamiltonian); rather, it is only the number of spins in each state that matters. Therefore we may write $H(\sigma) = H(n)$, where n is the number of, say, negative spins in spin configuration σ. Since there are $\binom{N}{n}$ spin configurations with n negative spins we have

$$Z = \sum_{n=0}^{N} \binom{N}{n} e^{\beta H(n)}. \tag{7.2}$$

If we further assume that the interaction matrix J and the external magnetic field h are constant, the definition

of the Ising Hamiltonian becomes:

$$H(n) = -J \sum_{\langle i,j \rangle} \sigma_i \sigma_j - h \sum_i \sigma_i \tag{7.3}$$

where the notation $\langle i, j \rangle$ indicates that the sum is taken over all adjacent pairs, counting each pair once (i.e. not $\langle j, i \rangle$ if we have already counted $\langle i, j \rangle$). Of course, as spins are not allowed to interact with themselves, we do not count the pair $\langle i, i \rangle$.

Now, we would like to derive a simpler expression for $H(n)$. We can do this by first altering the definition of the Hamiltonian, given above. Specifically. we will double count each adjacent pair (i.e. by including $\langle j, i \rangle$ as well as $\langle i, j \rangle$ in the summation) and we will considers spins to be adjacent to themselves (i.e. by including $\langle i, i \rangle$ in the summation). We will denote this new first term by $J \sum'_{\langle i,j \rangle} \sigma_i \sigma_j$. Upon computing this new summation we will adjust the result so that it is equivalent to the original summation in the Hamiltonian. To this end, first consider the contribution of the $N - n$ positive spins to the summation. Each positive spin will contribute $+1$ for each other positive spin, and -1 for each negative spin. Thus, the contribution of the positive spins to the summation is $(N - n)[(N - n) - n] = (N - n)(N - 2n)$. Similarly, each of the n negative spins will contribute $+1$ for each other negative spin and -1 for each positive spin. Therefore, the contribution of the negative spins to the summation is $n[n - (N - n)] = n(N - 2n)$. If we add each of these two contributions we have that for a system with n negative spins, $\sum'_{\langle i,j \rangle} J_{ij} \sigma_i \sigma_j = (N - 2n)^2$. To get the original summation, we need to adjust the new summation for our altered assumptions. To remove the contribution due to spins interacting with themselves, we need to subtract N from the new summation. Then, to remove the contribution due to counting each adjacent pair twice, we need only divide by 2, since the interactions are symmetric. Thus, we have $\sum_{\langle i,j \rangle} J_{ij} \sigma_i \sigma_j = \left[(N - 2n)^2 - N \right] / 2$.

The effect of the second term, $\sum_i h_i \sigma_i$, is more straightforward. The n negative spins will cancel out n positive spins, leaving $N - 2n$ remaining positive spins to add to the sum. Thus, $\sum_i h_i \sigma_i = h_i [N - 2n]$. Therefore,

$$H(n) = -J \left[(N - 2n)^2 - N \right] / 2 - h[N - 2n]. \tag{7.4}$$

This expression for the Hamiltonian will greatly reduce the computation time required in a Monte Carlo simulation of the 0D Ising model. If we plug this expression into equation 7.2 we have a simplified expression for the 0D partition function

$$Z = \sum_{n=0}^{N} \binom{N}{n} e^{J\beta \left[(2n-N)^2 - N \right] / 2 + h\beta [2n - N]}. \tag{7.5}$$

7.0.4 Lack of Phase Transition

For small N it is possible to apply equations 3.6 and 3.20 to obtain analytical expressions for the magnetization and the internal energy. The following were computed with Mathematica for $N = 4$:

$$Z = e^{(6J-4h)\beta} + 4e^{-2h\beta} + 6e^{-2J\beta} + 4e^{2h\beta} + e^{(6J+4h)\beta} \tag{7.6}$$

$$\langle M \rangle = \frac{-8e^{-2h\beta} + 8e^{2h\beta} - 4e^{(6J-4h)\beta} + 4e^{(6J+4h)\beta}}{4e^{-2h\beta} + 4e^{2h\beta} + 6e^{-2J\beta} + e^{(6J-4h)\beta} + e^{(6J+4h)\beta}} \tag{7.7}$$

$$U \equiv \langle E \rangle = -\frac{-8he^{-2h\beta} + 8he^{2h\beta} - 12Je^{-2J\beta} + (6J - 4h)\, e^{(6J-4h)\beta} + (6J + 4h)\, e^{(6J+4h)\beta}}{4e^{-2h\beta} + 4e^{2h\beta} + 6e^{-2J\beta} + e^{(6J-4h)\beta} + e^{(6J+4h)\beta}} \tag{7.8}$$

One can see that even for relatively small N, the calculations grow cumbersome quite quickly. Now, figure 7.1 shows a plot of the internal energy as a function of temperature in zero magnetic field, where we let $k = 1$ and

$J = 1$. Certainly we can see a sudden change in the energy as a function of temperature. However, notice that an increase in the system size both shifts the internal energy curve outwards and softens the transition between the low energy and high energy states. As $N \to \infty$ we expect the internal energy curve to approach a horizontal line. If the 0D model had a critical temperature, it would certainly increase with N. That is, it would not be an intensive property of the system. This violates our definition of phase transition and we thus conclude that the 0D model does not have a phase transition. Yet, as the sudden change in internal energy illustrates, the 0D model exhibits behavior similar to a phase transition. We will define this behavior as a *pseudo-phase transition.* This concept will become more clear in section 7.1 where we show the results of Monte Carlo simulations of the 0D Ising model. The equations above also imply that the mean magnetization is always zero for all system sizes. We will see in the next section, however, that the simulations of the 0D Ising model exhibit "pinning", whereby a net magnetization is observed. This illustrates the difference between a time average and an ensemble average, as discussed in chapter 3. It also illustrates that the 0D model does not exhibit ergodicity breaking at the pseudo-critical point as the magnetization will eventually flip signs.

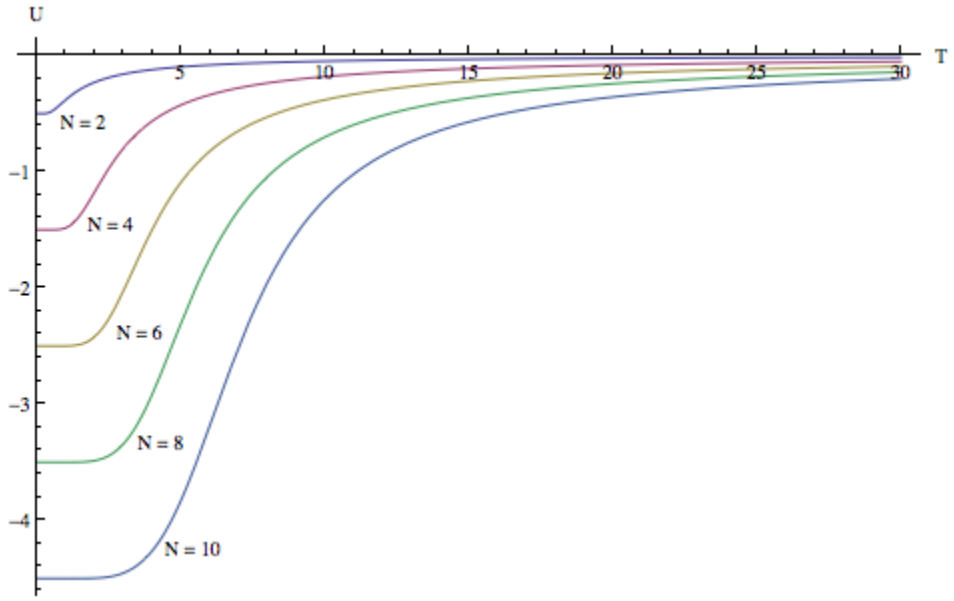

Figure 7.1: Internal energy as a function of temperature for a selection of system sizes.

7.1 Simulations of 0D

In the spirit of section 3.3.3, we will now show the results of a collection of Monte Carlo simulations of the 0D Ising model. As before, we will use the Metropolis algorithm.

We will begin by focusing on a system of $N = 100$ spins. As with the 2D simulations, for each simulation we will run for 1000 sweeps to reach equilibrium and then run for an additional 10,000 sweeps to calculate the mean magnetization M, the internal energy U, and the time-averaged correlation matrix C. The time-averaged correlation matrix will be calculated with a subsequence length of $L = 1000$ sweeps and an offset of $K = 1$ sweeps.

Figures 7.2 and 7.3 show the correlation matrices for a selection of temperatures. Notice the absence of the diagonal bands observed in the 2D simulations. However, the correlations increase just below a temperature of around 80, and decrease afterwards. This is reminiscent of a phase transition. Figure 7.4 shows the 2 norm of the correlation matrix as a function of T.

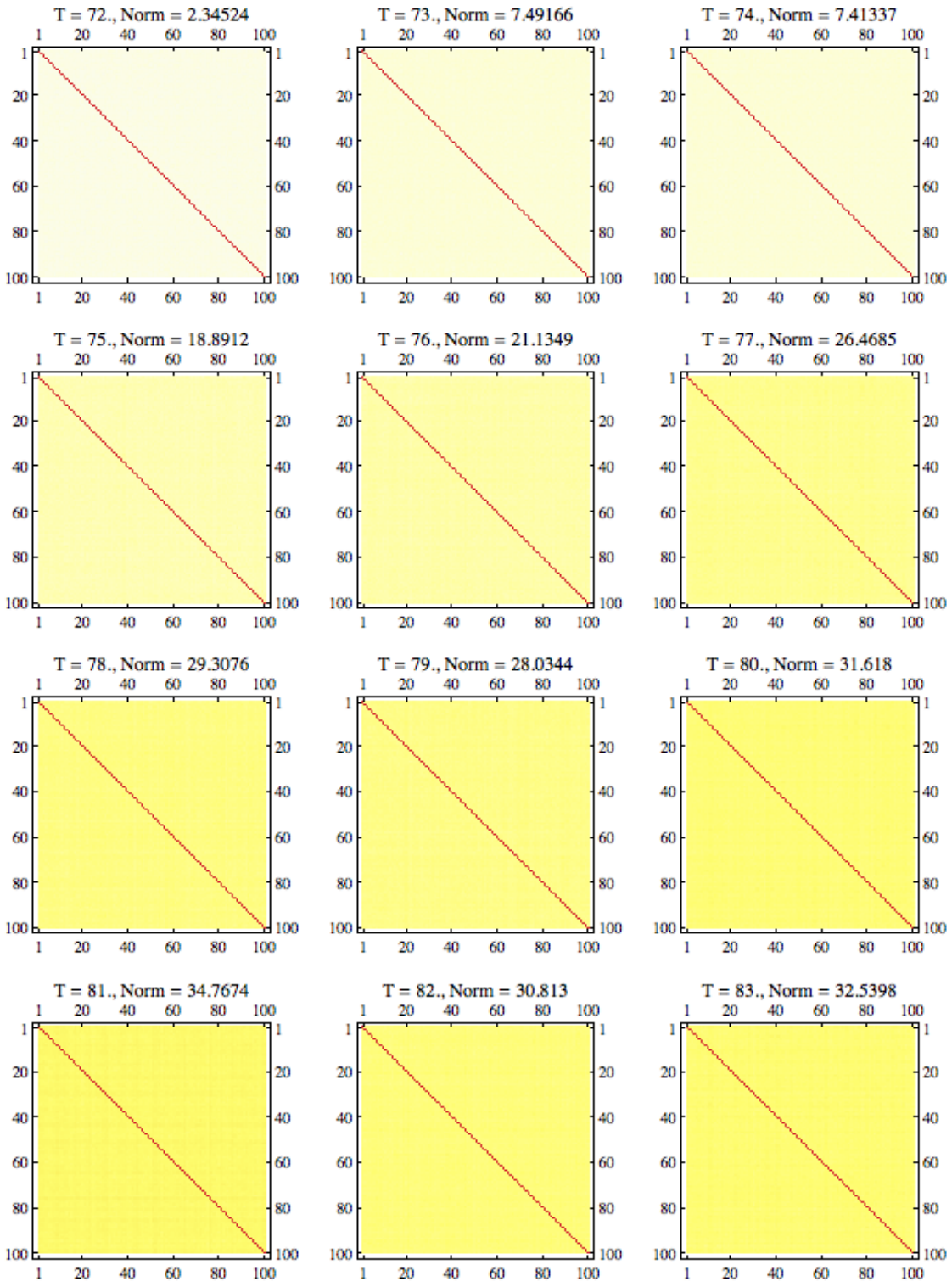

Figure 7.2: Correlation matrices of a 0D Ising model simulations (part 1).

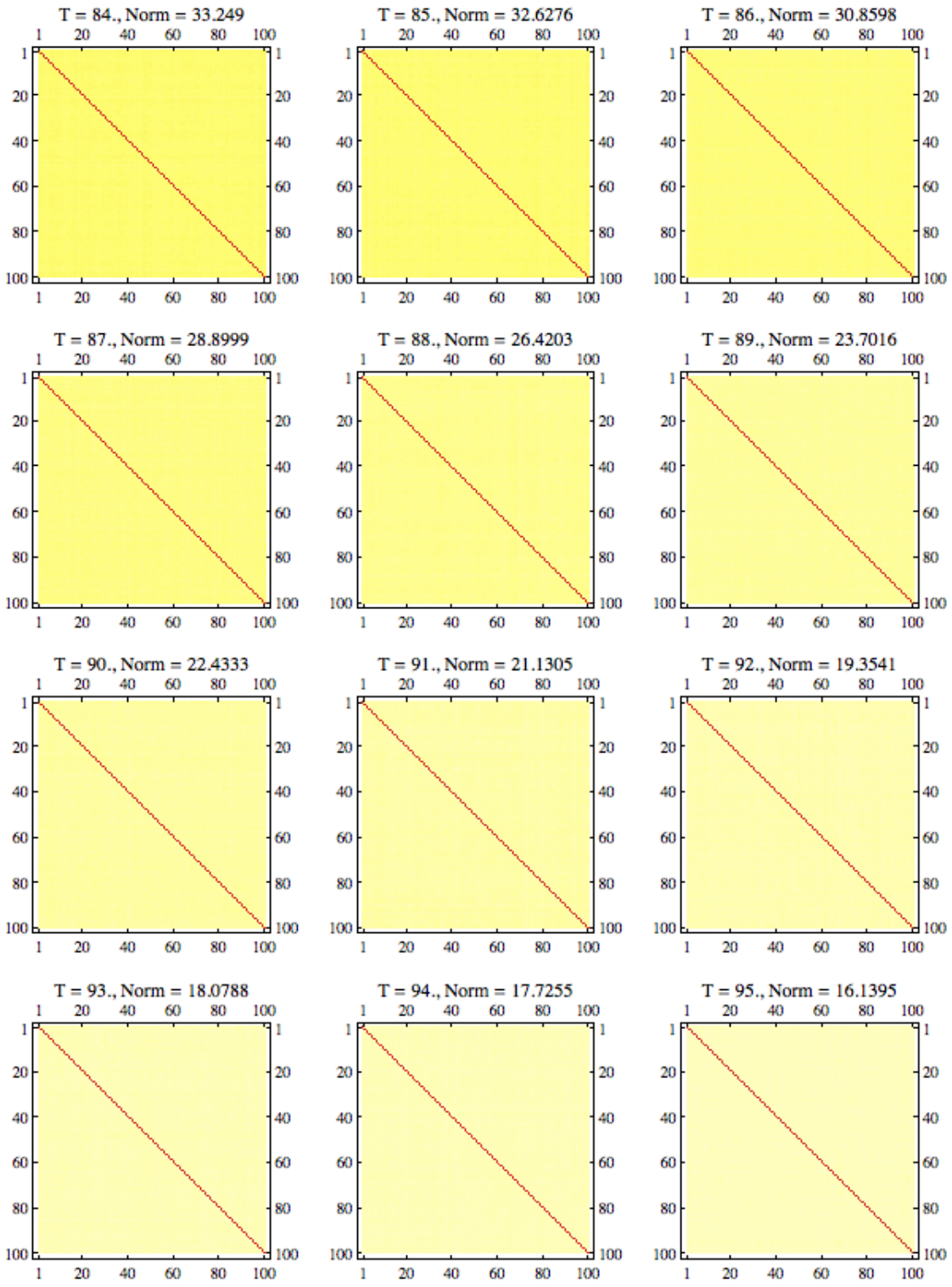

Figure 7.3: Correlation matrices of a 0D Ising model simulations (part 2).

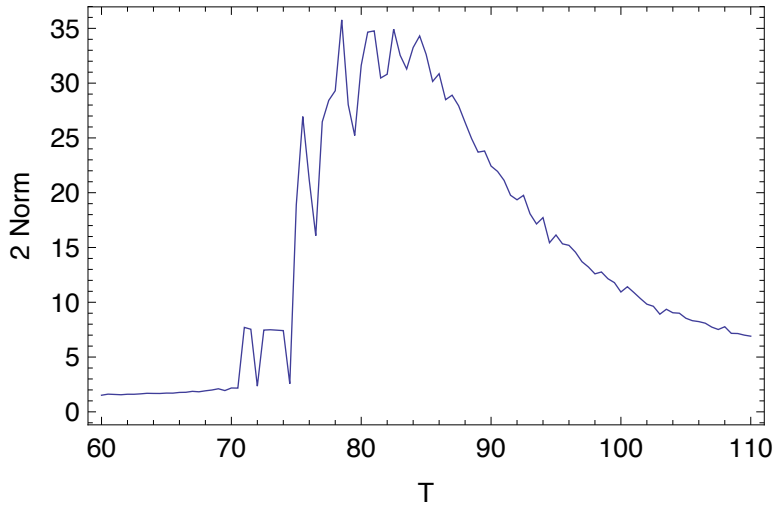

Figure 7.4: Matrix 2-norm as a function of temperature.

Figure 7.5 shows the internal energy and mean magnetization as a function of T. The plot of the internal energy seems to agree with the results predicted by the partition function for small N. However, the plot of the mean magnetization exhibits a "pinned" magnetization for low temperature. Recall that the partition function predicts a mean magnetization of zero for all temperatures. To explain this difference we offer the following explanation: a 0D Ising system does not experience ergodicity breaking at the pseudo phase transition. Over a finite amount of time, the 0D system may exhibit non-zero net magnetization. However, in the limit, the system will cross between spin up and spin down states, giving a net magnetization of zero. This is the magnetization calculated from the partition function. The difference corresponds to the difference in taking a finite time average of a macroscopic quantity and an ensemble average.

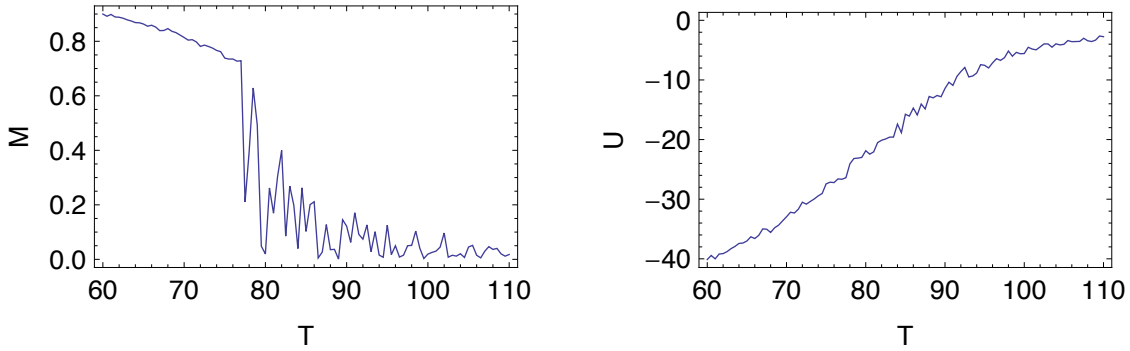

Figure 7.5: s.

The next two figures, 7.6 and 7.7, show U and M for a selection of system sizes. Here we can see that the transition temperature shifts outwards with increased system size. This is in agreement with the theoretical prediction of the partition function.

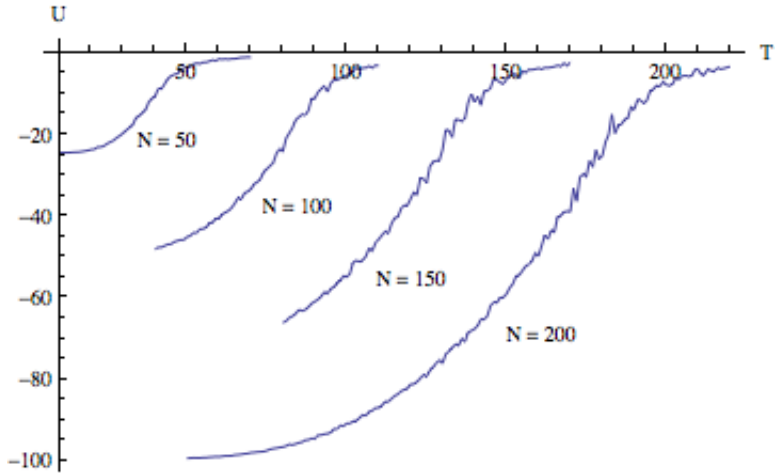

Figure 7.6: Internal energy from 0D simulations for different N.

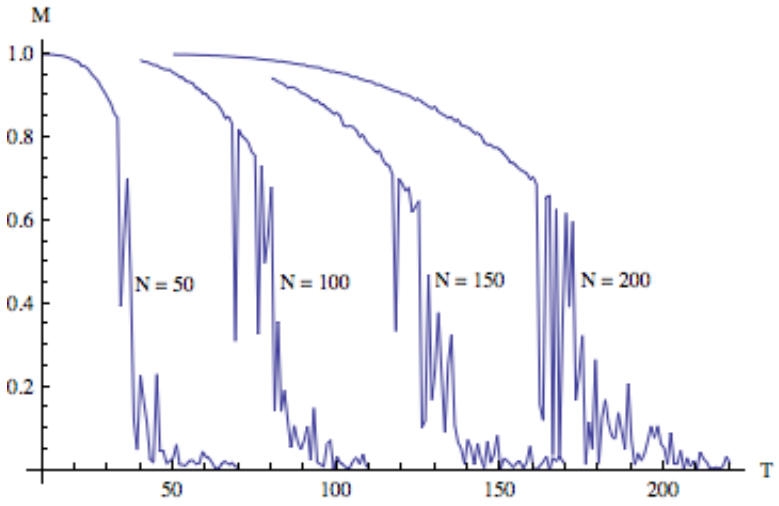

Figure 7.7: Mean magnetization from 0D simulations for different N.

Last, in figures 7.8 and 7.9, we show plots of the distribution of correlations and the staircase function for a variety of temperatures. Notice that the correlation plots do not exhibit the additional bumps of higher correlation that are characteristic of the 2D system near the critical point. Indeed we see little change in the distributions near the transition, other than than an outward shift in the mean. The observations in the staircase plots are similar: the additional bumps are not exhibited and the plots seem only to shift outward near the transition. Also, notice that the slope of the staircase plot is much steeper than in the 2D simulation.

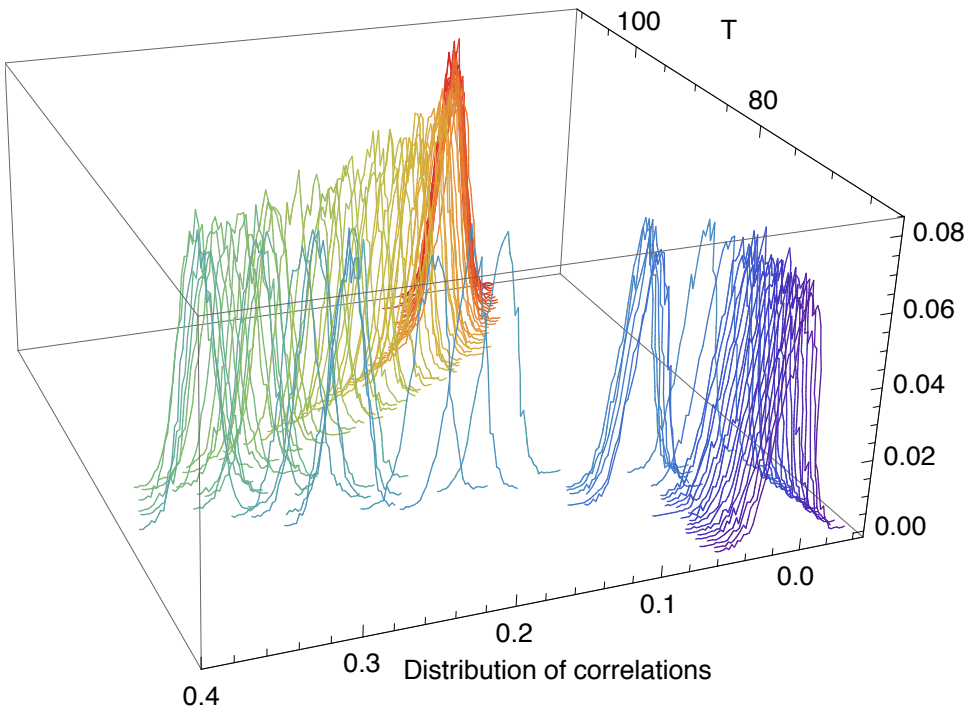

Figure 7.8: Distribution of correlations for a variety of temperatures.

.

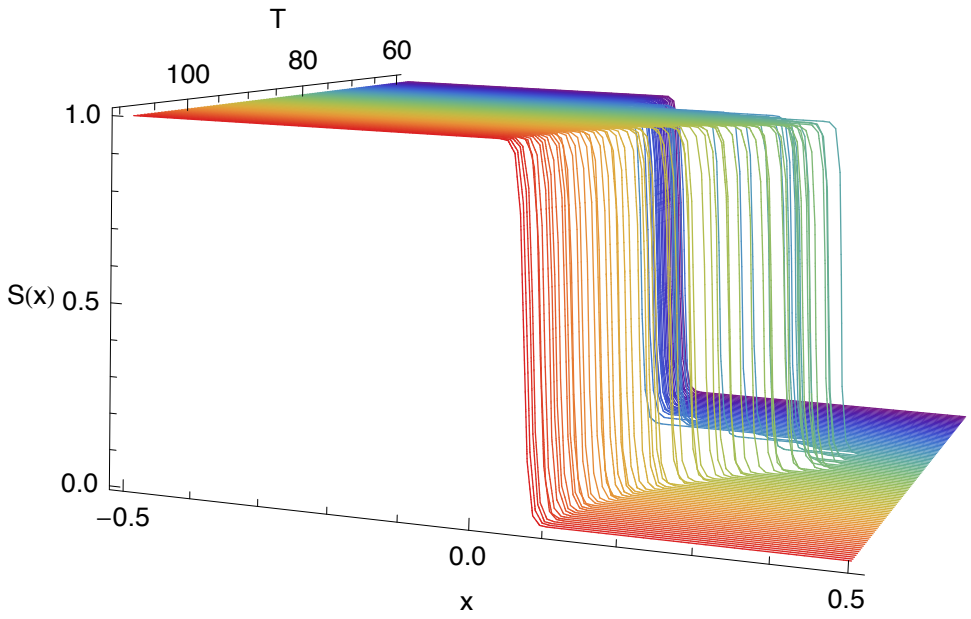

Figure 7.9: Staircase plots for a variety of temperatures.

7.2 With Random Coupling Matrix

As we argued earlier in the discussion of the 2D Ising model, we do not expect a stock market to be described by a Hamiltonian with constant coupling coefficients J_{ij}. The simulations below show that, as with the 2D model, randomly coefficients (on the interval $[0, 1]$, as before) do not substantially alter the behavior of the system, other than by lowering the critical temperature. The correlation matrices themselves are not shown as they are similar

to the results from figures 7.2 and 7.3.

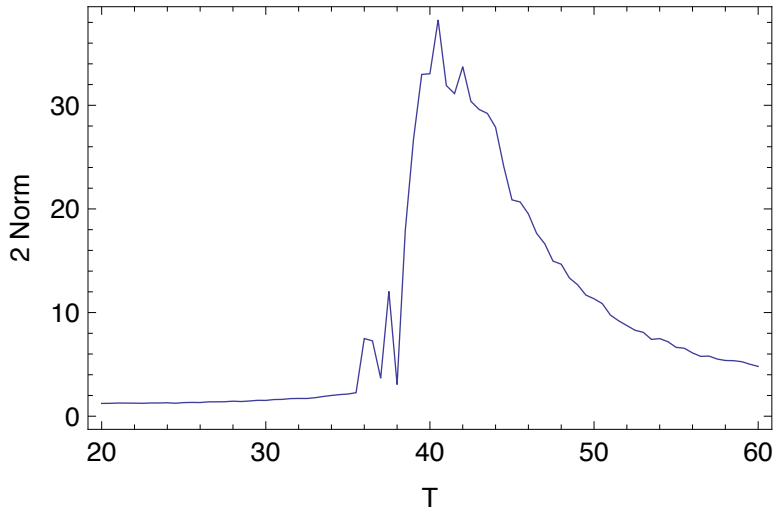

Figure 7.10: 2 norm as a function of temperature.

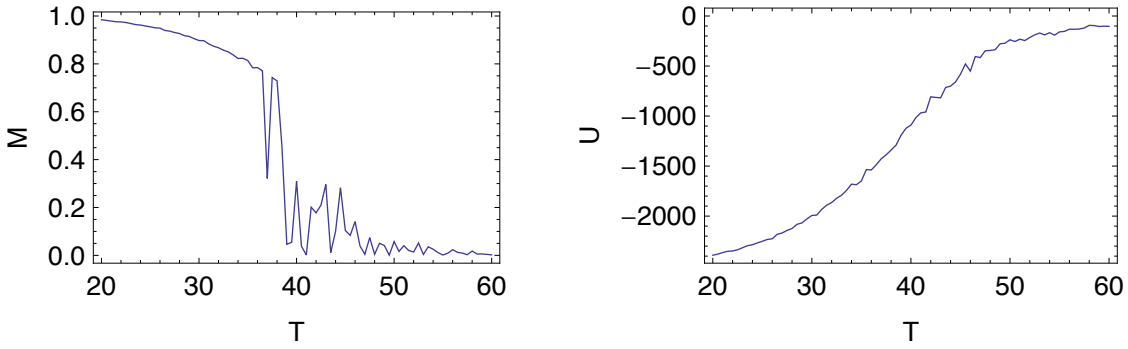

Figure 7.11: Mean magnetization and internal energy as a function of temperature.

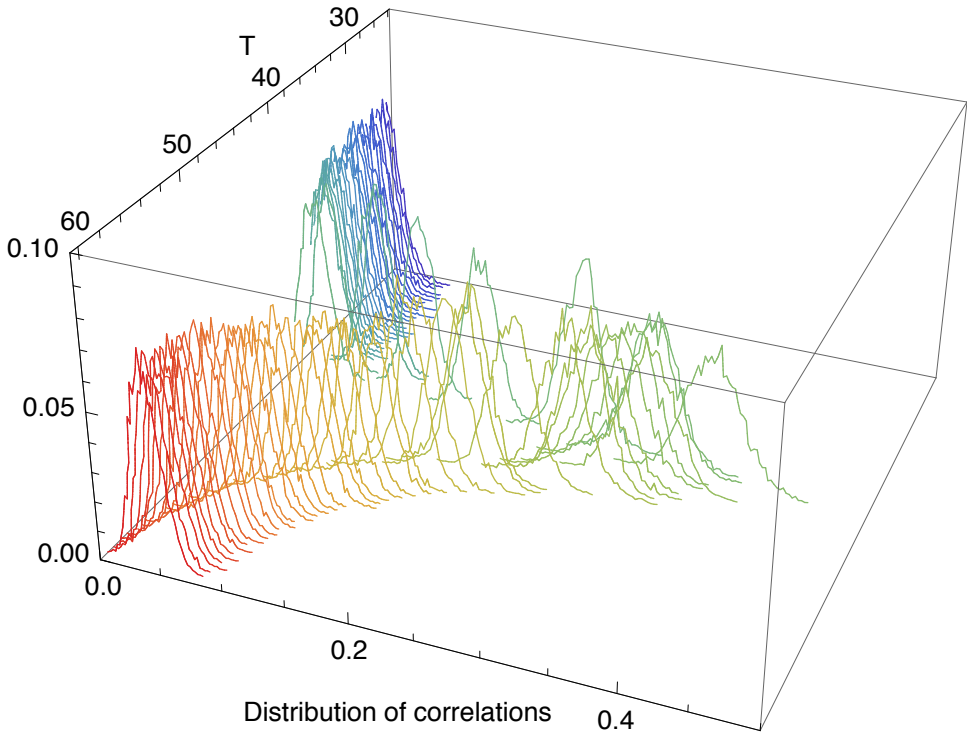

Figure 7.12: Histograms of the correlations for a variety of temperatures.

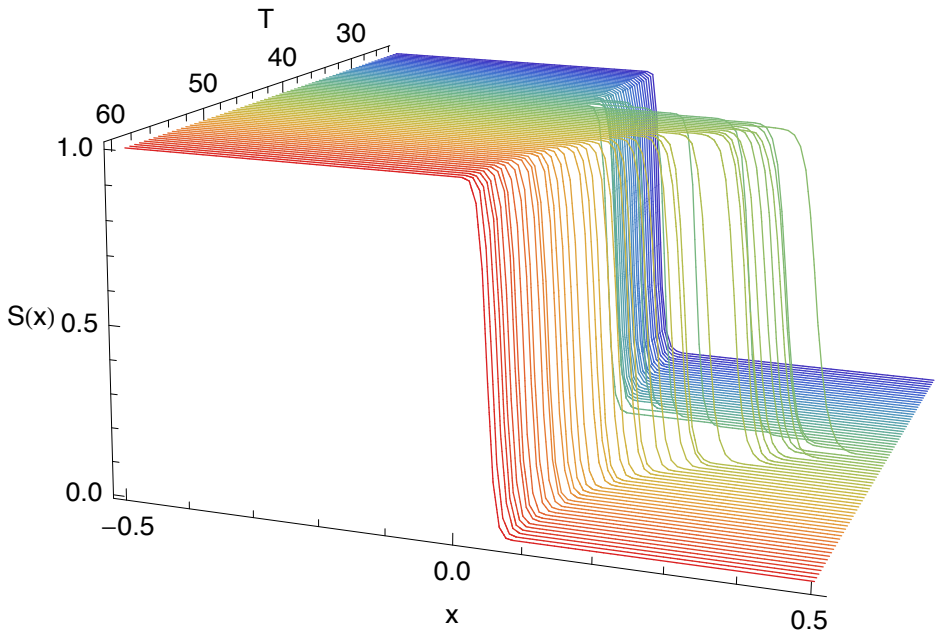

Figure 7.13: Staircase plots of the correlation matrix for a variety of temperatures.

Chapter 8

Conclusion

8.1 Summary of New Results

We briefly summarize the new methods and results developed in this thesis.

1. Scale invariance of the parameter λ_s^2, a measure of the non-Gaussian nature of the returns, does not appear to be a strong universal property of stock market crashes, although there does appear to be some correlation.

2. The black box Ising model problem is, in general, not solvable, although the histograms and staircase functions of the correlation matrices near the critical point do provide some information that may be used to distinguish between spatial dimensions.

3. Correlation matrices of intraday and intrahour stock data from the last 20 years *never* exhibit any features that suggest that a measure of distance between stocks exists.

4. The results in fact resemble the correlation matrices of a Zero-dimensional Ising model, which while a common pedagogical problem for small N, has not been analyzed systematically. The 0D Ising model exhibits an interesting *pseudo-phase transition*, where a macroscopic quantity (the internal energy) changes character at a critical temperature, but this is not an intensive property of the system. Simulations of the 0D Ising model exhibit "pinning" of the system in one state at lower temperatures, whereby only an ensemble of identically prepared systems equates to the thermodynamic averages.

5. The resemblance of the stock market to the 0D Ising model suggests that

   (a) stock market crashes will critically depend on market size in the way the pseudo-phase transition of the 0D model depends on system size.

   (b) as the coefficients of stock interaction vary, the "critical point" of the stock market may evolve in time.

   (c) the stock market may in fact be "pinned" when the correlation matrices are observed to be high.

   (d) a 0D matrix model with random and time varying coefficients may better describe the stock market.

6. Policy arguments drawn upon the analogy as originally proposed are potentially spurious until further research is conducted.

8.2 Further Study

Unlike physical systems, which are inevitably confined to 1D or higher and for which there exists a rich variety of possible symmetries that generate a vast plethora of different symmetry breaking phase transitions, the symmetry structure of 0D is extremely simple. This suggests that a very small space of possible 0D models exist. Since we have seen that it is the symmetries of the system that determine its critical behavior we suggest a more thorough investigation of symmetries of a 0D system. We also leave to further work the construction of a 0D model of a stock market, with random and time varying coefficients, and that may be used to predict distributions of returns, etc.

Bibliography

[1] Binyamin Appelbaum and Eric Dash. S&p downgrades debt rating of u.s. for the first time. *New York Times*, 6 August 2005.

[2] L Bachelier. Theorie de la speculation. *Annales Scientifiques de l'Ecole Normale Superieure*, 3:21–86, 1900.

[3] Richard T. Baillie and Tim Bollerslev. Intra-day and inter-market volatility in foreign exchange rates. *The Review of Economic Studies*, 58(3):565–585, 1991.

[4] Daniel Bernoulli. Exposition of a new theory of the measurement of risk. *Econometrica*, 22(1):23–36, 1954. English translation. Originally published in 1738.

[5] Fischer Black and Myron Scholes. The pricing of options and corporate liabilities. *Journal of Political Economy*, 81, 1973.

[6] Stefan Bornholdt. Expectation bubbles in a spin model of markets: Intermittency from frustration across scales. *Journal of Modern Physics C*, 12(5), 2001.

[7] B. Castaing, Y. Gagne, and E.J. Hopfinger. Velocity probability density functions of high reynolds number turbulence. *Physica D*, 46, 1990.

[8] Anirban Chakraborti, Ioane Muni Toke, Macro Patriaca, and Frederic Abergel. Econophysics review: 1. emprical facts. *Quantitative Finance*, 11(7), 2011.

[9] Rama Cont, Marc Potters, and Jean-Philippe Bouchaud. Scaling in stock market data: Stable laws and beyond. 1997.

[10] A. D. Cowper. *On the Motion of Small Particles Suspended in a Stationary Liquid, as Required by the Molecular Kinetic Theory of Heat*. Dover Publications, Inc., 1926. This is an english translation of Albert Einstein's 1905 paper "Uber die von der molekularkinetischen Theorie der Warme geforderte Bewegung von in ruhenden Flussigkeiten suspendierten Teilchen".

[11] Gerard Debreu. *The New Palgrave Dictionary of Economics*. Palgrave Macmillan, 2008. From the section entitled "Mathematical Economics".

[12] Eugene F. Fama. The behavior of stock-market prices. *The Journal of Business*, 38(1):34–105, 1965.

[13] Jens Feder. *Fractals*. Plenum Press, 1988.

[14] Niall Ferguson. The darwinian economy. In BBC Radio, editor, *The Reith Lectures*, 26 June 2012.

[15] Irving Fisher. The application of mathematics to the social sciences. *The seventh Josiah Willard Gibbs Lecture*, 13 December 1929. Read before a joint session of the American Mathematical Society and the American Association for the Advancement of Science.

[16] S. Ghashghaie, W. Breymann, P. Talkner J. Peinke, and Y. Dodge. Turbulent cascades in foreign exchange markets. *Nature*, 381(27), June 1996 1996.

[17] Malcolm Gladwell. *The Tipping Point: How Little Things Can Make a Big Difference*. Back Bay Books, 2002.

[18] Roy J. Glauber. Time dependent statistics of the ising model. *Journal of Mathematica Physics*, 4:294 – 307, 1963.

[19] Josef Honerkamp. *Statistical Physics: An Advanced Approach with Applications*. Springer, 1998.

[20] Kerson Huang. *Statistical Mechanics*. Wiley, 1987.

[21] Ernst Ising. Beitrag zur theorie des ferromagnetismus. *Zeitschrift fuer Anorganische und Allgemeine Chemier Physik*, 31(1):253–258, 1925.

[22] Taisei Kaizoji. A model of international financial crises. *Physica A*, 299, 2001.

[23] Ken Kiyono, Zbigniew R. Struzik, Naoko Aoyagi, Seiichiro Sakata, Junichiro Hayano, and Yoshiharu Yamamoto. Critical scale invariance in a healthy human heart rate. *Physical Review Letters*, 93(19), 2004.

[24] Ken Kiyono, Zbigniew R. Struzik, and Yoshiharu Yamamoto. Criticality and phase transition in stock-price fluctuations. *Physical Review Letters*, 96(068701), 2006.

[25] Ladislav Kristoufek. Rescaled range analysis and detrended fluctuation analysis: Finite sample properties and confidence intervals. *AUCO Czech Economic Review*, 4:315 – 329, 2010.

[26] Moshe Levy. Stock market crashes as social phase transitions. *Journal of Economic Dynamics & Control*, 32, 2008.

[27] Yanhui Liu, Parameswaran Gopikrishnan, Pierre Cizeau, Martin Meyer, Chung-Kang Peng, and H. Eugene Stanley. Statistical properties of the volatility of price fluctuations. *Physical Review E*, 60(2), 1999.

[28] Tony Long. March 10, 2000: Pop goes the nasdaq! *Wired Magazine*, 7 March 2007.

[29] Sam Mamudi. Lehman folds with record 613 billion dollar debt. *Market Watch*, 15 September 2008.

[30] Benoit Mandelbrot. The variation of certain speculative prices. *Journal of Business*, 36:394–419, 1963.

[31] Benoit Mandelbrot. *The Misbehavior of Markets: A Fractal View of Financial Turbulence*. Basic Books, 2006.

[32] Rosario N. Mantegna and H. Eugene Stanley. *An Introduction to Econophysics: Correlations and Complexity in Finance*. Cambridge University Press, 2000.

[33] Harry Markowitz. Portoflio selection. *Journal of Finance*, 7:77–91, 1952.

[34] J.F. Muzy, J. Delour, and E. Bacry. Modelling fluctuations of financial time series: from cascade process to stochastic volatility model. *The European Physical Journal B*, 17, 2000.

[35] M.E.J. Newman and G.T. Barkema. *Monte Carlo Methods in Statistical Physics*. Oxford University Press, 1999.

[36] Division of Market Regulation. Trading analysis of october 27 and 28, 1997. *U.S. Securities and Exchange Commission*, September 1998.

[37] Lars Onsager. Crystal statistics. i. a two-dimensional model with an order-disorder transition. *Phys. Rev.*, 65:117–149, 1944.

[38] C.-K. Peng, S. V. Buldyrev, S. Havlin, M. Simons, H. E. Stanley, and A. L. Goldberger. Mosaic organization of dna nucleotides. *Physical Review E*, 49(2), February 1994.

[39] Julianne Pepitone. Fannie mae and freddie mac delist from nyse. *CNN Money*, 7 July 2010.

[40] J.G. Powles. Brownian motion - june 1827. *Phys Educ.*, 13, 1978.

[41] Gheorghe Savoiu and Ion Iorga-Siman. Some relevant econophysics' moments of history, definitions, methods, models and new trends. *Romanian Economic and Business Review*, 3(3):29–41, 2008.

[42] Daniel V. Schroeder. *An Introduction to Thermal Physics*. Addison-Wesley, 1999.

[43] Franz Schwabl. *Statistical Mechanics*. Springer, 2 edition, 2006.

[44] Sitabhra Sinha, Arnab Chatterjee, Anirban Chakraborti, and Bikas K. Chakrabarti. *Econophysics: An Introduction*. Wiley-VCH, 1 edition, 2010.

[45] Richard Sole. *Phase Transitions*. Princeton University Press, 2011.

[46] Tiziano Squartini and Diego Garlaschelli. Jan tinbergen's legacy for economic networks: from the gravity model to quantum statistics. *Quantitative Finance*. Submitted on 11 April 2013.

[47] Robert A. Wood, Thomas H. McInish, and J. Keith Ord. An investigation of transactions data for nyse stocks. *The Journal of Finance*, 40(3), 1985.

[48] Rossitsa Yalamova and Bill McKelvey. Explaining what leads up to stock market crashes: A phase transition model and scalability dynamics. *Journal of Behavioral Finance*, 12, 2011.

[49] W.-X. Zhou and D. Sornette. Self-organizing ising model of financial markets. *European Physical Journal B*, 55, 2007.